FaSSIF-C, a Cholesterol containing biorelevant intestinal model medium for development and test of oral drug formulations

Dissertation

Zur Erlangung des akademischen Grades

“Doktor der Naturwissenschaften”

im Promotionsfach Pharmazie

am Fachbereich Chemie, Pharmazie und Geowissenschaften

der Johannes Gutenberg-Universität Mainz

Pooneh Khoshakhlagh

geb. in Rasht, Iran

Mainz, 2015

dedication

1. Acknowledgement

2. Table of contents

Abbreviations

API,	active pharmaceutical ingredient
BCS,	biopharmaceutics classification system
cmc	critical micelle concentration
cmc_e	critical micelle concentration of added exipient
DLS,	dynamic light scattering
DOPC,	1,2-di-oleoyl-sn-glycero-3-phosphocholine
Egg-PC,	Egg-phosphatidylcholine
FaSSGF,	fasted state simulated gastric fluid
FaSSIF,	fasted state simulated intestinal fluid
$FaSSIF_{mod}$,	fasted state simulated intestinal fluid, bicarbonate-HEPES buffered
FaSSIF-C,	fasted-state simulated intestinal fluid with cholesterol
FeSSGF,	fed state simulated gastric fluid
FeSSIF,	fed state simulated intestinal fluid
$FeSSIF_{mod}$,	fed state simulated intestinal fluid, bicarbonate-HEPES buffered
FeSSIF-C,	fed-state simulated intestinal fluid with cholesterol
FDA,	Food and Drug Administration
GI,	gastrointestinal
HBSS,	Hank's buffered salt solution
HEPES,	4-(2-hydroxyethyl)-1-piperazineethanesulfonic acid
IVIVC,	in-vitro in-vivo correlation
MMC	migrating motor complex
MTT	tetrazolium salt, 3-(4,5-dimethylthiazol-2-yl)-2,5-diphenyl tetrazolium bromide
NP,	nanoparticle
PC,	phosphatidylcholine
POPC,	1-palmitoyl-2-oleoyl-sn-glycero-3-phosphocholine
PSDi,	particle size distribution by scattering intensity (DLS raw data)
PSDv,	particle size distribution, particle volume scaled
SALS	small angle light scattering
SANS,	small angle neutron scattering
SASX	small angle X-ray scattering
SCoF,	simulated colonic fluid
SDS,	Sodium dodecyl sulfate
SIF,	simulated intestinal fluid

SGF, simulated gastric fluid

Soy-PC, soybean phosphatidylcholine

TC, taurocholate

TM transport medium

TDOC, taurodeoxycholate

TM, transport medium

1. Introduction

The Biopharmaceutics Classification System (BCS) describes the solubility in water and the intestinal permeability as the rate limiting steps for an effective oral drug delivery. For BCS classes II and IV a sub-classification according to sub-specification of acid (a), base (b) and neutral (c) have been proposed[1].

For the accurate prediction of solubility and permeability of APIs the choice of appropriate media for *in vitro* test is critical. For BCS class II and IV compounds it seems sensible to use the media that mimic the gastrointestinal tract because the human intestine has a higher solubilizing capacity than pure water or simple buffer systems.

Biorelevant media have been proposed to mimic *in vivo* condition based on knowledge of the composition of the GI tract in different nutritional states and physiochemical properties such as pH, viscosity, osmolality, and surface tension. During the last decade a lot of attempts have been made to make these media more similar to the body's environment.

In the human intestinal fluid, even in fasted state, different solubilizing species such as phospholipids, bile salts and cholesterol are detected[2] . These substances originate from biliary secretions in the duodenum. The fed state simulated intestinal fluid (FeSSIF) and fasted state simulated intestinal fluid (FeSSIF) are biorelevant media to simulate the upper part of the small intestine. To have a more realistic biorelevant model media all of the main components that are found in the GI tract are required. In this work new biorelevant media, FeSSIF -C and FaSSIF-C, containing cholesterol as a missing part of the old FeSSIF and FaSSIF were developed and the effect of the cholesterol on solubility and nanoparticle structure of some BCS class II drugs was investigated.

The structure development upon the dilution of the fed state bile model to FaSSIF showed that bile salt-lipid micelles change to liposome after dilution[3]. Therefore, the kinetics of the nanoparticle structure development in the gastro-intestinal model fluids were investigated.

With many of poor water soluble drugs, different ways have been used to improve their solubility. Surfactants, lipids and polymers are important excipients employed for this purpose[1]. Hence, the effect of some surfactants on solubilization and transit nanoparticle structure development in $FaSSIF_{mod}$ and FaSSIF-C with Fenofibrate as a BCS class II was investigated.

1.1 Physiology of gastrointestinal tract

The Gastrointestinal (GI) system is responsible for digestion of food, vitamin and drug absorption. GI conditions such as pH, fluid composition and hydrodynamics strongly affect the bioavailability of drugs. The GI system is composed of three major parts which are relevant for bioavailability studies: the stomach, small intestine and large intestine.

1.1.1 Stomach

The stomach is a hollow muscular organ and continues the digestive process that began in the mouth. This organ is divided into two functional regions; the fundus and the antrum. The gastric juice contains hydrochloric acid, bicarbonate, pepsinogen, gastric lipase, mucins, and bile salts as the main components. Gastric acid plays a key role for activation of pepsin from pepsinogen. Pepsin initiates protein digestion in the food into peptide fragments. The Gastric lipase causes 15% to 20% of total fat digestion[4, 5].

1.1.2 Small intestine

The small intestine is the most important part for digestion and absorption of the GI tract with a length of about 5.5m[6, 7].It is divided into three segments: the duodenum, the jejunum and the ileum. The large surface of the human small intestine makes it ideal for absorption[7]. The fold of Kerckring, the vili and the microvilli provide huge area of surface [4] The chyme moves into the duodenum by the rhythmic muscular action of the stomach wall (peristalsis) and it simulates the release of secretin. This hormone increases the flow of pancreatic juice and bile[8]. The pancreatic juice contains several hydrolytic enzymes and bicarbonate. The most important role of bile is improving the efficacy of lipid digestion by formation of transit nanoparticle system. This develops from micelles to liposomes including food components, with pH of 6.8 to 7 at the end of the duodenum[3].

The small intestine plays a large role in the human water homeostasis. Daily, about 9 L of fluid enter the small intestinal and about 7 L of that is reabsorbed by ileocecal junction[4].

1.1.3 Large intestine

The large intestine (cecum, colon and rectum) is the last part of the GI. The main functions of the large intestine include fermentation by large bacterial population, reabsorption of water and electrolytes as well as elimination of indigestible food. The large intestine has fewer and less efficient absorption mechanisms than the small intestine[4].

1.2 Important physiological factors in gastrointestinal absorption

Drug absorption from oral formulations is affected by various physiological factors including the gastric emptying rate, volume and composition of gastrointestinal (GI) fluids, the pH and buffer capacity of these fluids, viscosity, osmolality , surface tension, bile secretion, digestive and metabolic enzymes, the presence of intestinal barriers and transporters[4].

1.2.1 Transit time

1.2.1.1 The gastric emptying rate

The gastric emptying rate is the frequency of entering of the drug and food compounds from the stomach into the small intestine and is one of the critical factors that influence the plasma concentration of the orally administered drugs. This rate is variable depending on the drug formulation and the content of the stomach (such as pH, temperature, volume, and viscosity of the meal). Furthermore, inter and intra individual day to day variation in gastric section affects the rate of gastric time[4, 9, 10,11]. In the fed state only particles smaller than 2 mm can pass the pylorus. Larger, nondigestible objects emptying occurs during phase III of the migrating motor complex (MMC)[12, 13].

The emptying mechanisms of the liquids and solids are different. Liquids distribute rapidly through the stomach and are emptied immediately following first order kinetics. Solids food emptying pattern is biphasic. In this process a lag phase is observed during which only little emptying occurs. Afterwards extensive emptying following first order kinetics occurs[14, 15].

1.2.1.2 Small intestinal transit time

The small intestinal transit time in health persons is three to five hours. This time does not seem to be influenced by food intake and the dosage form type[4, 9, 10]. An increase in the transit time enhances the possibility for absorption of poor permeable and poor soluble drugs.

1.2.1.3 Colon transit time

The ascending colon transit time in human is reported to be about 13h. This transit time is independent of the type of formulation[10].

1.2.2 GI fluid volume and composition

The composition and volume of gastrointestinal fluids have a major role in solubility, and thereby absorption of drugs in the gastrointestinal tract. For instance, the presence of amphiphiles in the intestine plays an important role in solubilization of poor soluble drugs[16].

The resting fluid volume of the stomach is 30-50 ml and the volume of the stomach changes after meal intake up to 1.5 L. The intestinal volume in the Fasted state is 45-319 ml and 20-156 ml in fed state as determined by magnetic resonance imaging[16]. Fasting volume of the ascending colon is ca. 203 ± 75 ml. This volume expands by 10% after feeding in healthy persons[17].

1.2.3 GI pH and buffer

There is a general trend of increasing of pH from stomach to jejunum. The pH value of the fasted stomach is reported to be about 1.7 up to 3.3 (median 2.5), while that of the duodenum is 5.6-7 (median of 6.3). The jejunum has a pH value of 6.5-7.8 (median of 6.9). The buffer capacity of the stomach has been determined to be between 13.3-19 mM/ΔpH (median 14.3) and 5.6 to 8.5 mM/ΔpH for the duodenum. The buffer capacity of the jejunum in general is reported to be lower than the buffer capacity of the duodenum (median 4 mM/ΔpH)[1, 18-22].

The difference in pH between gastric fasted and fed state is because of the administered food. In fed state the gastric pH increase from 4.5 to 6.7. The secreted hydrochloric acid slowly reduces the pH[11]. As a result of the pretreatment in the stomach, the effect of food on the pH of the intestine is smaller. The duodenum pH has been reported to be between 5.4 and 6.5 (median 6.0). The jejunal fluid has a pH of 6.1. The buffer capacity for gastric, duodenal and jejunal fluids in fed state is higher as compare to fasted state. The gastric buffer capacity has been reported as 19.5 mM/ΔpH. The duodenal buffer capacity is between 24 and 30 mM/ΔpH, while jejunal fluid has 13.9 mM/ΔpH[1, 19, 20, 23, 24].

1.2.4 Viscosity, osmolarity and surface tension

There is no report about the viscosity of the fasted state of the gastric fluid and intestinal fed and fasted state. In the fed state, the value of the gastric viscosity is between 10-2000 Pa.s[10, 25].

Osmolarity can affect the disintegration of a formulation. The osmolarity is higher in fed state as compared to fasted state. The osmolality of the gastric juice in fasted state is in the range of 119-221 mOsm (median of 202mOsm) and shows increase to a value of 388mOsm after meal intake. In the duodenal fluid, osmolarity is in the range of 137-224 mOsm (median 197 mOsm) and 276-416 mOsm in fasted state and fed state, respectively. Osmolality in jejunal fluid in fed state shows increase as compared to gastric and duodenal fluids. The

osmolarity in the jejunum has been reported to be 200-300 mOsm (median 280mOsm). No report about the osmolarity of the fed jejunal fluids has been reported[1, 18, 19, 22, 26].
The surface tension of a medium has influence on the wetting speed of drugs and excipients. The gastric surface tension in fasted state is about 41 to 46 mN/m and in fed states, 30 to 31 mN/m. Surface tension in the upper small intestine is from 28- 46 mN/m and from 27-37 mN/m in fasted and fed states, respectively. In the colon, surface tension is 39 mN/m in fasted states and 43mN/m in fed state[10, 27].

1.2.5 Bile micelle

Bile is a complex fluid containing water, inorganic salts, cholesterol, lecithin, bile salts and bilirubin that flows through the biliary duct into the small intestine [28, 29]. Bile is necessary for lipid digestion and removal of excess cholesterol from the body by direct excretion or after conversion to bile acids. Bile micelles and liposomes increase the solubility and dissolution rate of hydrophobic drugs as well as decrease the unbound drug fraction and effective permeability[10, 30, 31]. The bile is also an excretion path for lipophilic toxins[32].
In the body, the gall bladder volume after an overnight fast is 17-25 ml[10, 33] . In the fasted state about 30% of bile is directly released into the duodenum. [10] When lipidic food from the stomach reaches the duodenum cholecystokinin is released by the endocrine cells of the small intestine. This hormone stimulates the gallbladder to contract and causes the gallbladder to be emptied up to 75 %. In this state, the bile is diluted by the fluids from the stomach at different rate[10, 34].
There is a dynamic change of bile concentration. In humans the bile acid concentration in the stomach is low[35 11]. The small intestine has higher concentration of mixed micelles since the gall bladder empties its contents into the duodenum. During the transit of fluids in the small intestine water is reabsorbed and the concentration of the bile increases about two fold. The concentration of the bile derived micelles might be slightly higher in the upper jejunum than in the duodenum. The average bile salt concentration in early jejunum is ca. 3mM in fasted state and ca. 5-15mM in fed sate. Most of the bile acids are reabsorbed passively in the jejunum and actively at the end of the ileum by apical sodium dependent bile acid transporter (ASBT; SLC10A2). The composition of the fluid secretion in the fed state is more dynamic than in the fasted state. In the fed state, the bile micelle concentration depends on the food[4, 10, 26, 35, 36]. In the colon the bile concentration is very small, because most of the bile is reabsorbed at the small intestine[35]. The bile concentration shows a big difference of individual variation according to gender and race[35, 37]

Bile acids are disk-shaped amphiphilic molecules with hydrophobic and hydrophilic domains at the opposite sites of the rigid steran ring system. They are biological detergents that are synthesized stepwise by oxidation and modification of the cholesterol in the liver[38]. Bile acids are at neutral pH highly soluble in water and form micelles at concentrations above the critical micelle concentration (cmc)[39]. They also partition into lipid bilayers such as vesicles with lecithin and cholesterol. These structures will reduce the toxicity of the bile acids. The surface of the bile micelles is negatively charged due to the presence of sulfate or carboxylate groups. In bile acids all hydroxyl groups are located on the same face of the steran plane. This results in somewhat different behavior from regular surfactants.[2, 10, 40]. In the fasted state human intestinal fluid contains three predominant bile salts: taurocholate, glycocholate and glycochenodeoxycholate. The sum of these bile salts contributed about 70%-75% to the total bile salts concentration in human small intestine[2, 22, 41-44].

Phospholipids are the most important lipids observed in the human intestinal fluid. They have amphiphilic structure that can aggregate to bilayer structures (e.g. liposomes or mixed micelles) in which the hydrophilic head groups are oriented towards the surface and the hydrophobic hydrocarbon chains towards the interior[45, 46]. In the human body phospholipids from bile and food are substrate for the phospholipase secreted by the pancreas. In the human small intestine the main phospholipids are lecithin and its hydrolysis product lysolecithin[26, 47, 48].

Cholesterol is a hydrophobic molecule which contains one polar hydroxyl group and a rigid non-polar steroid ring structure with a branched hydrocarbon tail. The solubility of pure cholesterol in aqueous solution is very low. In the human bile cholesterol is solubilized by formation of micelle and vesicles with bile salts. A supersaturation of the cholesterol will happen when either too much cholesterol or insufficient bile salt and lecithin are secreted. Excess cholesterol is kept in vesicles (ie, spherical bilayers of cholesterol and phospholipid, without bile salts) or in cholesterol crystals, which can develop to gall stones. Biliary cholesterol is non-esterified and accounts for 97% of the total sterol in the bile. In the gut cholesterol is taken up at two regions (early jejunum, late ileum/colon). The enterohepatic circulation stabilizes the cholesterol concentration in the intestinal system. [30, 49-53].

1.2.6 Enzymes and bacteria

Pepsin and lipases play important roles in the oral absorption of drugs. In the fasted state, the pepsin concentration changes between 0.1 and 1.3 mg/ml and in fed state ranges from 0.26 to

1.72 mg/ml. Lipase is critical for lipid based formulations and its activity is 11.4 to 43.9 U/ml in fed state[10, 27].

There are some populations of bacteria in the gastrointestinal tract (Enterococci, Clostridia, Lactobacilli, Bacteriodes and gram positive anaerobes). The prevalence of bacteria in different part of GI tracts depends on various factors such as pH, mucin secretion, and diet. These bacteria can degrade some foods and drugs [2,10, 54].

1.2.7 Gastro intestinal barriers and transporters for drug permeation

Dissolved drug should pass the physical barrier consisting of a mucus layer and intestinal cells of enterocytes to reach the blood circulation. Mucus is a hydrophilic secretion that may limit diffusion of strongly lipophilic drugs and decrease their permeability. However the most important barrier for drug permeation is the intestinal monolayer of epithelial cells[55, 56]. In addition to physical barriers, biochemical barriers (intestinal metabolism and efflux) have crucial effect on GI drug permeability[56, 57].

Several different uptake transporter proteins like peptide transporter, organic cation transporters, ATP-binding cassette transporters, etc. are localized on the apical (brush border) membrane of enterocytes at specific intestinal locations. These transporters catalyse the entry of non-membrane-permeable molecules into the blood circulation[1, 58, 59].

1.3 Important parameters of gastrointestinal drug absorption

1.3.1 Solubility

Drug solubility in the gastrointestinal tract is an important parameter, because the maximum amount of the drug dissolved in this fluid is limited by the solubility and only free drug molecules in solution will be available for absorption across the intestinal epithelium. Therefore, the bioavailability of orally administered drugs is to some extent influenced by the solubility in the GI tract. Poor aqueous solubility could present a problem for development of the drug formulation of new drugs, e.g. of the BCS classes II and IV[10, 16]. Methods usually used to improve the solubility of poor soluble drugs include use of salt form, increase of specific surface area by reduction of particle size, change of crystal form (polymorphism/amorphism) and preparation of solid dispersion. Solubility enhancing excipients can be used in formulations to solve solubility problems. Such excipient include water-soluble organic solvent, hydrophilic polymers and cyclodextrins, medium chain triglyceride, long chain triglyceride, phospholipid and surfactants[60].

Supersaturation can improve the solubility of drugs. The drugs in the state of supersaturation are kinetically soluble in solution at concentrations above their thermodynamic equilibrium. If the supersaturated drug solution exist in GI for an adequate time, it may result in an enhanced flux across the intestinal wall and improve the absorption[61].

1.3.2 Dissociation constant (pKa)

The dissociation constant, pKa, is a key physicochemical parameter of the drug that affects some biopharmaceutical characteristics .The solubility of weak acids and bases is dependent on their dissociation constant and the local pH of the dissolution medium. pK_a affects solubility, dissolution rate and permeability of the drugs[10, 62].

1.3.3 Particle size

The particle size of active ingredients and excipients is an important physical characteristic for pharmaceutical products. Reducing particle size can aid the formulation of the drug with poor water solubility. Particle size analysis is possible by microscope, laser diffraction, dynamic laser scattering (DLS)[10]and solution scattering methods such as small angle light scattering (SALS), small angle X-ray scattering (SASX) and small angle neutron scattering (SANS). The latter method can distinguish formulation components by deuterium contrast variation[63, 64].

1.3.4 Disintegration

Disintegration is the first step preceding the drug absorption of a solid dosage form. In this step the formulation disintegrates to granules and releases solid particles of active pharmaceutical ingredient (API). A delay in disintegration of the solid dosage form will affect the overall release of the API, as well as the pharmacokinetics[10].

1.3.5 Dissolution rate

Drug dissolution is a dynamic process by which drug is transferred from solid state into a solvent per unit time[10]. For dissolution of the solid formulation the properties of the formulated drug and intrinsic physicochemical properties of the drug molecule play a crucial role[62]. For lipophilic drugs the dissolution is a rate limiting step[65].

1.4 Biorelevant media

Biorelevant media simulate the fasted and fed state of the gastrointestinal tract to reproduce the physiological situation in the formulation development and tests[66, 67, 68].These media are developed based on knowledge of the composition of the GI fluids in different nutritional state with respect to physicochemical properties such as pH, buffer capacity, ionic strength and surface tension[2]. They have been proposed to predict the *in vivo* drug absorption and have been modified with time[69]. Biorelevant media are useful tools for the early stage of drug discovery and development for finding the biopharmaceutical behavior of the compounds. They are also useful for drug formulation development and the establishment of *in vitro-in vivo* correlations (IVIVC), which leads to a decrease in the numbers of animal experiments in bioavailability and bioequivalence studies. The solubility and dissolution tests in these media can show a better forecast of pharmacokinetic profiles of drugs than compendial media[70, 71]. Cell and tissue compatible biorelevant media also allow studying the drug transport for *in vitro* models[16, 72-77].

1.4.1 Media to simulate the gastric condition in the fasted state

The simulated gastric fluid (SGF) for the fasted state contains hydrochloric acid, sodium chloride, pepsin and water .The pH of that was adjusted to 1.2. Synthetic surfactant, like sodium lauryl sulfate (SDS) or Triton-X has been proposed to reduce the surface tension to physiological values[78, 79]. This medium induces solubilization effects greater than under physiological conditions[80]. Fasted state simulated gastric fluid (FaSSGF) was developed as a medium to reflect the actual gastric composition in the fasted state according to physiological data. This medium contains pepsin and low amount of bile salt and lecithin[81].

Table1-1. Composition of media to simulate the fasted state in the gastric condition[66,78,79,81]

Components	SGF_{SLS}	SGF_{Triton}	FaSSGF
Sodium lauryl sulfate (%W/V)	0.25/0.05	-	
Triton X 100(%W/V)	-	0.1	
Pepsin (mg/ml)	-	-	0.1
NaTC[µM]	-	-	80
Lecithin [µM]	-	-	20
NaCl	34.2	34.2	34.2
pH	1.2	1.2	1.6
Osmolality (mOsm/kg)	180.5±3.6	157.7±2.9	120.7±2.5

1.4.2 Media to simulate the gastric condition in the fed state

In the fed sate, the composition of the stomach fluid highly depends on the composition of the food ingested and time[19, 82]. The perfect medium to show the gastric condition in the fed state should have nutritional and physicochemical properties of the meal, e.g. the standard breakfast recommended by the US FDA[83]. Homogenized long-life milk (3.5% fat) and complete nutrition products (Ensure ®Plus) were two alternatives as the dissolution media to simulate fed condition in the stomach. Both of them have a similar composition to a breakfast meal. Ensure ®Plus is better for the simulation of the gastric condition after administration of a high fat meal. In both media some weaknesses like pH, pepsin, etc. were evident. Variation in source and season of the milk may cause differences in the results[67, 83-86].

Table1-2. Composition of media to simulate the fed state in the gastric condition[66,69]

Components	Early	Middle(FeSSGF)	Late
NaCl (mM)	148	237.02	122.6
Acetic acid (mM)	-	17.12	-
Sodium acetate (mM)	-	29.75	-
H_3PO_4(mM)	-	-	5.5
NaH_2PO_4 (mM)	-	-	32
Milk/Buffer	1:0	1:1	1:3
HCl /NaOH	q.s. pH 6.4	q.s. pH 5	q.s. pH 3
pH	6.4	5	3
Osmolality (mOsm/kg)	559	400	300

Early refers to the first 75min, middle from 75 to165 minutes and late after 165 min of the gastric condition after meal digestion

The variability of the gastric composition was reflected by "snapshot" milk-based media and gradually digested milk during in vitro release test. In "snapshot" media three phases (early, middle and late) were designed. The composition of the media were based on pH, buffer capacity and osmolality of the gastric condition during the first 75min (early), from 75-165 min (middle), and after 165 min (late) development of meal digestion. The "middle" medium (FeSSGF) is suggested as the most appropriate for simulating the postprandial condition of the stomach[66, 69 35].

1.4.3 Media to simulate the small intestinal condition in the fasted state

Simulated Intestinal Fluid (SIF) is the simplest medium for the simulation of small intestine, which is used for quality control tests. Thus it cannot be an optimum condition for *in vitro/in vivo* correlations. This medium does not have most aspects of physiological conditions in the small intestine (buffer capacity, bile, surface tension, osmolality and volume of intestinal content). It only represents the pH condition in the jejunum (pH of 6.8) and contains pancreatin [70, 84].

The medium FaSSIF has been introduced to simulate the proximal small intestine under fasting condition. Sodium taurocholate (bile salt) and phospholipids (lecithin) in the rate of 4:1 are added to this medium. Osmolality and buffer capacity with the pH of the mid-duodenum to proximal ileum (6.5) have been considered for this medium[67, 79].

During the last decade FaSSIF has been updated. In FaSSIF-V2 [69] the amount of the lecithin has been reduced from 0.75mM to 0.2 mM and the osmolality decreased from 270 to180 mOsm/kg. In this medium the buffer changed from phosphate (pK'a = 7.1) to maleate (pK'a = 6.2). However, in the small intestine the native buffer is bicarbonate. Bicarbonate buffer contains volatile carbon dioxide in physical and chemical form. Possible gas loss during the application may change the pH and buffer capacity. This kind of buffer is not easy to use, at least in a passive system[66, 69, 87].

In update of FaSSIF to FaSSIF $_{mod6.5}$ a cell compatible bicarbonate-glucose buffer, HBSS, was used. This buffer contains 4.167 mM $NaHCO_3$, 0.779 phosphate and 25 mM glucose (supplemented HBSS) and 10 mM HEPES (Pk_a=7.5 at 25 °C) to improve the buffer capacity. The pH was adjusted to 6.5 with 0.1 M HCl [88].

1.4.4 Media to simulate the small intestinal condition in the fed state

The conditions in the proximal small intestinal in fasted state and in fed state are different. After ingesting a meal, the second part of duodenum has a higher concentration of mixed micelles [68]. As a result of food digestion some buffer species like amino acids will be released from proteins, which play an important role in pH and buffer capacity. Thus it is not simple to simulate the buffer species in fed state[66 ,89].

Fed state simulated intestinal fluid (FeSSIF) was suggested to reflect this environment better[79, 83]. FeSSIF is a medium with higher concentrations of sodium taurocholate and phospholipids as compared to FaSSIF. In addition, the buffer capacity and osmolality is higher.

Jantratid et al.[69] improved the composition of FeSSIF according to the finding that the pH in the upper small intestine decreased rather slowly after a meal intake[19]. As in the stomach, "snapshot" media were developed to reflect the digestion process. Three phases ("early", "middle" and "late") were defined to represent different time frames of the composition of small intestine after food ingestion. In addition the lipolysis products glyceryl monooleate and sodium oleate were added to the media. FeSSIF –V2 has been suggested as representative postprandial condition in the small intestine. In this medium the bile salt /phospholipids levels was changed from 4 to 5. The buffering species was changed to maleate and the osmolality was decreased. In this medium lipolysis products were added (OA/MO: 0.16) which is lower than physiological value[69].

Table1-3. Composition of media to simulate the fasted state in the small intestine[66, 72, 75, 84]

Components	FaSSIF	FaSSIF-V2	$FaSSIF_{mod}$
NaCl[mM]	105.85	68.62	137.931
KCl [mM]	-	-	5.333
$CaCl_2$[mM]	-	-	1.261
$MgCl_2$ [mM]	-	-	0.493
$MgSO_4$ [mM]	-	-	0.407
$NaHCO_3$ [mM]	-	-	4.167
KH_2PO_4 [mM]	28.65	-	0.441
Na_2HPO_4 [mM]	-	-	0.338
HEPES [mM]	-	-	10.0
Glucose [mM]	-	-	25.0
NaOH [mM]	8.7	34.8	-
Maleic acid [mM]	-	19.12	-
Acetic acid [mM]	-		-
NaTC [mM]	3	3	3
Lecithin [mM]	0.75	0.2	0.75
Fatty acid [mM]	-	-	-
Monoglycerides [mM]	-	-	-
pH	6.5	6.5	6.5
Osmolality (mOsm/kg)	270±10	180±10	311.7±0.6

FeSSIFmod6.5, the cell compatible model medium, is different from FeSSIF in some aspects. In this medium, HBSS as bicarbonate buffer, was supplemented to 25 mM glucose and 10 mM HEPES. pH was adjusted to 6.5, which refer to the middle of the duodenum[88].

Table1-4. Composition of media to simulate the fed state in the small intestine[66, 75, 84, 88]

Components	FeSSIF	Early	Middle	Late	FeSSIF-V2	$FeSSIF_{mod}$
NaCl [mM]	173	145.2	122.8	51	125.5	137.931
KCl [mM]	-	-	-	-	-	5.333
$CaCl_2$ [mM]	-	-	-	-	-	1.261
$MgCl_2$ [mM]	-	-	-	-	-	0.493
$MgSO_4$ [mM]	-	-	-	-	-	0.407
$NaHCO_3$ [mM]	-	-	-	-	-	4.167
KH_2PO_4 [mM]	29.68	-	-	-	-	0.441
Na_2HPO_4 [mM]	-	-	-	-	-	0.338
HEPES [mM]	-	-	-	-	-	10.0
Glucose [mM]	-	-	-	-	-	25.0
NaOH [mM]	101	52.5	62.3	72	81.65	-
Maleic acid [mM]	-	28.6	44	58.09	55.02	-
Acetic acid [mM]	144	-	-	-	-	-
NaTC [mM]	15	10	7.5	4.5	10	15
Lecithin [mM]	3.75	3	2	0.5	2.0	3.75
Sodium oleate [mM]	-	40	30	0.8	0.8	-
Glyceryl monooleate [mM]	-	6.5	5	1	5	-
pH	5.0	6.5	5.8	5.4	6.5	6.5
Osmolality (mOsm/kg)	635±10	400±10	390±10	390±10	240±10	325.7±0.6

Early, middle and late represent different time frames of the composition of small intestine after food ingestion

1.4.5 Media to simulate the proximal colon condition

Based on the limited knowledge about the condition in large intestine, the medium that simulates this region was according to pH considerations without attention to the potential of food effect. In the colonic environment there are large numbers of bacteria. These bacteria digest foods that are not digested earlier. Major intestinal segment products are carbohydrate and fatty acids. Fotaki *et al.* developed colonic fluid (SCoF) to simulate the composition and physiochemical characteristics of colon fluid according to pH and short chain fatty acid concentration. SCoF has a pH of 5.8 and contains acetate buffer to represent at least one of the typical ions of this part of the GI tract[66, 91].

Table1-5. Composition of media to simulate the proximal colon[66,91]

Components	SCoF
NaOH [mM]	157
Acetic acid [mM]	170
pH	5.8
Osmolality (mOsm/kg)	295
Ionic Strength	0.16

Recently, the content of ascending colon in healthy volunteers under fasting and fed conditions were evaluated. The data showed that free water content, pH, buffer capacity, osmolality, surface tension, short chain fatty acid and bile acid content are important parameters in bioavalibility studies of this region. Based on these data there are some attempts to develop new biorelevant media for colonic fluids[35, 66].

1.5 Model drugs

1.5.1 Fenofibrate

Fenofibrate, 2-(4-(4-chlorobenzoyl) phenoxy)-2-methyl-propanoic acid, 1-methylethylester, is a third generation of fibrate drugs[92]. This drug is a neutral and lipophilic molecule (log P=5.24). It is practically insoluble in water, with aqueous solubility of about 0.3 µg/ml at 37 °C. According to the BCS class, Fenofibrate is a BCS-II drug (low solubility and high permeability)[93-95].

Fenofibrate is used to treat Primary hypercholesterolemia, combined dyslipidemia, remnant hyperlipidemia, endogenous hyperlipidemia and mixed hyperlipidemia (Friedrickson type IIa, IIb, III, IV, and V dyslipidemia, respectively)[96].

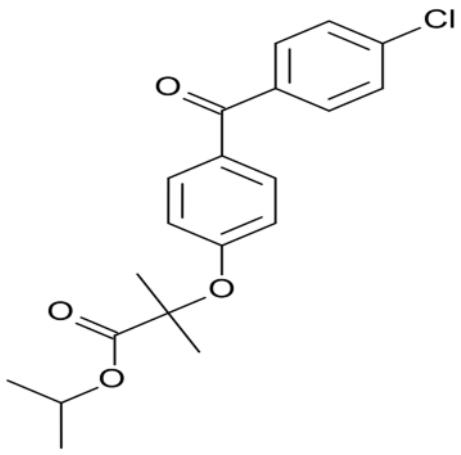

Figure1-1: Structure of Fenofibrate

Fenofibrate is hydrolysed in the intestinal wall and liver by esterases to fenofibric acid (active metabolite) after uptake. Fenofibric acid activates the nuclear transcription factor PPAR-alpha and they heterodimerise with the retinoic acid-X. The dimer binds to peroxisome proliferator-response elements and controls the key genes of lipid metabolism[97-100].

Fenofibrate has low bioavalibility and the absorption of this drug increases with the intake of food in the gastrointestinal tract[101, 102]. Fenofibric acid is 99% bound to plasma proteins. Fenofibrate and fenofibric acid do not undergo oxidative metabolism. Fenofibric acid is primarily conjugated with glucuronic acid and eliminated. Most of the dose is excreted in the urine and only a small fraction is eliminated via feces. This drug is eliminated with a half-life of about 16h[101, 103].

Trying to increase the solubility of Fenofibrate led to different formulations of this drug. The initial dosage of the non-micronized tablet was 300 mg daily, taken with food. The solubility of these micronized formulation increased by reducing the particle size. The initial dosage of this formulation reduced to 200 mg. To have the bioavailability of the Fenofibrate independent of food insoluble drug delivery-microparticle Fenofibrate tablets were developed. In these formulation 160mg of Fenofibrate is bioequivalent to 200 mg of the micronized drug capsule[104]. By reducing the particle size to the nano scale, the bioavailability of the drug increased and dosage reduced to130mg and 145mg. These formulations do not show interaction with food[101, 105].

1.5.2 Danazol

Danazol, 17α -Pregna-2,4-dien-20-yno [2,3-d]-isoxazol-17-ol, an ethisteroneon derivative is an gonadotropin inhibitor[106]. It is a neutral and lipophilic drug (log P=4.53). Danazol is

practically insoluble in water, depicting an aqueous solubility of about 1 µg/ml at 37 °C. According to the BCS class, this drug belong to BCS class II[26, 107, 108].

Danazol has been used in the treatment of endometriosis, fibrocystic breast disease as well as for hereditary angioedema. This drug suppresses ovarian steroid genesis like other progestins. Danazol has also been used to reduce immunoglobulin concentrations and alter the serum complement activity. It displaces testosterone from the sex hormone-binding globulin (SHBG) which results in an increase of the serum testosterone level. Additionally, this drug directly stimulates androgen and progesterone receptors[109-113].

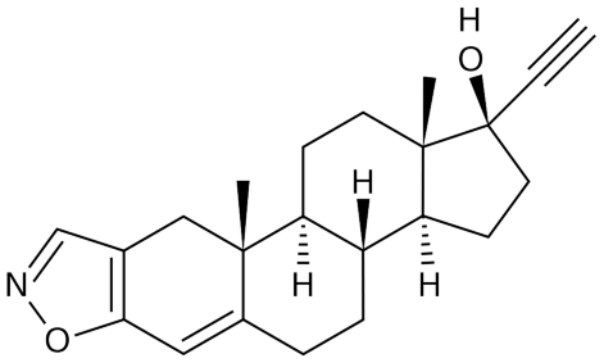

Figure1-2: Structure of Danazol

Danazol has a hepatic metabolism and metabolizes to ethisterone and 17-hydroxymethylethisterone[113]. The half-life of this drug is about 3-6 hours in single dose, and 26 hours in repeating administration. It is eliminated via urine and feces. Bioavailability studies indicate that blood levels do not increase proportionally with the increase of the administered dose. When the dose is doubled, the plasma levels changes only by about 35% to 40%[113].

Danazol capsules for oral administration contain 50 mg, 100 mg, or 200 mg active substance[113].

1.5.3 Carbamazepine

The chemical structure of Carbamazepine is similar to the tricycle antidepressants. This drug is a derivative of iminostilbene with a carbamoyl group at 5 position[114, 115]. Carbamazepine is a neutral, lipophilic compound (log P: 2.45) that can easily pass the blood/brain barrier. It is practically insoluble in water, with aqueous solubility about 170 µg/ml at 25 °C[116, 117].

Carbamazepine binds to sodium and potassium channels and slows down the influx of these ions into neurons. Thus, it has a stabilizing effect on the synaptic transmission. Based on this effect this drug may have anticonvulsant efficacy and can be used in the treatment of

trigeminal neuralgia. Carbamazepine blocks the reuptake of norepinephrine and shows 25% activity of imipramine. This drug is a competitive adenosine antagonist[114, 118-120].
Carbamazepine is indicated for use as an anticonvulsant drug. This drug is also useful for trigeminal neuralgia. Benefit of Carbamazepine in glossopharyngeal neuralgia has been reported[120-122].

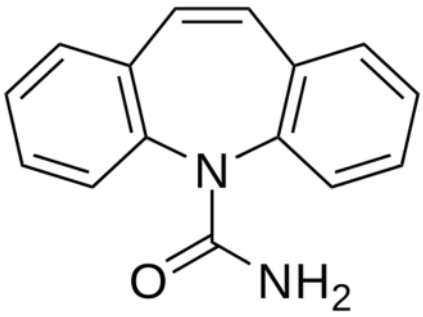

Figure1-3: Structure of Carbamazepine

Carbamazepine has slow but well absorption after oral administration (100% bioavalibility)[113, 120]. The achieving of the peak serum concentration is variable between 2-12h. The half-life of the drug is relatively long (31-35h). The protein binding is approximately 70-80%. The drug can induce its own metabolism by hepatic enzymes. The Metabolic degradation of Carbamazepine starts with an oxidation. At first, the drug changes to a 10, 11-epoxide metabolic that has anticonvulsant activity and then to the 10, 11-dihydroxide. One-third of the 10, 11-dihydroxide will be conjugated as the glucuronide and eliminated and two-third of the elimination occurs in free form. The drug is excreted by the urine and feces[123, 124].
Carbamazepine is available for oral administration as 100 and 200 mg tablets, extended release tablets of 100, 200, and 400 mg, and as a suspension of 100 mg/5 mL)[113, 118].

1.5.4 Griseofulvin

Griseofulvin is a neutral and lipophilic drug (log P=2.18). It is practically insoluble in water, with aqueous solubility about 15–30 µg/ml at 37 °C. According to the BCS class, this drug belongs to the BCS class II drugs[107, 120, 125-127].
Griseofulvin is an antifungal drug that is administered orally for the treatment of ringworm infections of the skin, hair, and nails, namely: tinea corporis, tinea pedis, tinea cruris, tinea barbae, cradle cap or other conditions caused by *Epidermophyton*, *Trichophyton* and *Microsporum* fungi[127-129].

The drug is a fungistatic, binds to tubulin, interfering with microtubule function and inhibiting fungal cell mitosis. Griseofulvin is deposited in the keratin precursor cells and shows a

enhanced affinity for diseased tissue. The drug is tightly bound to the new keratin which becomes highly resistant to fungal invasions[127, 128, 130].

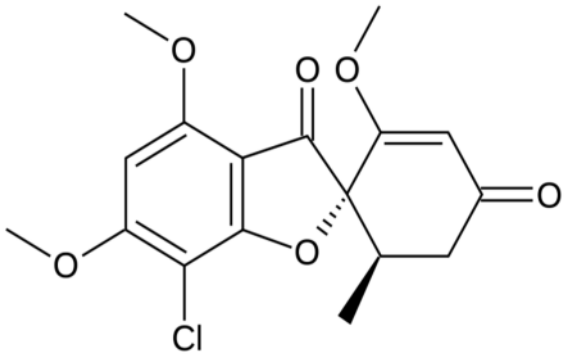

Figure1-4: Structure of Griseofulvin

Griseofulvin is metabolized by the liver to 6-desmethylgriseofulvin and its glucuronide conjugated. Griseofulvin is poorly absorbed from the GI with values ranging from 27 to 72% of an oral dose. Absorption is significantly enhanced by administration with or after a fatty meal[113, 128, 129, 131]. It has a variable elimination half-life in plasma (9 to 21 hours). It is excreted in the urine mostly in the form of metabolites. About one-third of a single dose of griseofulvin is excreted unchanged by the faeces. The efficiency of gastrointestinal absorption of ultramicrocrystalline Griseofulvin is approximately 50% increased as compared to the conventional microsize Griseofulvin[128, 131].

This drug for oral administration (tablet and suspension) contains 125 mg, 250 mg and 500 mg active substance[131].

1.6 Aims of the thesis

The main aim of the thesis was to simulate the second part of the duodenum more closely to the *in vivo* condition to better predict drug absorption by developing a new biorelevant media. Surfactants used in drug formulation were added to the developed biorelevant media to assess their effect.

The specific goals were:

- Investigation of the nanoparticle structure development in the gastro-intestinal model fluid $FaSSIF_{mod6.5}$ from several phospholipids at various water content relevant for oral drug administration.
- Development of new biorelevant media, FeSSIF-C and FaSSIF-C, to mimic the physiological condition. FaSSIF- C was studied in three aspects: biocompatibility, drug solubilizing capacity and structural investigation of the colloidal systems by combined DLS and SANS.
- study the tracing of mixed nanoparticles from drug, surfactants and biorelevant media ($FaSSIF_{mod}$ and FaSSIF-7C) by parallel drug solubilization study and dynamic light scattering DLS.

2. Materials and Methods

The materials and methods of this work are presented in the published text of the cumulative results section. However, the general description of methods used are summarized in this section.

2.1 Solubility study

The solubility of a drug is a key important parameter in biopharmaceutical modeling. Equilibrium solubility is defined as the concentration of a system when chemical compound in the solid state is in equilibrium with a solution of that compound. Traditionally, the equilibrium solubility of the pharmaceutical particles are measured by the shake flask method. In this method an excess amount of the drug is added to the medium and shaken for a predetermined time, usually 24h or longer. After saturation, the fluid and undissolved solid drug are separated by filtration or sedimentation. When using sedimentation (usually with a centrifuge), the first supernatant can be recentrifuged to avoid contamination (double centrifuge method). The amount of the solute contained in the sample is measured by UV, HPLC or the LC-MS method[1, 10].

2.2 Size measurements

2.2.1 Dynamic light scattering (DLS)

DLS is one of the most common methods used to determine the size of particles. This method determines the size according to the Tyndall effect (scattering) and the Brownian motion of the particles in a sample.

In DLS, the characteristic time of fluctuation in the scattered intensity is estimated. This depends on the diffusion coefficient of the particles undergoing Brownian movement. When the laser light hits the moving particle, the light intensity changes depends on the particle size, similar as in X-ray and neutron scattering. Additionally the motion results in a size dependent fluctuation of interferences resulting from the light of several particles. Smaller particles move rapidly and large particles move more slowly. The quantitative data of the fluctuation of light intensity versus time can be calculated by equation 2-1, which is known as autocorrelation function[113, 132].

$$g^2(\tau) = \frac{\langle I(t) * I(t+\tau) \rangle}{\langle I(t) \rangle 2} \qquad \text{(equ.2-1)} \quad \text{Autocorrelation function}$$

scattered intensity at an arbitrary time = $I(t)$

scattered intensity at a delay time $\tau = I(t + \tau)$,

the normalized autocorrelation function of the scattered intensity = $g^2(\tau)$

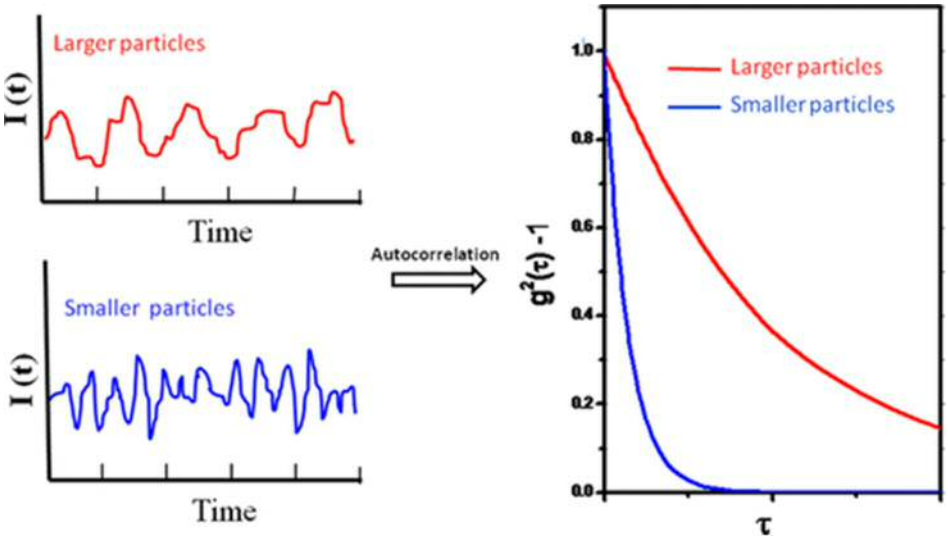

Figure2-1: Schematic representation of the fluctuations in the intensity of scattered light and the corresponding autocorrelation functions from suspensions of different size particles[132].

The correlation time corresponds to the particle diffusion coefficient D. The relation between the size of the particles and its velocity because of Brownian motion is defined by employing Stokes-Einstein equation(eqn. 2-2), which allows us to replace the time scale by a radius scale yielding the intensity scale (raw) particle size distribution function S(r) (PSD_i in the Malvern nomenclature)[132].

$$D = \frac{K_b T}{6\pi\eta r}$$

(equ.2-2) Stokes−Einstein diffusion law

D =diffusion coefficient

K_b = Boltzmann's constant

T = absolute temperature

η = solvent viscosity

r = particle radius

The evaluation of the intensity scaled raw particle size distribution $S(r)$ to mass-weighted (volume) particle size distributions $C_m(r)$ was done according to common scattering laws is depicted in equations 2-3 and 2-4 for massive particles as $C_{m3}(r)$ and for hollow particles of constant membrane span (liposomes) as $C_{m2}(r)$.

$$C_{m3} = \frac{S(r)}{r^3}$$ (equ.2-3) Particle mass distribution $C_{m3}(r)$ for solid particles, micelles

$$C_{m2} = \frac{S(r)}{r^2}$$ (equ.2-4) Particle mass distribution $C_{m2}(r)$ for liposomes

$S(r)$ = Particle size distribution

2.2.2 Small-Angle Neutron Scattering (SANS)

SANS is one of the most powerful techniques that investigates the structure and dynamics of materials on the nanometer scale (1 - 100 nm). Neutron scattering is an excellent technique, but it is an expensive method. In contrast to X-ray small angle scattering (SAXS), it can distinguish components of formulations by D_2O-contrast.

In this technique the beam is elastically scattered by a sample. Detector records the scattered radiation. The scattering profiles is called the scattering vector q (momentum transfer)[133]. This vector is modulus of the resultant between the incoming wave, k_i, and scattered neutron wave, k_s and is calculated from the neutron wavelength λ and the half scattering angle Θ, according to equation below.

$$\vec{q} = \vec{k}_i - \vec{k}_s = \frac{4\pi}{\lambda} \sin \Theta$$

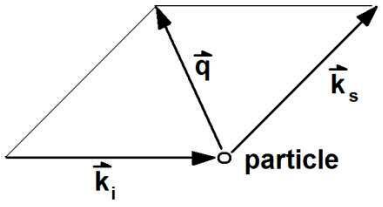

(equ.2-5) Scattering vector, momentum transfer, and graphical equivalent (right)

By the Guinier and Kratky-Porod plots the radius of gyration R_g of the liposomes as well as the bilayer thickness d can be calculated. The radius of gyration R_g is the geometric averaged distance of the scatters (atoms) from the center of the object. In solid sphere samples it is by a factor of $(5/3)^{1/2}$ smaller as the outer particle radius r. The thickness scattering profile $I_d(q)$, membrane thickness d and liposome size s from SANS are evaluated by equations 2-7 to 2-10. r_m is equivalent to membrane radius and R_d is thickness radius[3]:

$$\ln(I(q)) = \ln(I_0) - \frac{Rg2}{3}q^2$$ (equ.2-6) Logarithmic Guinier equation

$$\ln(Id(q)) = \ln(Id_0) - R_d^2 q^2$$ (equ.2-7) Logarithmic Kratky−Porod equation

$$I_d(q) = I(q) * q^2$$ (equ.2-8) Thickness scattering profile $I_d(q)$

$$d = R_d \sqrt{}_{12}$$ (equ.2-9) Membrane thickness *d*

$$S = 2r_m + d \cong 2 R_g + d$$ (equ.2-10) Liposome size *s* from SANS

2.3 Cytotoxicity assay (MTT assay)

The MTT test is a colorimetric assays that is widely used for determination of cytotoxicity and viability of cells. This assay is based on the reduction of the yellow tetrazolium salt, 3-(4,5-dimethylthiazol-2-yl)-2,5-diphenyl tetrazolium bromide (MTT), to a blue colored formazan product by mitochondrial enzymes present only in living, metabolically active cells[134, 135]. The obtained formazan dye is proportional to the number of vital cells. In this work the test was used for toxicity estimation with Caco-2 cells at 1h incubation.

3. Results

The results of this thesis are presented in cumulative form. Each of the result chapters contains one of the four papers. The result chapters are copies of the published manuscript versions. The figures and tables were re-numbered for this thesis by adding the paper-number, i.e. as fig. 3.3-5 for the figure 5 of the third paper (3). This allows the reference in the general discussion (chapter 4).

The results are published in the following peer reviewed publications. The contents were previously discussed in the contributions at international conferences, listed in chapter 6

3.1 "Nanoparticle Structure Development in the Gastro-Intestinal Model Fluid FaSSIF$_{mod6.5}$ from several Phospholipids at various Water Content relevant for oral Drug Administration"

Pooneh Khoshakhlagh, Raphael Johnson, Thomas Nawroth, Peter Langguth, Lars Schmueser, Nadja Hellmann, Heinz Decker, Noemi Kinga Szekely. Eur. J. Lipid Sci. Technol. **2014**, 116, 1155–1166.

3.2 "Fasted-State Simulated Intestinal Fluid "FaSSIF-C", a Cholesterol containing Intestinal Model Medium for *in vitro* Drug Delivery Development"

Pooneh Khoshakhlagh, Raphael Johnson, Peter Langguth, Thomas Nawroth, Lars Schmuese, Nadja Hellmann, Heinz Decker, Noemi Kinga Szekely. J. Pharmaceutical Sciences **2015**, 104 (7), 2213–24.

3.3 "Bifurcation of the Nanoparticle-Excipient mediated Drug Solubilization Pathways of oral Formulations in the Gastro-Intestinal model Fluid FaSSIF$_{mod6.5}$"

Thomas Nawroth, Pooneh Khoshakhlagh, Philipp Buch, Raphael Johnson, Peter Langguth, Lars Schmueser, Nadja Hellmann, Heinz Decker, Noemi Kinga Szekely. International Journal of Pharmaceutics, submitted.

3.4 "Excipient effect on the colloidal structure and drug solubility gap in cholesterol containing biorelevant intestinal medium (FaSSIF-7C) with Fenofibrate"

Pooneh Khoshakhlagh, Philipp Buch, Raphael Johnson, Peter Langguth, Thomas Nawroth, Lars Schmueser, Nadja Hellmann, Heinz Decker, Noemi Kinga Szekely. J. Pharmaceutical Sciences, submitted.

3.1. Nanoparticle Structure in FaSSIF$_{mod6.5}$

"**Nanoparticle Structure Development in the Gastro-Intestinal Model Fluid FaSSIF$_{mod6.5}$ from several Phospholipids at various Water Content relevant for oral Drug Administration**"

Pooneh Khoshakhlagh, Raphael Johnson, Thomas Nawroth, Peter Langguth, Lars Schmuese, Nadja Hellmann, Heinz Decker, Noemi Kinga Szekely

Eur. J. Lipid Sci. Technol. 2014, 116 (9), 1155–1166

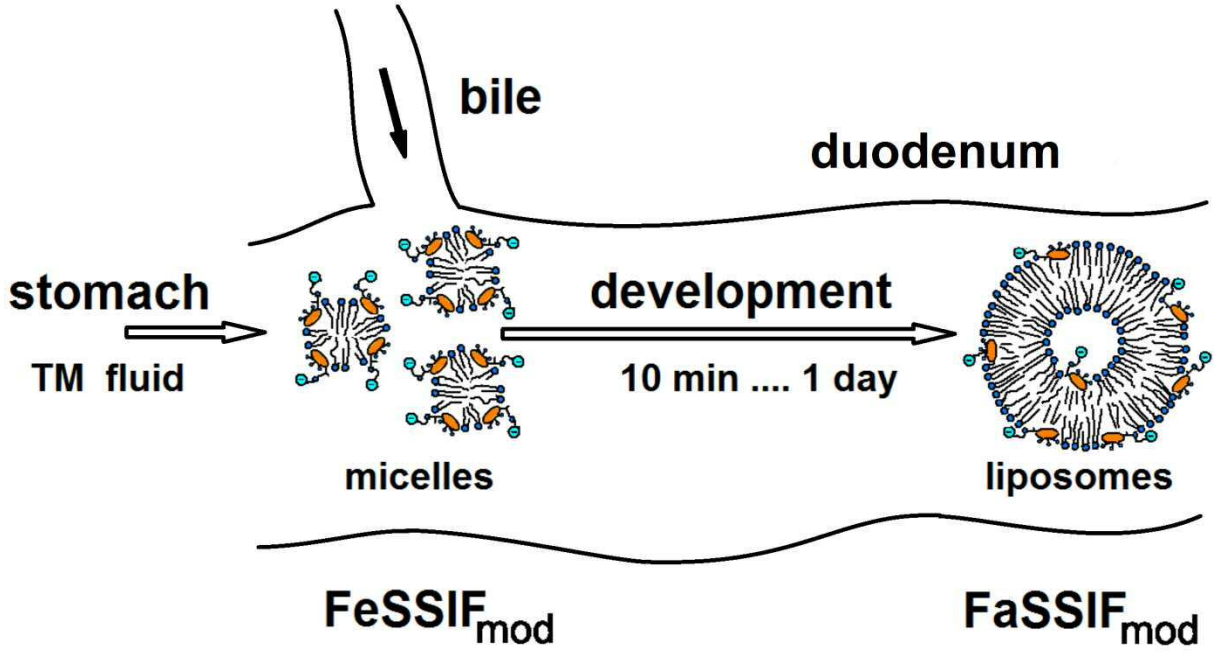

Formation and decay of liposomes and micelles from bile in the duodenum was studied, due to their role as an intermediate for resolution and uptake of hydrophobic drugs (BCS II, IV). The physiological conditions studied may vary individually and due to diseases.

"Nanoparticle Structure Development in the Gastro-Intestinal Model Fluid FaSSIF$_{mod6.5}$ from several Phospholipids at various Water Content relevant for oral Drug Administration"

Pooneh Khoshakhlagh, Raphael Johnson, Thomas Nawroth, Peter Langguth, Lars Schmuese, Nadja Hellmann, Heinz Decker, Noemi Kinga Szekely

Eur. J. Lipid Sci. Technol. 2014, 116 (9), 1155–1166

Running title: GI-model fluid structure kinetics

3.1.1. Abstract

The characteristics of intestinal model fluids were investigated at conditions, which simulate the passage from the middle to the end of the duodenum. The formation and decay of liposomes and micelles in model bile fluids were studied, because of their role as an intermediate host for the resolution and uptake of hydrophobic drugs (BCS classes II, IV). The conditions, which may influence the formation of these nanoparticulate intermediates were studied, i.e. the lipid composition of the bile, the preparation method, the time of the passage through the modelled duodenum segment and the concentration, which results from the variable dilution of the bile by mixing with the transfer medium representing the fluid arriving from the stomach. The variation of the lecithin entity revealed an equivalence of Egg–lecithin of a high purity (99%) with its main component 1-palmitoyl-2-oleoyl-sn-glycero-3-phosphocholine POPC, while 1,2-di-oleoyl-sn-glycero-3-phosphocholine DOPC resulted in a slight delay of the micelle-liposome conversion. The FeSSIF preparation method was best with the sequential-film method, while the bile-film method yielded comparable results; the shake method showed a slightly different kinetics of the nanoparticle conversion. The time and concentration dependence of the formation and decay of lipidic nanoparticles indicates that these strongly depend on the passage time (speed) and bile dilution rate. The corresponding physiological conditions at healthy persons may vary *in vivo* individually and due to diseases. The studied conditions cover typical physiological conditions, which should be taken into consideration in the exploration of *in vitro* tests of formulations of hydrophobic drugs.

Keywords: Biorelevant media, kinetics, FaSSIF, DLS, SANS

Abbreviations:

BCS, biopharmaceutics classification system
DLS, dynamic light scattering
DOPC, 1,2-di-oleoyl-sn-glycero-3-phosphocholine
Egg-PC, Egg-phosphatidylcholine
FeSSIF, fed state simulated intestinal fluid
FaSSIF, fasted state simulated intestinal fluid
FeSSIF$_{mod}$, fed state simulated intestinal fluid, bicarbonate-HEPES buffered
FaSSIF$_{mod}$, fasted state simulated intestinal fluid, bicarbonate-HEPES buffered
HBSS, Hank's buffered salt solution
HEPES, 4-(2-hydroxyethyl)-1-piperazineethanesulfonic acid
NP, nanoparticle
POPC, 1-palmitoyl-2-oleoyl-sn-glycero-3-phosphocholine
PSDi, particle size distribution by scattering intensity (DLS raw data)
PSDv, particle size distribution, particle volume scaled
SANS, small angle neutron scattering
Soy-PC, soybean phosphatidylcholine
TC, taurocholate
TM, transport medium

3.1.2. Introduction

Intestinal model fluids are a tool for the *in vitro* investigation of drug formulations for oral administration. *In vitro* solubility and permeability studies at nearly physiological conditions are the key for an improvement of the bioavailability of drugs, which is difficult for hydrophobic materials, i.e. drugs of the classes II and IV of the Biopharmaceutics Classification System BCS[136]. *In vivo* the chyme containing the drug from stomach emptying undergoes in the first half of the duodenum a pH shift. After subsequent addition of bile and pancreatic juice[4, 10] it depicts a slightly acidic pH (6.5), while the concentration varies depending on the composition of the meal and fluid intake. In parallel intestinal nanoparticles (micelles and liposomes) develop from the bile components, food and drug in a dynamic process. After passing the duodenum, bile acids are reabsorbed in the ileum by a bile acid transporter[10, 16, 26, 36], while the lecithin component is cleaved by lipases and later absorbed.
In vitro biorelevant media such as fasted state simulated intestinal fluid (FaSSIF) and fed state simulated intestinal fluid (FeSSIF) are established tools to predict the absorption of several drugs *in vivo* [67, 69]. These media simulate some aspects like pH, osmolality, surface tension and solubilization capacity of drugs. The composition contains lecithin and taurocholic acid (TC) to mimic bile micelles and liposomes in the small intestine[10, 137,16]. Bile micelles and liposomes have an important role in increasing the solubility and dissolution rate of hydrophobic drugs[10, 138] . In the last decade, the biorelevant media have been improved towards a higher similarity to the body condition[16]. Kataoka et al. suggested new intestinal fluids (FeSSIF$_{mod}$, FaSSIF $_{mod}$) based on the bicarbonate buffer cell culture medium HBSS and improvement of the buffer capacity by addition of HEPES. Partly the pH was adjusted to 6.5[88], as in the duodenum centre. For a shorter style, we name in this paper the pH adjusted media FeSSIF$_{mod}$ and FaSSIF$_{mod}$ as a synonym of FeSSIF$_{mod6.5}$ and FaSSIF$_{mod6.5}$. Biorelevant media can be prepared by several methods[139, 140], which were compared in this study. In addition, the media have been produced from different sources and grades of lecithin and sodium taurocholate. *In vivo*, a mixture of bile salts is more relevant than pure sodium

taurocholate [89]. Prior studies assumed that FaSSIF, which is prepared by a 1:5 dilution of FeSSIF, represents the duodenal conditions. However, this composition may vary depending on the amount of fluid intake, and upon meals. Thus this parameter was varied in this study. Furthermore we investigated the influence of three different lecithins, [1-palmitoyl-*2*-oleoyl-sn-glycero-3-phosphocholine (POPC), 1,2-di-oleoyl-sn-glycero-3-phosphocholine (DOPC), and Egg-phosphatidylcholine (Egg-PC)] on the size and development of nanoparticles in biorelevant media. The structure of lipidic nanoparticles in solution can be estimated by dynamic light scattering DLS and small angle scattering, with best contrast using neutrons, i.e. neutron small angle scattering SANS. In this study we applied DLS for multiple long term kinetic studies, and SANS for precise reference investigation of a few samples.

3.1.3. Material and Methods

3.1.3.1. Material

1-Palmitoyl-2-oleoyl-sn-glycero-3-phosphocholine (POPC, ≥99%), 1,2-di-oleoyl-sn-glycero-3-phosphocholine (DOPC, ≥99%), egg *L-a*-lecithin 3-sn-phosphatidylcholin (Egg-PC, ≥99%) *and* sodium taurocholate hydrate (NaTC, ≥97%) were purchased from Sigma-Aldrich (Steinheim, Germany). HEPES was purchased from Merck. Glucose and chloroform (HPLC grade) were purchased from Carl Roth. HBSS (Gibco14025) was purchased from Life Technologies (Paisley, UK).

3.1.3.2. Preparation of Transport medium

The transport medium (TM) was cell compatible buffer HBSS containing 4.167 mM $NaCO_3$ and 0.779 phosphate, supplemented with 19.45 mM glucose (final 25 mM) and 10 mM HEPES. The pH was adjusted to 6.5 with 0.1 M HCl. Finally the medium was sterile filtered (0.2 μm).

3.1.3.3. Preparation of FeSSIF$_{mod}$

3.1.3.3.1 shake method

Into three separate tubes, 1.5 ml suspensions of 3.75mM of Egg-PC, POPC and DOPC, each with 15mM Na-TC in TM were prepared. The suspensions were stirred for about 15 minute at 37° C, and then agitated in an orbital shaker at 100 rpm overnight at 37°C.

3.1.3.3.2 bile-film method

For each of the lipids, Egg-PC, POPC and DOPC, the lipid and NaTC were deposited in glass tubes and resolved with methanol and chloroform (1:5 v/v). The solvent was removed in a vacuum with a rotational evaporator model R-3 (Büchi, Flawil, Switzerland). After drying of the film in a vacuum, 1.5 ml TM was added to each tube to obtain 3.75 mM of each lipid and 15 mM of NaTC. The tubes were vortexed at room temperature for 5 minutes at 30 Hz with a Bioblock TopMix Vortexer (Fisher Scientific Inc., Waltham, MA, USA). The solutions (1.5 ml) were kept overnight at 37^0C for equilibration yielding FeSSIF$_{mod}$.

3.1.3.3.3 sequential -film method

A stock solution of Egg-PC in chloroform (100mg/ml) was prepared. A known amount of the stock solution (3.75mM in the final volume) was administered into a glass tube with a gas tight syringe (Hamilton). The solvent was removed with a rotational evaporator as with the bile-film method. 1.5 ml of 15 mM of sodium taurocholate in transport medium was added to

the tube. The tube was vortexed for 5 minutes at 30 Hz with a Bioblock TopMix Vortexer (Fisher Scientific Inc., Waltham, MA, USA). The solution was kept overnight at 37^{0}C for equilibration yielding FeSSIF$_{mod}$.

3.1.3.4. Preparation of FaSSIF$_{mod}$ in different dilution

To prepare the final solutions, FaSSIF$_{mod}$, different dilutions of FeSSIF$_{mod}$ (1:3, 1:4,1:5 ,1:7, 1:10 = FeSSIF:TM) from the methods were prepared manually in a short time (< 2 s), incubated unstirred at 37°C, and analyzed for up to two days. In this paper all dilutions of FeSSIF$_{mod}$ are called FaSSIF$_{mod}$, independent of the dilution rate.

3.1.3.5. Particle size estimation by Dynamic Light Scattering DLS

The particle size distributions were estimated by dynamic light scattering DLS using a Zetasizer Nano-ZS device, Malvern, Worcestershire, UK. The raw size distributions (by scattered light intensity; PSDi) were evaluated yielding volume contributions of micelles and liposomes as done in our previous investigation [3]: For a component analysis (fig.3.1-3 and 3.1-5 to 3.1-8) the raw intensity data were exported as text file with the Zetasizer Software V6.2, and scaled in Origin^{tm} 6.0, Northampton, MA, US after completing the radius values (the procedure and an example is shown in www.mpsd.de/DLS_dataexport_Malvern.html with the template "DLS_Malvern_d-template.txt"). Particles smaller than 20 nm were identified by size as micelles (massive), larger as liposomes[3]. The raw intensity data were scaled to particle volume contributions PSDv for micelles as for massive particles as rough estimate by $1/r^3$ yielding the volume (~ mass) contribution using the Zetasizer Software V6.2 (Malvern Instruments Ltd.), for liposomes the scaling by $1/r^2$ was done with Origin^{tm}.

3.1.3.6. Particle structure estimation by Neutron small angle scattering SANS

The precise structure estimation of the nanoparticles in the intestinal model fluid in a regime of <100 nm particle size was done with neutron small scattering SANS. The experiments were done with the Instrument KWS-2 at the FRM-II reactor using a cold neutron source beam at the Heinz Maier-Leibnitz Zentrum MLZ, Munich-Garching. The samples were prepared with 71 % D_2O-buffer for improving the contrast, but avoiding possible aggregation problems (at high D_2O content). The scattering experiments were done with neutrons of 0.453 nm wavelength at a sample-detector distance of 7.68 m. The momentum transfer q was estimated as $q = (4 * \pi / \lambda) \sin(\theta)$, where λ is the wavelength of the radiation and θ is half of the scattering angle. After normalization to beam intensity (monitor and subtraction of empty cuvette and buffer scattering), the scattering profiles were evaluated according to the Guinier approximation for small momentum transfer q[141] , and by Kratky-Porod plot of the layer scaled intensity $I_d = I(q)*q^2$ yielding the span of the liposome membranes[142, 143]. The size s_l of the liposomes was calculated from the radius of gyration R_g and the layer span d_l of phospholipid membranes as $s_l = 2 * R_g + d_l$ [142]. The size of micelles s_m was estimated as $s_m = 2 * R_g*\sqrt{(5/3)}$ assuming nearly spherical particles. The micelle contribution was calculated as contribution as $a_m = 100\% *c_2 / (c_1 + c_2)$, where the liposome contribution was $c_{01} = I_{01}/(R_{g1}^2*R_d)$, the micelle contribution $c_{02} = I_{02}/Rg_2^3$. The final evaluation and plots were done with Origin^{tm} 6.0, using the formalisms presented earlier[3].

3.1.4 Results

The gastrointestinal model fluids were prepared with the procedures shown in fig. 3.1-1. The model fluid for the fed state FeSSIF$_{mod}$ were prepared by three methods: (i) in the "shake method" solid lipid, bile acid and buffer were collected in a flask, which was subsequently stirred and shaken overnight; (ii) in the "bile-film method" lipid and bile acid were resolved in methanol - chloroform (1:5), dried with a rotational evaporator and subsequently resolved in TM by vortexing and incubation at 37°C; and (iii) in the "sequential- film method" first a film of pure lipid was prepared by resolving in chloroform, removal of the solvent with a rotational evaporator and vacuum drying. Then the lipid was suspended by vortexing with a bile acid solution in TM and subsequent incubation overnight at 37°C. The bile-film method revealed homogenous suspensions, while the preparation of the mixed bile-lipid film was difficult (foam, spilling). The optimal sequential-film method yielded homogenous suspensions after fast lipid film preparation. The FeSSIF$_{mod}$ preparation by the film methods was nearly complete even after 2 h. For comparison all media were incubated the same way.
The model fluid for the FaSSIF$_{mod}$ was in all cases prepared from the FeSSIF$_{mod}$ by manual dilution with transport medium in a relation of 1:3 to 1:10, as reported below. The formation of liposomes from the micelles after dilution of FeSSIF to FaSSIF was observed up to two days by two methods: dynamic light scattering DLS as laboratory method revealed the nanostructure composition at moderate resolution at various sample compositions in a size range of 2 nm to 5 µm (signal filter limit of the Malvern DLS). Neutron small angle scattering SANS was used for a few samples for a precise structure analysis in a limited size range (<100 nm; detector distance limit of the KWS-2 instrument).

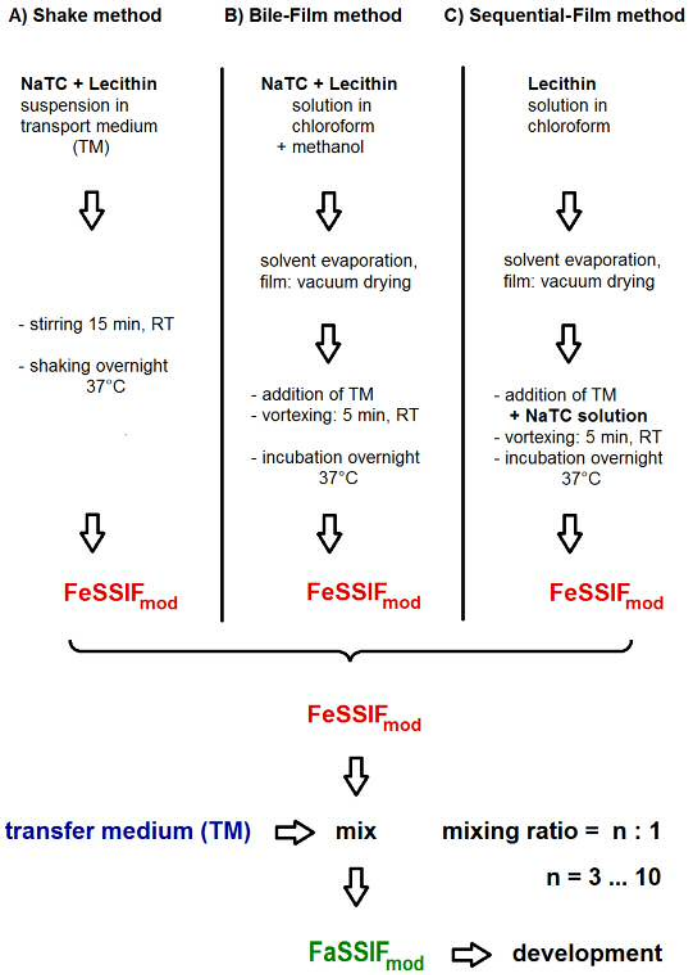

Fig. 3.1-1: Sketch of the preparation methods of the gastro-intestinal model fluids FeSSIF$_{mod}$ and FaSSIF$_{mod}$: Concentrated FeSSIF$_{mod}$ is obtained by the A) shake method, B) bile-film method, or C) sequential-film method. The final model FaSSIF$_{mod}$ develops in time after dilution of FeSSIF$_{mod}$ with transfer medium TM.

3.1.4.1 Static particle size estimation with DLS and SANS

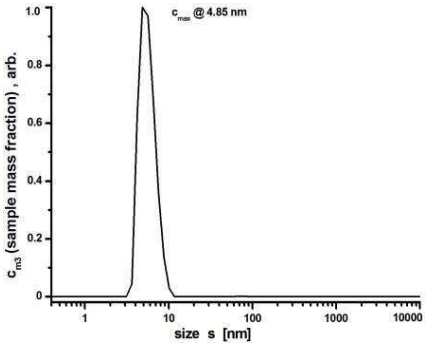

Fig. 3.1-2: The structure investigation of gastro-intestinal model fluid FeSSIF$_{mod}$ by DLS indicates small nanoparticles of 4.85 nm size, which are assigned to lipid-bile micelles.

The result of the DLS structure analysis of FeSSIF$_{mod}$, prepared by the shake method is shown in fig. 3.1-2. The raw data (scattering intensity related data PSDi) were scaled to mass (volume) related data c_{m3} by division by the third exponential of the radius^3, as usual for massive particles. By the size of s_{m1} = 4.85 nm, the nanoparticles in FeSSIF$_{mod}$ were identified as small micelles.

The structure investigation of intestinal model fluid FaSSIF$_{mod}$ from Egg-PC after 1 h development from FeSSIF$_{mod}$ by DLS and neutron small angle scattering SANS is shown in fig. 3.1-3 and 3.1-4. The DLS study (fig. 3.1-3A-C) yielded an overview. The representation of the data as A) intensity raw data PSDi, and particle size distribution PSDv as B) mass (volume) related particle size distribution c_{m3} (massive particle assumption); C) mass (volume) related hollow particle size distribution c_{m2} showed one main component, where the apparent particle size with a liposome particle assumption yielded s_l = 37.8 nm.

The detailed nanoparticle structure of 1h old FaSSIF$_{mod}$ in 71% D_2O-TM estimated by SANS is shown in fig. 3.1-4 (i) as scattering profile, (ii) as size analysis by a Guinier plot, and (iii) as layer analysis by a Kratky-Porod plot. Fig. 3.1-4B indicated a mixture of two particle populations with a major component R_{g1} = 13.65 ± 0.11 nm, I_{o1} = 2.103 ± 0.31, and a minor component, due to the zero angle scattering ratio, of R_{g2} = 5.96 ± 1.56 nm, I_{o2} = 0.4023 ± 0.02, which were identified as liposomes and large micelles by size. The layer analysis by the Kratky-Porod plot in fig. 3.1-4C revealed a membrane span of d_l = 5.51 ± 0.44 nm from a thickness radius R_d = 1.561 ± 0.126 nm. The high error was caused by the overlap at the right side of (C) with the second Guinier region of (B). The liposome size s_l was calculated[142] as $s_l = 2 * R_{g1} + d_l$ = 32.8 ± 0.66 nm. The size of the large micelles was calculated as $s_{m2} = 2*R_{g2}*\sqrt{(5/3)}$ = 15.4 ± 4.0 nm, the contribution as $a_m = 100\% * c_2 / (c_1 + c_2) = \sim 21\%$ (w/w).

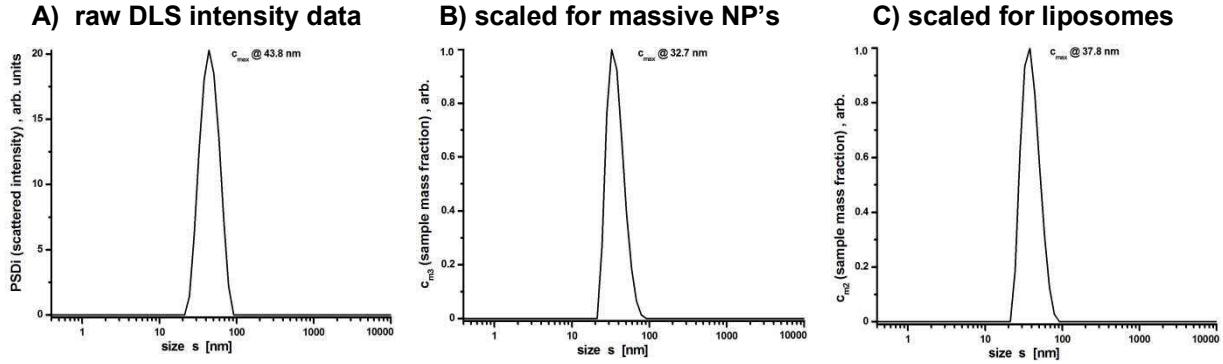

Fig.3.1-3: Structure investigation of the intestinal model fluid FaSSIF$_{mod}$ from Egg-PC after 1 h development from FeSSIF$_{mod}$ by dynamic light scattering DLS, represented by: **A)** scattering intensity related particle size distribution PSDi (raw data), and volume (mass) related particle size distributions PSDv as **B)** volume related particle size distribution c_{m3} (massive particle assumption); **C)** volume related size distribution c_{m2} for hollow particles with a constant membrane span d_l, yielding s = 37.8 nm.

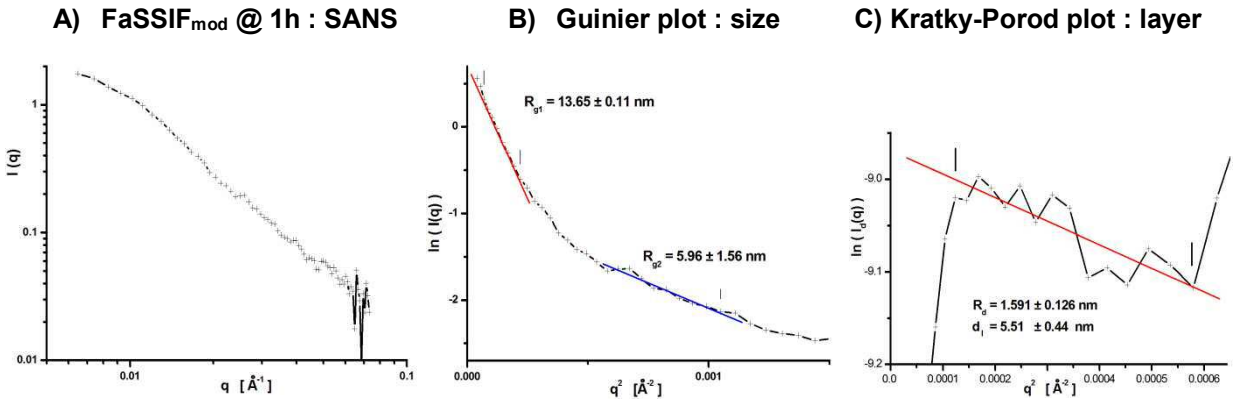

Fig.3.1-4: The detailed nanoparticle structure of 1h old FaSSIF$_{mod}$ estimated by neutron small angle scattering SANS is shown in **A)** as scattering profile, **B)** as size analysis by the Guinier plot indicating a mixture of at least two particle populations (liposomes R_{g1} = 13.65 nm, and micelles, R_{g2} = 5.96 nm), and **C)** shell span estimation by the Kratky-Porod plot indicating the presence of membranes (d_l = 5.5 nm). The Kratky-Porod range in (C) is the curved region between the two linear Guinier regions in (B).

3.1.4.2 Time resolved analysis of particle size in FaSSIF$_{mod}$ at digestion conditions

3.1.4.2.1 Structure development in FeSSIF$_{mod}$, prepared from DOPC

The structure development of particles in intestinal model media containing DOPC during two days after dilution of FeSSIF$_{mod}$ prepared by the shake method and the bile-film method at various mixing ratios is shown in figure 3.1-5. The predominant particles in all dilutions in the first two minutes were micelles (particles < 20 nm), depicting an average size between 12 nm to 17 nm (from mass/volume scaled DLS data c_{m3}). During temporal development (fig. 3.1-5A,B), there was in case of the shake method (A) a general increase in the particle size indicating the formation of liposomes after ≥10 min at all dilutions greater than 1:3. In case of the bile-film method (B) a temporal liposome formation occurred in the 1:3 sample in a time range of 10 to 60 min. Large liposomes (particles > 40 nm) appeared with the shake method at 1:4 and 1:5 dilutions after ≥ 30 minutes, with the bile-film method at 1:4 dilutions after ≥ 30 minutes, both with ongoing increase up to one day. The increase of the particle size with time was small with the shake method in dilutions 1:3, 1:7 and 1:10, and with the bile-film method in the dilution 1:10. The dependence of the particle size on the dilution factor appeared at least bi-phasic. In the 1:5 dilution sample the particle size increased with the shake method to 35nm (in 1 h) and 41nm (24h), with the bile-film method to 30 nm (in 1 h) and 38 nm (24h). The cut profiles with DOPC showed at 1h development (fig. 3.1-5C,D) with both methods (duodenal passage in healthy persons) a plateau. At 1 day development (pharma-lab standard, maximal time in disease) (fig. 3.1-5E,F) both methods depicted a peak in the nanoparticle size at a FaSSIF$_{mod}$ dilution rate of 1:4.

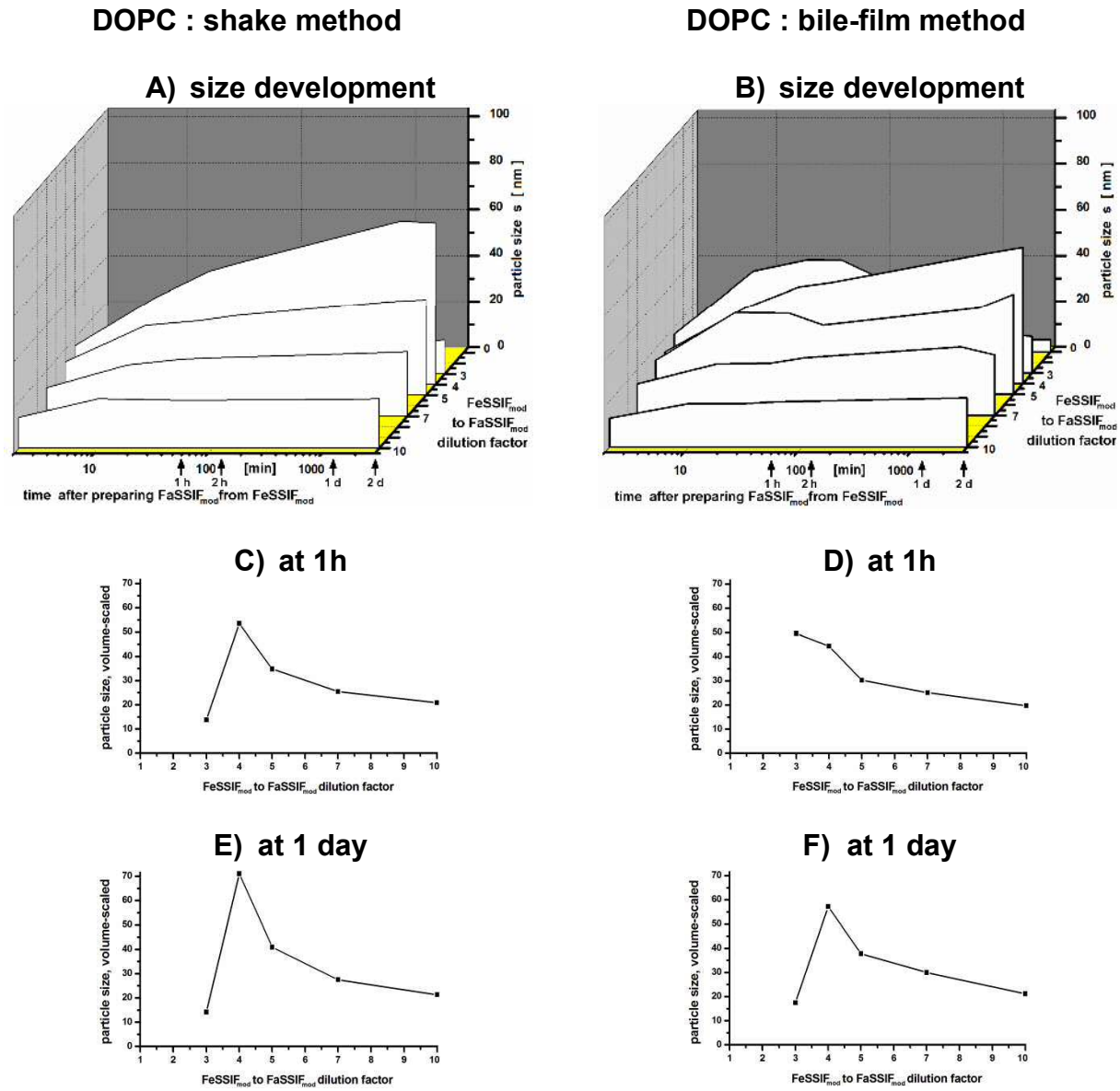

Fig.3.1-5: Nanoparticle structure development in DOPC, **left:** prepared by the shake method, and **right:** by the bile-film method, during two days after dilution of FeSSIF$_{mod}$ at various mixing ratios, i.e. water consumption upon drug administration: **A,B)** 3D-plot of development in time and dilution rate; **C,D)** cut at 1 h (duodenal passage time in healthy persons); **E,F)** cut at 1d (delayed digestion, lab standard).

3.1.4.2.2 Structure development in FeSSIF$_{mod}$, prepared from POPC

The structure development of particles in intestinal model media containing POPC during two days after dilution of FeSSIF$_{mod}$ prepared by the shake method and the bile-film method at various mixing ratios is shown in figure 3.1-6. The predominant particles in all dilutions in the first two minutes were micelles (particles < 20 nm), depicting an average size between 10 nm to 20 nm with the shake method and 12 nm to 22 nm with the bile-film method (mass/volume scaled DLS data c_{m3}). During temporal development (fig. 3.1-6A,B), there was a general increase in the particle size indicating the formation of liposomes after ≥10 min at all dilutions greater than 1:3. Large liposomes (particles > 40 nm) appeared at a dilution of 1:5 after ≥ 30 minutes, with ongoing increase up to one day, and at 1:7 dilution at two days with the bile-film method.

With the shake method, in the 1:4 dilution a short particle size peak (39 nm) developed at 30 min, with subsequent decrease to 20 nm (60 min – 2d), while at 1:3 dilution a short peak of d=28 nm appeared at 60 min and the increase of the particle size with time in dilutions 1:3 and 1:10 were small. With the bile-film method the increase of the particle size with time in dilution 1:10 was limited to 33 nm after one day.
The dependence of the particle size on the dilution factor appeared bi-phasic. In the 1:5 dilution the particle size increased to 77 nm (in 1 h) and 101 nm (24h) with the shake method, and 64 nm (in 1 h) and 95 nm (24h) with the bile-film method. The cut profiles at 1h development (duodenal passage in healthy persons) (fig. 3.1-6C,D) and at 1 day development (pharma-lab standard, maximal time in disease) (fig. 3.1-6E,F) revealed with POPC a peak in the nanoparticle size at a FaSSIF$_{mod}$ dilution rate of 1:5.

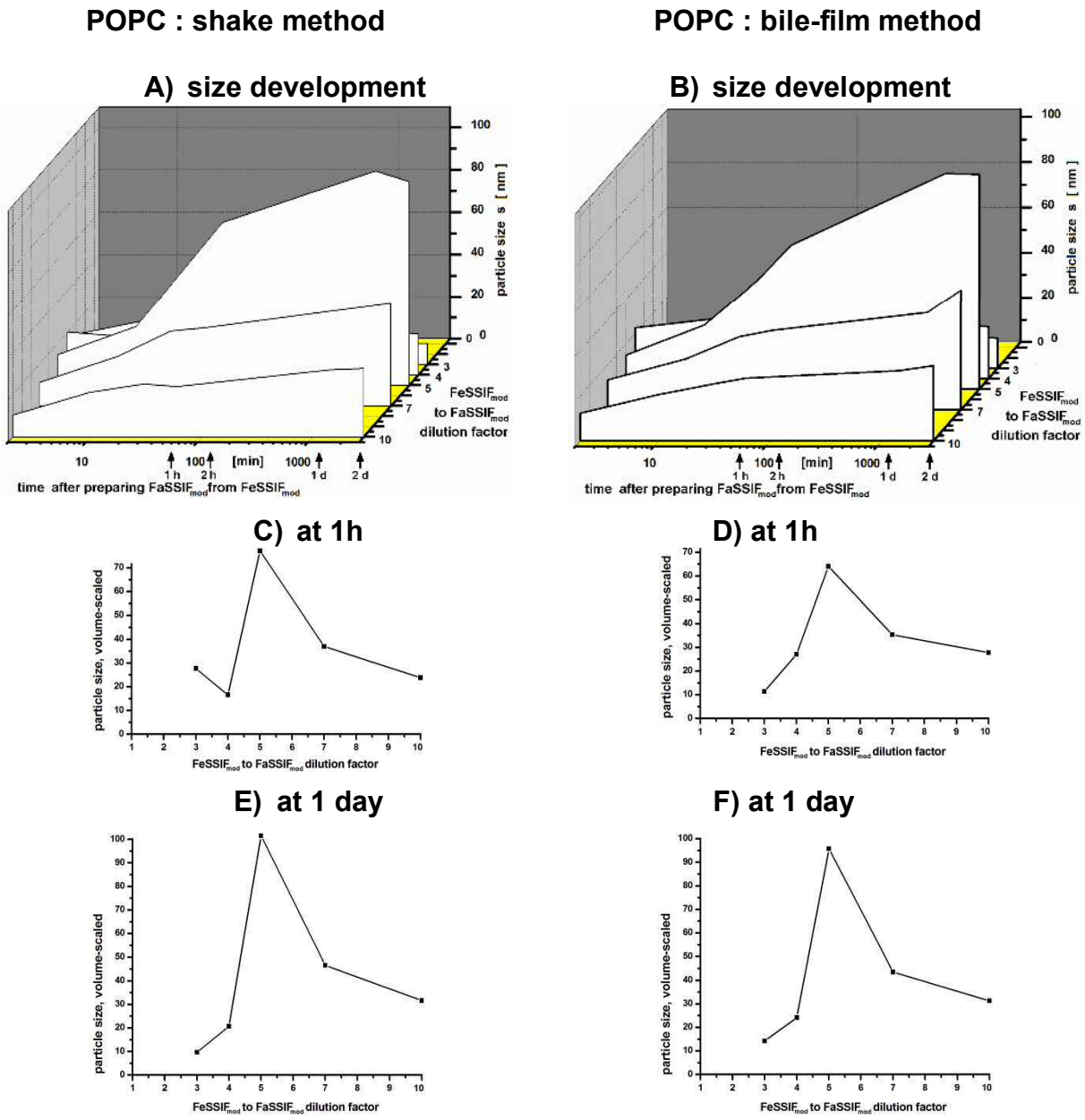

Fig.3.1-6: Nanoparticle structure development in POPC, **left:** prepared by the shake method, and **right:** by the bile-film method, during two days after dilution of FeSSIF$_{mod}$ at various mixing ratios, i.e. water consumption upon drug administration: **A,B)** 3D-plot of development in time and dilution rate; **C,D)** cut at 1 h (duodenal passage time in healthy persons); **E,F)** cut at 1d (delayed digestion, lab standard).

3.1.4.2.3 Structure development in FeSSIF$_{mod}$, prepared from Egg-PC

The structure development of particles in intestinal model media containing Egg-PC during two days after dilution of FeSSIF$_{mod}$ prepared by the shake method and the bile-film method at various mixing ratios is shown in figure 3.1-7. The predominant particles in all dilutions in the first two minutes were micelles (particles < 20 nm), depicting an average size between 14 nm to 20 nm with the shake method, and 10 nm to 19 nm with the bile-film method (mass/volume scaled DLS data c_{m3}).
During temporal development (fig. 3.1-7A,B), there was a general increase in the particle size indicating the formation of liposomes after ≥ 10 min at all dilutions greater than 1:3. Large liposomes (particles > 40 nm) appeared at a dilution of 1:4 after ≥ 10 minutes, with ongoing

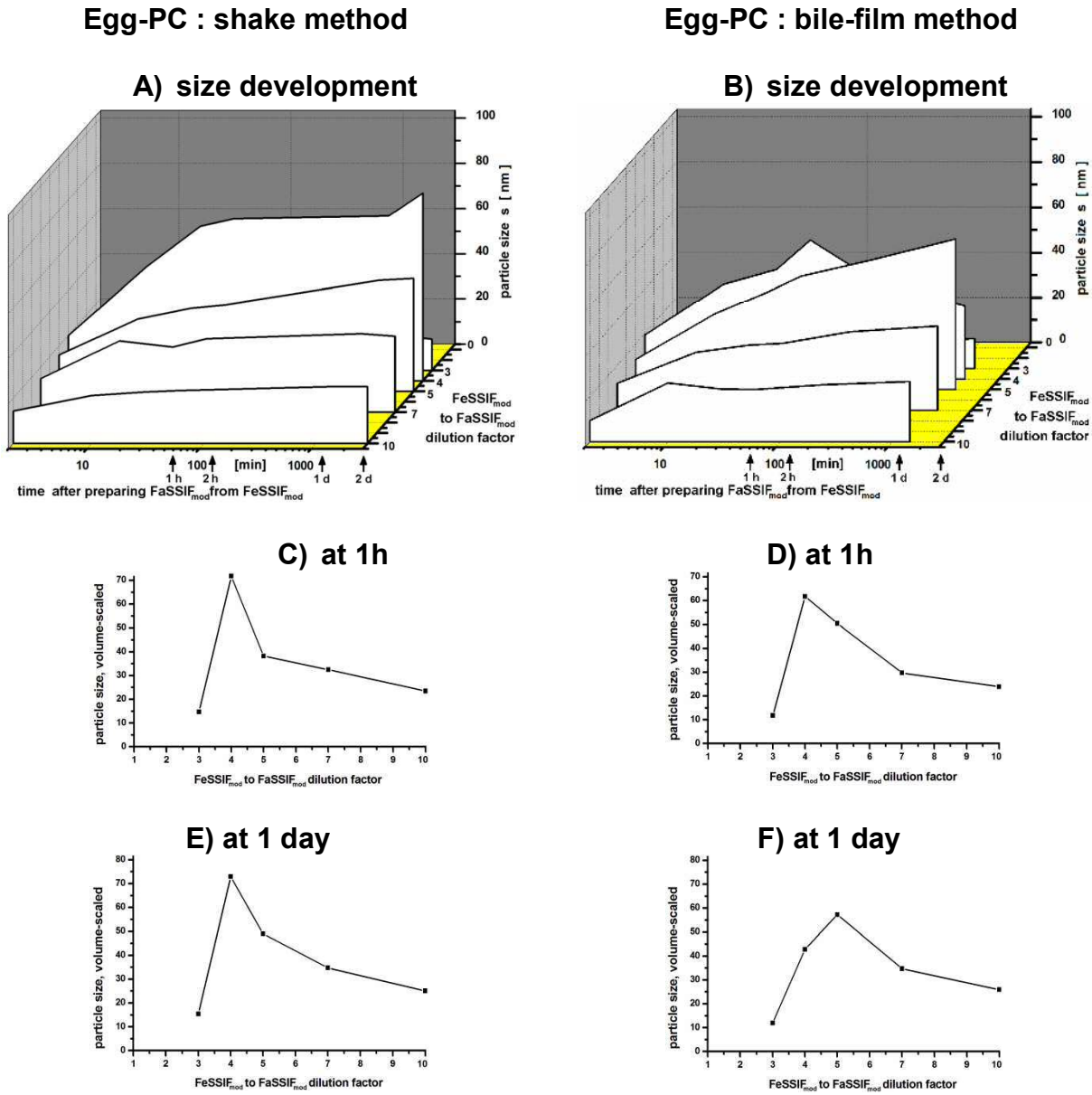

Fig.3.1-7: Nanoparticle structure development in Egg-PC, **left:** prepared by the shake method, and **right:** by the bile-film method, during two days after dilution of FeSSIF$_{mod}$ at various mixing ratios, i.e. water consumption upon drug administration: **A,B)** 3D-plot of development in time and dilution rate; **C,D)** cut at 1 h (duodenal passage time in healthy persons); **E,F)** cut at 1d (delayed digestion, lab standard).

increase up to one hour, followed by a plateau upon one day. In the 1:5 diluted sample an ongoing increase in the particle size occurred during one day with the shake method (A), while particle sizes of 38nm (1 h) and 48nm (24h) occurred. The particle size in the 1:7 and 1:10 diluted samples was stable after 10 minutes. With the bile-film method (B) the size increase lasted two days, while particle sizes of 50nm (1 h) and 66nm (24h) occurred. The dependence of the particle size on the dilution factor appeared to be at least bi-phasic for all samples.

The cut profiles at 1h development (duodenal passage in healthy persons) (fig. 3.1-7C,D) revealed with Egg-PC and both methods a peak in the nanoparticle size at a FaSSIF$_{mod}$ dilution rate of 1:4. At 1 day development (pharma-lab standard, maximal time in disease) (fig. 3.1-7E,F) the shake method resulted in a size peak at a dilution rate of 1:4,while with the bile-film method (fig. 3.1-7F) it showed a peak at a FaSSIF$_{mod}$ dilution rate of 1:5.

The particle structure development in intestinal model media containing Egg-PC prepared by the sequential-film method at various mixing ratios after dilution of FeSSIF$_{mod}$ in figure 8 resembled that of the bile-film method (fig. 3.1-7B). The predominant particles in all dilutions in the first two minutes were micelles (particles < 20 nm), depicting an average size between 9 nm to 26 nm (mass/volume scaled DLS data c_{m3}), with the exceptions of 29 nm at 1:4 dilution (t>2 min. and 26 nm at 1:5). During temporal development (fig. 3.1-8A), there was a general increase in the particle size indicating the formation of liposomes after ≥ 10 min at all

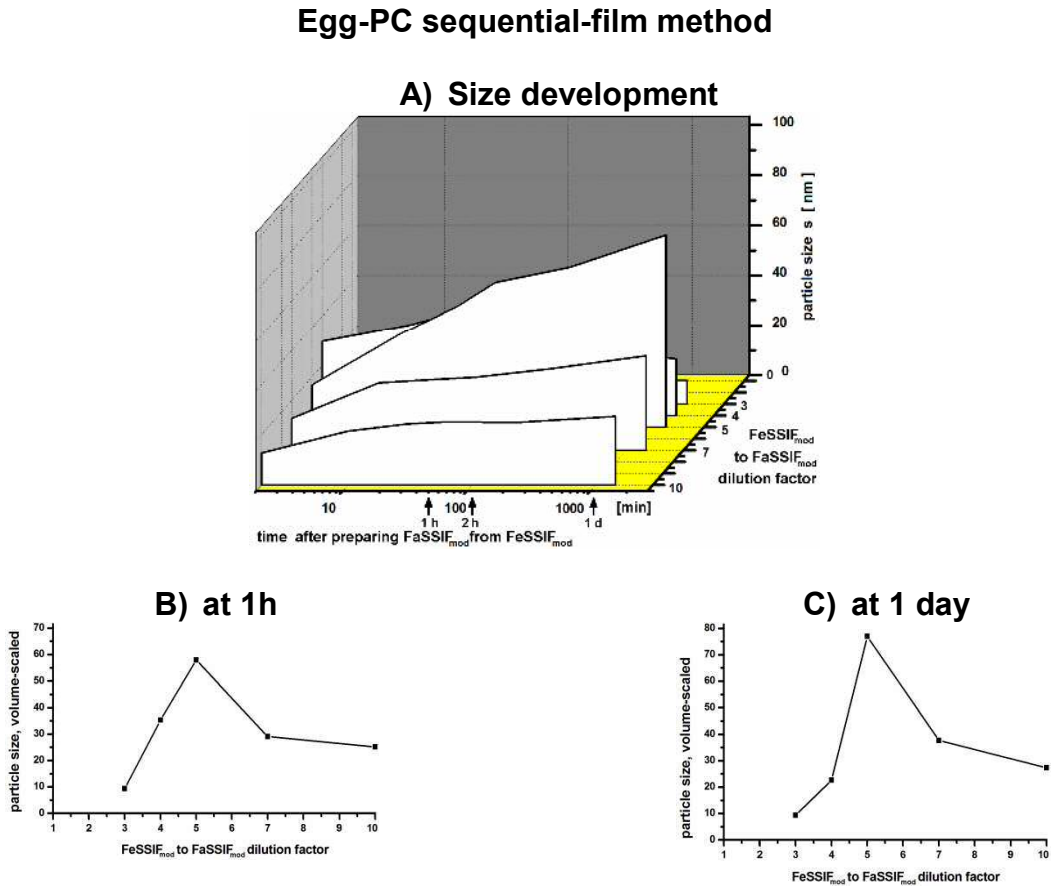

Fig.3.1-8: Nanoparticle structure development in Egg-PC, prepared by the sequential-film method during 2 days after dilution of FeSSIF$_{mod}$ at various mixing ratios, i.e. water consumption upon drug administration: **A)** 3D-plot of development in time and dilution rate; **B)** cut at 1 h (duodenal passage time in healthy persons); **C)** cut at 1d (delayed digestion, lab standard).

dilutions greater than 1:3. At 1:3 dilution the particles did not exceed 10 nm size (micelles). Large liposomes (particles > 40 nm) appeared at 1:5 dilution after ≥ 30 minutes, with ongoing increase up to one day. The particle size in the 1:10 diluted sample led to a plateau of d = 25 nm after one hour. The dependence of the particle size on the dilution factor appeared to be at least bi-phasic. In the 1:5 dilution sample the particle size increased to 58 nm (in 1 h) and 77 nm (24h). The cut profiles with Egg-PC and the sequential-film method at 1h development (duodenal passage in healthy persons, fig. 3.1-8B) and at 1 day development (pharma-lab standard, maximal time in disease (fig. 3.1-8C) showed a peak in the nanoparticle size at a FaSSIF$_{mod}$ dilution rate of 1:5.

3.1.5. Discussion

The oral route is the most preferred and convenient way of the drug administration. However, there are limitations for drugs with poor solubility and permeability (BCS classes II and IV). These lipophilic drugs can undergo a complex formation leading to solubilization and uptake with other hydrophobic materials, which can enter from the native bile, food and from drug formulations. The secretion of bile in the human body improves the digestion and uptake of lipophilic materials from food and supplements, e.g. lipids, vitamins and drugs [4, 10, 144].

The intestinal fluid of the duodenal gut section is modelled in pharmaceutical studies with model fluids, FeSSIF for the fed state, and FaSSIF for the fasted state, i.e. upon intake of food and drinks. Various methods have been employed in the preparation of FeSSIF and FaSSIF [139, 140]. In this study we use fluids with an improved bicarbonate-HEPES buffering system, i.e. FeSSIF$_{mod6.5}$, FaSSIF$_{mod6.5}$ [88, 145] and the corresponding transfer medium TM, which models the fluid entity entering from the stomach after pH-shift to pH6.5 in the middle of the duodenum. As a simplification, we name here all the dilutions of FeSSIF$_{mod}$ as "FaSSIF$_{mod}$", independent of the dilution rate.

This study compares three different methods of preparing FeSSIF$_{mod}$ and subsequently FaSSIF$_{mod}$ from three lecithin entities and sodium taurocholate: the "shake method", the "bile-film method" and the "sequential-film method" (fig.1). The shake method is a simple method to prepare FeSSIF$_{mod}$ and FaSSIF$_{mod}$ from solid materials and does not involve any organic solvent. The extended shaking at 37°C could lead to lipid hydrolysis. Moreover this method is only convenient when *one* lipid is involved, in order to avoid a risk of a non-homogenous mixture. The shake method was difficult to apply in a reproducible way and revealed partly in a liposome peak at one hour development at low mixing ratios, as compared to the film methods (fig. 3.1-5 - 3.1-7: C,D). The film methods are applicable to lipid mixtures which result in a thin and homogenous film and at the end produce homogenous FeSSIF$_{mod}$ mixtures. The preparation of FeSSIF$_{mod}$ by the bile-film method was more difficult as compared to sequential-film method, due to problems in the film formation (foam, spilling, delayed evaporation). For a bile-film, about 4-5 hours is needed for the complete evaporation of the methanol from the mixed lipid-bile solution, but the alcohol is needed for the solubilization of the bile acid.

These problems are avoided in the sequential-film method, which gave a similar product as the bile-film method, but was easier and faster to apply, especial in the film preparation step. Here a solution of sodium taurocholate in transport medium is added to the dry lipid film for the FeSSIF$_{mod}$ preparation. The intermediate FeSSIF$_{mod}$ is mostly ready after two hours and can be stored frozen (-24°C).

The human bile fluid and the intestinal fluids contain lecithin (PC) as a major component, which forms complexes with other amphiphilic materials[16, 146] . This organ specific lipid contains palmitoyl-oleoyl-lecithin (POPC) as predominant entity, which is also the major component of Egg-lecithin (Egg-PC). In the intestinal model fluid studies until now, PC species from several origins have been used, POPC, DOPC, Soy-PC and Egg-PC, while the latter two were mainly used [16, 147]. DOPC and POPC are used for precise physicochemical and biochemical studies. According to literature bile salts, phospholipids and ionic strength of the media influence the particle size and structure of colloids[148], and drug solubilization and uptake, especially for drugs of the BCS classes II and IV. The development of FaSSIF$_{mod}$ from FeSSIF$_{mod}$, which simulates the situation of drug administration together with fluid or food[10] , shows the development of liposomes and other nanoparticles at a physiological correct time (20min-2h).

We have compared DOPC (fig. 3.1-5), POPC (fig3.1-.6) and Egg-PC (fig. 3.1-7, 3.1-8) with the different preparation methods stated above to prepare intestinal model fluids FeSSIF$_{mod}$ and FaSSIF$_{mod}$ to resolve the effect of different lecithins on the size, kinetics and amount of lipophilic nanoparticle in these media. By the DLS experiments with FeSSIF$_{mod}$ (fig. 3.1-2A-C), there was no detectable difference in particle size in FeSSIF$_{mod}$ (~ 5nm) with the lipids and methods used in the first part of the preparation. In the second step the uptake relevant model fluid FaSSIF$_{mod}$ was prepared and studied upon dilution of FeSSIF$_{mod}$ by the transfer medium TM as a model for the material arriving from the first half of the duodenum. The formation of larger nanoparticles, which are possible uptake mediators of hydrophobic drugs, was studied by DLS and SANS. The static DLS investigation of FaSSIF$_{mod}$ after 1h of development (fig. 3.1-3) revealed the formation of nanoparticles of ~38 nm size, which were identified as liposomes by the size[3]. The precise neutron scattering investigation (fig. 3.1-4) showed that this is a mixture of two particle populations, liposomes (33 nm) and large micelles (15.4 nm), while that seen in the simpler DLS experiment is the major component. The presence of liposomes was proven with SANS by the lamellar structure with a membrane span of d_l = 5.5 nm (fig. 3.1-4C).

The time resolved study (fig. 3.1-5 - 3.1-8) covered the time range of 10 minutes to 1 day, which are the limits of the physiological transit time through the duodenum in ill and healthy persons. The average time for a healthy human is assumed as 20-60 minutes. In this time regime liposomes (33 nm) and in parallel large mixed lipid-bile micelles (15 nm) develop from the small micelles in FeSSIF (5 nm, fig3.1-2), as depicted in fig. 3.1-4 (SANS after 1h). The mixing ratio of bile and intestinal fluid, in our study of the model fluids, FeSSIF$_{mod}$ and TM yielding FaSSIF$_{mod}$, varies at different physiological conditions by food and fluid uptake. In most pharmaceutical studies a ratio of 1:5 is assumed as biorelevant medium, while it varies *in vivo*. In the figures 3.1-5 - 3.1-8, a mixing rate variation from 1:3 to 1:10 was applied with various lipid and FeSSIF$_{mod}$ variations. Additionally to the 3D-structure development profiles, two cuts were supplied which compare the dependence of the nanoparticle size on the intestinal fluid dilution at typical physiological development times: 1 h as example for a healthy person, and 1 day as example for a disease accompanied with delayed digestion, e.g. constipation. The results indicate that the intestinal model fluids contain liposomes as major component mostly at a dilution ration of 1:5, while this nanoparticle entity is formed in a slow process during 20 min to hours. The liposome formation kinetics depends on the dilution rate, lipid and at a lower level on the FeSSIF$_{mod}$ preparation method. With DOPC (fig. 3.1-5) and POPC (fig. 3.1-6) the liposome formation continued up to one day. With Egg-lecithin, which resembles the human bile lipid, the liposome concentration led to a constant plateau after two

hours, while the major part was already formed in the span between 10 minutes and one hour – the typical transit time through the second part of the duodenum *in vivo*.

3.1.6. Conclusion

The particle characteristics of intestinal model fluids were investigated at conditions, which simulate the passage from the entry of the bile in the middle of the duodenum until the end of this gut segment. The formation and conversion of liposomes and micelles was studied, because of their role as intermediate host for resolution and uptake of hydrophobic drugs, i.e. those of the BCS classes II and IV. The conditions, which may influence the formation of these nanoparticulate intermediates were studied, i.e. the lipid composition of the bile, the preparation method, the passage time through the modelled duodenum and the concentration, which results from the variable dilution of the bile by mixing with transfer medium representing the fluid arriving from the stomach. The variation of the lecithin entity revealed an equivalence of Egg–PC of a high purity (≥ 99%) with its main component POPC, while the standard lipid of biochemical membrane studies DOPC resulted in a slight delay of the micelle-liposome conversion. The FeSSIF preparation method was best with the sequential-film method, while the technically more difficult bile-film method yielded comparable results; the shake method showed a slightly different kinetics, probably because of the extended hydration of the solid lipid. The time and concentration dependence of the formation and disintegration of lipidic nanoparticles indicates that the concentration of these particles strongly depends on the time and dilution rate. The physiological conditions at healthy persons may vary individually and due to diseases. The studied conditions cover typical physiological situations. Exploration of in vitro dissolution tests of formulations of hydrophobic drugs should take these considerations and findings of this study into consideration.

3.1.7. Acknowledgments

We are thankful for the funding by the German ministry of science and education BMBF, grant 05KS7UMA; the Forschungszentrum Jülich FZJ, Jülich Centre of Neutron Science JCNS, outstation at the FRM2 reactor Munich Garching; and support by the Dr. Georg-Scheuing Stiftung, Mainz. This work was contributed to the OrBiTo project (http://www.imi.europa.eu/content) as side ground.

Conflict of interest: There are no financial or commercial conflicts of interest.

References

The references are included (re-numbered) in the general reference section (5) of this thesis

3.2. FaSSIF-C", a Cholesterol containing Intestinal Model Medium

"**Fasted-State Simulated Intestinal Fluid "FaSSIF-C", a Cholesterol containing Intestinal Model Medium for *in vitro* Drug Delivery Development**"

Pooneh Khoshakhlagh, Raphael Johnson, Peter Langguth, Thomas Nawroth, Lars Schmuese, Nadja Hellmann, Heinz Decker, Noemi Kinga Szekely

Journal of Pharmaceutical Sciences 2015, 104 (7), 2213–2224

Running title: "FaSSIF-C"

3.2.1. Abstract

A set of biorelevant media 'FaSSIF-C' for the *in vitro* study of intestinal drug dissolution in the duodenum was developed. These contain cholesterol at the same levels as in human bile: The cholesterol content of FaSSIF-7C is equivalent to healthy female, FaSSIF-10C to healthy male persons, and FaSSIF-13C to several disease cases which lead to gallstones. The fluids were studied in three aspects: biocompatibility, intestinal nano-structure, and solubilizing power of hydrophobic drugs of the BCS class II. The biocompatibility study showed no toxic effects in a Caco-2 cell system. The drug solubilizing capacity towards Fenofibrate, Danazol, Griseofulvin, and Carbamazepine was assessed as example. It varied with the cholesterol content widely from a 4-fold improvement to a 2-fold reduction. The nanostructure study by dynamic light scattering and neutron small angle scattering indicated vesicles as the main component of FaSSIF-C in equilibrium (>1h), but at high cholesterol content larger particles were observed as a minor contribution. The neutron experiments indicated the presence of complex micelle-vesicle mixtures, even after one hour development of fed state bile model to FaSSIF. The results indicate that cholesterol affects some drugs in solubilzation and particle size in intestinal model fluids.

Keywords: In vitro models, biorelevant media, drug solubility, lipids, micelle, light-scattering, DLS, SANS, FaSSIF, Caco-2 cells

3.2.2. Introduction

Lipophilic drugs of the BCS[136] classes II and IV are subject of drug formulation development during the last decade. However, many of these drugs do not have sufficient solubility and that makes them undesirable for *in vivo* studies[136, 144].

In vitro studies of orally administered dosage forms ensure the reliability and efficacy of the ultimate product. They lead to a reduction of animal tests and bioavailability studies[79, 149]. *In vitro* models should be reliable and easily reproducible tools to mimic *in vivo* environment to study drugs[150].

In vivo, the intestinal fluid is mixed (after the gastric emptying and pH-shift) with the secretions of bile and pancreas in the middle of the duodenum at pH 6.5. As a result, the physiological intestinal fluid contains at the entrance of the drug uptake competent region

(jejunum, ileum) a mixture of amphiphilic materials (bile acids, lipids), nanoparticles and a cocktail of about 10 hydrolytic enzymes at pH 6.8 – 7.2[151,4] .
The essential role of bile acids and lecithin (the main lipid of bile) is the solubilization of lipophilic food and cofactors by incorporating the substance into mixed bile salt micelles, liposomes, and other nanoparticles[138, 152]. In addition to bile acid and lecithin, cholesterol is a further lipophilic component of bile[37]. The intestinal level of this important transport mediator is stabilized physiologically by the enterohepatic circulation system[153]. The cholesterol content, as referred to the total amphiphiles, in females' bile is almost 7% and around 10% in males[37]. However, the cholesterol content of bile increases up to 13% in some diseases[49]. As cholesterol has low solubility in water, its solubility in the bile depends strongly on the concentration of bile acids and lecithin. This is a consequence of the solubilization properties of the formation of mixed particles with cholesterol. In the process of solubilization and absorption of the lipophilic drug substances, the presence of lipids and development of their digestion products such as monoacylgycerides, lysolecithin, and free fatty acids are essential. Thus, several drugs show a food effect in bioavailability[52, 138, 154-156].
The artificial intestinal model media, fasted-state simulated intestinal fluid (FaSSIF) and fed-state simulated intestinal fluid (FeSSIF), simulate the conditions in the second half of the duodenum. The traditional forms of FeSSIF and FaSSIF have been introduced to forecast the solubility and permeability of drugs in gastrointestinal composition in the duodenum[67,83]. They have several deficiencies, such as limited pH stability, buffer capacity, phosphate buffer, osmolality, lipid composition, and lipid to bile acid ratio. During the last decade biorelevant media have been updated to improve the predictions of oral formulations[16, 83, 87, 91, 149]. In the recent models, $FaSSIF_{mod6.5}$ and $FeSSIF_{mod6.5}$ for the conditions in the late duodenum (pH6.5), the fluids were stabilized by addition of glucose and HEPES (4-(2-Hydroxyethyl)piperazine-1-ethanesulfonic acid, N-(2-Hydroxyethyl) piperazine-N′-(2-ethanesulfonic acid) to Hank's buffered salt solution (HBSS) bicarbonate buffer[88]. These model fluids were further used for studies of in *vitro-in vivo correlation* of drug solubility and uptake and the associated lipid-bile nanoparticle dynamics[87, 157-160] .
In this study, we investigated how the addition of cholesterol in *in vitro* media influences drug solubility and associated lipid nanostructures, that is, a more similar model of human bile. The media were based on pH-stabilized simulated intestinal fluids $FaSSIF_{mod6.5}$[88, 157, 158]. In the new fluids, "FaSSIF-C", the effect of different cholesterol concentrations on the particle size distribution was examined. The solubilizing capacity of four example drugs from BCS class II, low-solubility, and high-permeability compounds, was determined. The occurrence and role of intermediate nanoparticles, micelles, and vesicles, was estimated by quantitative dynamic light scattering (DLS). The biocompatibility of the medium was tested for cytotoxicity and proliferation in a Caco-2 cell culture model.

3.2.3. Experimental

3.2.3.1 Materials

Danazol (≥98%), Griseofulvin, Carbamazepine, cholesterol, lecithin, and sodium taurocholate (TC) hydrate (≥97%) were purchased from Sigma-Aldrich (Steinheim, Germany). Fenofibrate was purchased from Labochim (Hamburg, Germany). HEPES was obtained from Merck

(Darmstadt, Germany). The following materials were purchased from Life Technologies (Darmstadt, German): HBSS (Gibco 14025), Dulbecco's modified Eagle medium (DMEM) containing 4.5g/L Glucose, GlutaMax™ and phenol red (Gibco 61965), nonessential amino acids (NEAA; Gibco 11140-035), fetal bovine serum (FBS; Gibco 10270-106), 0.25% trypsin-ethylenediaminetraaceticacid (1 mM), and antibiotic-antimycotic mixture (10,000 U/ml penicillin G, 10,000 mg/ml streptomycin sulfate, Gibco 10923392) . The colorless medium for the cell test was DMEM containing 4.5g/L glucose (Gibco 31053). Glucose, dimethyl sulfoxide (DMSO) HPLC grade, chloroform HPLC grade and 3-(4,5-dimethylthiazol-2-yl)-2,5-diphenyltetrazolium bromide (thiazolyl blue, "MTT-reagent") were purchased from Carl Roth (Karlsruhe, Germany). The Caco-2 cell line was purchased from American Type Culture Collection (Rockville,Maryland).

3.2.3.2 Methods

All experiments were done at least three times.

3.2.3.2.1 Intestinal Model Media Preparation

Neutral pH-stabilized transport medium (TM)[88] was prepared from HBSS by addition of 19.45 mM glucose and 10 mM HEPES and pH adjustment to 6.5 with 0.1 M HCl. It contains finally 25 mM glucose, as the cell culture medium. The gastro-intestinal model media were prepared according to Table 1 with a total amphiphile concentration (TC + lecithin + cholesterol) of 18.75 mM for fed-state and 3.75 mM for fasted-state media. The $FeSSIF_{mod6.5}$ and FeSSIF-C samples were prepared by the sequential-film method[161] from stock solutions of lecithin and cholesterol (100 mg/ml in chloroform). For each of the samples (final 7.5 mL FeSSIF-C), aliquots of the lipid stock solutions were mixed with Hamilton syringes in glass tubes. The solvent was removed with a rotational evaporator, model R-3 (Büchi, Flawil, Switzerland), at stepwise decreasing pressure (150–10 mbar) during 30 min. The lipid films were dried at 5 mbar for 3 h. The sodium TC was dissolved in TM (7.5 mL) and added to the tubes. The tubes were vortexed for 5 min at 30 Hz with a Bioblock TopMix Vortexer (Fisher Scientific Inc., Waltham, Massachusetts). The solutions were kept overnight at 37^0C for equilibration yielding $FeSSIF_{mod6.5}$ or FeSSIF-C and then diluted 1:5 with TM to prepare the final solutions ($FaSSIF_{mod6.5}$ or FaSSIF-C).

Table3.2-1: Composition of the intestinal model media

Cholesterol contribution [amphiphil mol%]	Fed state intestinal model medium	Lecithin [mM]	Bile acid [mM]	Choles-terol [mM]		Fasted state intestinal model medium	Lecithin [mM]	Bile acid [mM]	Choles-terol [mM]
0	$FeSSIF_{mod}6.5$	3.75	15	0		$FaSSIF_{mod}6.5$	0.75	3	0
2	FeSSIF-2C	3.75	14.63	0.37		FaSSIF-2C	0.75	2.926	0.074
4	FeSSIF-4C	3.75	14.25	0.75		FaSSIF-4C	0.75	2.85	0.15
7	FeSSIF-7C	3.75	13.69	1.31		FaSSIF-7C	0.75	2.738	0.262
10	FeSSIF-10C	3.75	13.13	1.87		FaSSIF-10C	0.75	2.626	0.374
13	FeSSIF-13C	3.75	12.56	2.44		FaSSIF-13C	0.75	2.512	0.488

3.2.3.2.2 Drug Solubility Study

Excess amount of the drugs (~20 mg) were added to the intestinal model media (3 mL) in glass stoppered tubes (16 x 100 mm, borosilicate glass 3.3) and incubated at 37^0C, 35% speed, 60 min^{-1}, in a 3047 shaking waterbath, (Köttermann, Haenigsen, Germany). After 24 hours the samples (2 x 1.5 mL) were centrifuged for 10 min, 800g (HF-130 centrifuge; TOMY KOGYO, Fokushima, *Japan*). Then 2 x 1 mL of the supernatant was transferred to new tubes and again centrifuged for 5 min as before. The drug concentration in the second supernatant was immediately (1 min) estimated photometrically (*UV-1700 PharmaSpec;, Shimadzu, Kyoto, Japan*). The wavelength was 290 nm for Fenofibrate, 289 nm for Carbamazepine, 285 nm for Danazol, and 291 nm for Griseofulvin. The signal of a drug-free reference sample for each of the media compositions was taken as a reference. The drug content was then calculated using nondrug-saturated calibration factors for each media condition, that is, an individual calibration curve was estimated for each data point in the Figure 3.2-1 (24 calibration profiles). At high concentration, results of the supernatant solutions were verified by 1:1and 1:4 dilutions with blank medium. Test estimations with additional methanol (50%) did not differ in the result; thus, the cosolvent addition was omitted. The chosen photometric assay was shown by test samples to work well with protein-free model media, in contrast to human intestinal fluid HIF, where HPLC analysis is necessary.

3.2.3.2.3 Particle Size Estimation by DLS

The particle size distribution was estimated[161] after centrifugation (removal of excess drug) by DLS[162] with Zetasizer Nano-ZS (Malvern, Worcestershire, UK), which has an upper particles size limit of 5.6 µm. Thus, the particle contributions for large particles of greater than 1 µm were taken as semiquantitative (symbols in Fig. 3.2-2 and 3.2-5). All samples were measured three times at 37^0C. The raw size distributions (by scattered light intensity; PSD-I) were evaluated to mass contributions as performed in our previous investigation[3, 161]. The data export and evaluation procedure with the Zetasizer Software V6.2, and mass contribution scaling for liposomes, plates in Origin 7.0 (Northampton, Massachusetts) is shown in www.mpsd.de/DLS_dataexport_Malvern.html .

3.2.3.2.4 Particle Structure Estimation by Small-Angle Neutron Scattering

The precise structure estimation of the nanoparticles in the intestinal model fluid in a regime of <100 nm particle size was performed with small-angle neutron scattering (SANS)[133]. The experiments were carried out with the Instrument KWS-2 [163] at the FRM-II reactor using a cold neutron source beam at the Heinz Maier-Leibnitz Zentrum (Munich-Garching, Germany). The samples were prepared with 71 % D_2O-buffer for improving the contrast, but avoiding possible aggregation problems at high D_2O content. The scattering experiments were carried out with neutrons of 0.453 nm wavelength at sample-detector distances of 1.81 and 7.68 m. The primary data evaluation until the radial average of the SANS profiles was carried out at the FRM-II reactor using the QTIKWS software of the JCNS (Garching, Germany). In

a second step, the scattering profiles were evaluated using Origin 7.0, after subtraction of buffer scattering, according to the Guinier approximation for small momentum transfer (q). The momentum transfer (q) was estimated as $q = (4*\pi / \lambda) \sin(\theta)$, where λ is the wavelength of the radiation and θ is half of the scattering angle. The plots were carried out with Origin 7.0.

3.2.3.2.5 Cultures of Caco-2 Cells

After initial culturing with 2% antimycoplasmic solution Mycokill, the Caco-2 cells (passage75) were cultured in 75cm^2 flask in an incubator at 37°C with 5% CO_2. The culture medium was DMEM supplemented with 10% FBS, 1% NEAA, and 1% antibiotics solution (penicillin-streptomycin)[164]. The passaging was performed weekly with one intermediate feeding. At near confluency, the cells were transferred to 96-well plates and seeded at a density of 3000 cells per well and incubated for 48h for cell adhesion and formation of cell plaques (~100 cells, 20% confluence). The confluence at the toxicity test end was 50-70%.

3.2.3.2.6 Cytotoxicity Assay on Caco-2

Forty-eight hours after seeding cells to the multiwell plates, the culture medium was removed and replaced with TM, $FaSSIF_{mod6.5}$ and FaSSIF-7C (180 µl), and the cells were incubated for 1 h (drug incubation). Then, the drug medium was exchanged with fresh culture medium for a further hour (recreation). For the cell viability estimation using the "MTT-test",[165, 166] the medium was removed and 180 µl of Thiazolyl blue in colorless medium ("MTT-reagent", 0.5 g/L) was added and incubated at 5% CO_2, 37°C for 1 h (cellular MTT dye formation). After removal of the reagent medium, the Formazan crystals were solubilized by addition of 180 µl DMSO, incubation for 30 min in a CO_2-incubator at 37°C and subsequent agitation with a multichannel pipette (threefold). The dye DMSO extracts were transferred to a nonsterile 96-well plate, which avoids light scattering by cell debris. The optical densities were measured at 560 nm (signal) and 690 nm (background using the TECAN F200 plate reader). The difference values ($E_{560} - E_{690}$) were kinetically evaluated with Origin7.0 (Microcal, Northampton, Massachusetts).

3.2.4. Results

3.2.4.1 Drug Solubility Studies

Figure 3.2-1 shows the saturation solubility of four lipophilic drugs in intestinal model media of different cholesterol content; the range of healthy person equivalence is indicated by a box; the upper limit (13%) is associated with disease conditions leading to gallstones.

3.2.4.1.1 Fenofibrate

Figure 3.2-1a shows the saturation solubility of Fenofibrate in the model media. The solubility profile shows that the cholesterol content has a strong effect on the drug solubility. The solubility of Fenofibrate was increased by cholesterol by a factor of up to 3.78 in a

complex profile: at low concentration (< 4%), the cholesterol effect was very limited. The solubility enhancement depicted a factor of 3.00 at 7% cholesterol (FaSSIF-7C) and 3.78 at 10% (FaSSIF-10C) as compared to cholesterol-free $FaSSIF_{mod6.5}$. At high cholesterol content of 13% (FaSSIF-13C), the enhancement factor decreased to 2.31.

3.2.4.1.2 Carbamazepine

Figure 3.2-1b depicts the solubility profile for Carbamazepine in intestinal model media. For this drug, the effect of the cholesterol was very limited. The solubility of Carbamazepine was slightly reduced by cholesterol by a factor of up to 0.87 (= 1/1.15) at 7% cholesterol (FaSSIF-7C). In the concentration range of greater than 7%-13% cholesterol, an average increase by 11%, as compared to the drug solubility in FaSSIF-7C (minimum), was observed. The drug solubility at 13% cholesterol was 96.87 % of that in $FaSSIF_{mod6.5}$.

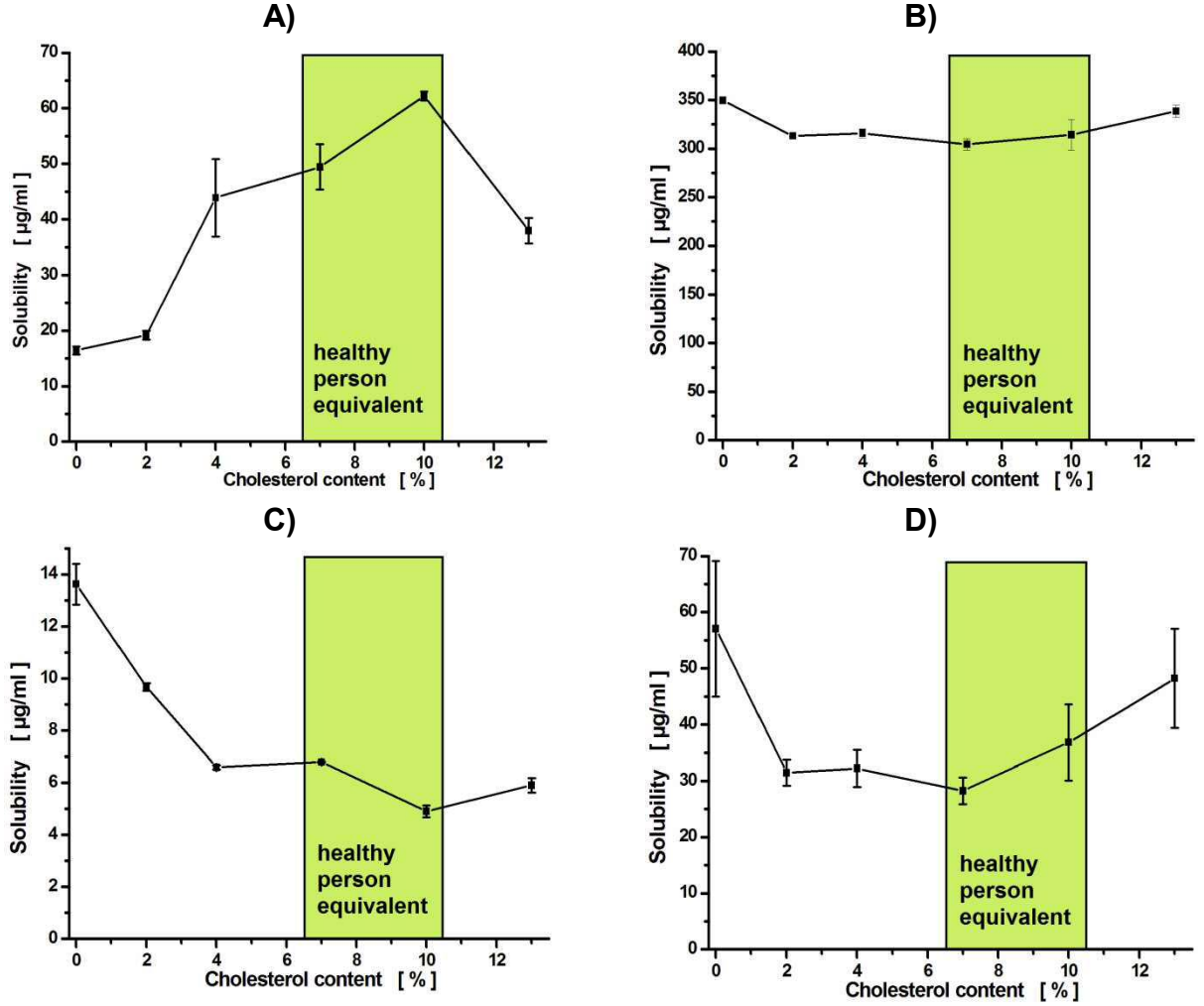

Fig.3.2-1. Solubility of **A)** Fenofibrate, **B)** Carbamazepine, **C)** Danazol and **D)** Griseofulvin in gastrointestinal model fluids FaSSIF-C containing various amounts of cholesterol. The physiologically related fluids contain 7% (female), 10% (male) and 13% (disease) cholesterol (mol% of amphiphiles; sodium taurocholate + lecithin+ cholesterol), the range for healthy persons is indicated by the box. The difficult samples of high cholesterol content (13%) are qualitatively shown for comparison only.

3.2.4.1.3 Danazol

Figure 3.2-1c shows the saturation solubility of Danazol in intestinal model media. The solubility profile shows that cholesterol has a considerable effect on the drug solubility. The solubility of Danazol was reduced by cholesterol by a factor of up to 0.36 (= 1/2.78). The cholesterol-related decrease developed in two steps: At low concentration (< 4%), the cholesterol effect was limited. The solubility decrease depicted a factor of 0.50 (= 1/2.00) at 7% cholesterol (FaSSIF-7C) and 0.36 (= 1/2.78) at 10% (FaSSIF-10C) as compared to cholesterol-free $FaSSIF_{mod6.5}$. At high cholesterol content of 13% (FaSSIF-13C), the decrease factor did not change further.

3.2.4.1.4 Griseofulvin

Figure 3.2-1d shows the saturation solubility of Griseofulvin in intestinal model media. The solubility profile shows that cholesterol has a significant effect on the solubility. The solubility of Griseofulvin was reduced by cholesterol by a factor of up to 0.495 (= 1/2.02). The cholesterol-related reduction of the drug solubility developed gradually: at low concentration (4%), the cholesterol effect reduced the drug solubility to a value of 0.53 (= 1/1.89). In the intermediate regime, the solubility decrease depicted a factor of 0.495 (= 1/2.02) at 7% cholesterol (FaSSIF-7C) and 0.645 (= 1/1.55) at 10% (FaSSIF-10C) as compared to cholesterol-free $FaSSIF_{mod6.5}$. At high cholesterol content of 13% (FaSSIF-13C), the solubility modification factor increased again to 0.845 (= 1/1.18) of the cholesterol-free medium.

3.2.4.2 Particle Size Studies with Quantitative DLS and SANS

3.2.4.2.1 Drug-Free Reference (Blank)

The apparent size of particles in various intestinal model media containing no drug but cholesterol, as estimated by DLS, is shown in Figure 3.2-2. The main particles in all media were vesicles depicting an average size between 70 nm to 25 nm before and after sample centrifugation. There was a general decrease in particle size in all media with increasing amount of cholesterol. In samples depicting a cholesterol content of at least 7 %, larger colloidal species (d > 200 nm) and some big particles were observed as minor component (qualitatively for s > 1 μm). The occurrence, apparent size, and content of these large particles are indicated in Figures 3.2-2 and 3.2-5 by colored symbols for samples after centrifugation. The dependence of the particle size of FaSSIF-C without drug on the cholesterol content developed in two steps, that is, a low cholesterol regime (<3%), and a medium to high cholesterol regime (>3%). The results for very high cholesterol content (13%) are shown for comparison only, as part of the material was removed by the centrifugation, which was necessary below for the excess drug removal.

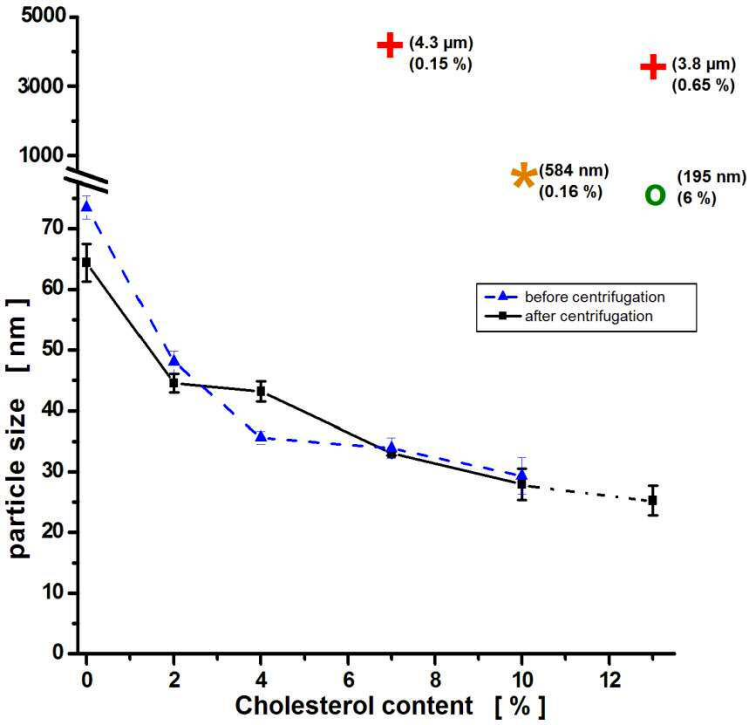

Fig.3.2-2: *Average* nanoparticle size of gastrointestinal model fluids FaSSIF-C containing various amounts of cholesterol without drug before (▲) and after centrifugation (■). At high cholesterol content additional large particles appear as minor components, which are indicated for the samples after centrifugation as symbols off size scale (+, *, o). The difficult samples of high cholesterol content (13%) are qualitatively shown for comparison only.

The structure of the intestinal model fluids was investigated more precisely with SANS. By technical reasons, the method was limited to particles of smaller than 100 nm size. The contrast of the nanoparticles to the solvent was improved by 71 % D_2O, which is pharmaceutically equivalent to the light water medium[3]. As depicted in Figure 3.2-3, even with cholesterol free $FaSSIF_{mod6.5}$, the scattering profile (Fig. 3.2-3a) appeared as a multicomponent mixture. The particle size analysis by Guinier plots[141] contained separate straight lines for up to five different nanoparticle entities. In parallel, the nanostructure developed with time[3]. As example, the data in Figure 3.2-3b were obtained from a 3-h old $FaSSIF_{mod6.5}$ sample, that in Figure 3.2-3c from a 47-min old specimen. The radius of gyration R_g of these components, R_{g1} = 12.78 ± 1.67 nm, R_{g2} = 7.554 ± 0.79 nm , R_{g3} = 5.34 ± 0.44 nm , R_{g4} = 4.53 ± 0.16 nm and R_{g5} = 3.394 ± 0.046 nm correspond to particle diameters, d_1 = 30.30 ± 4.31 nm, d_2 = 17.90 ± 2.04 nm, d_3 = 12.66 ± 1.14 nm , d_4 = 10.74 ± 0.38 nm and of d_5 = 8.05 ± 0.11, after scaling by 2 R_g *√(5/3), for spheres. At times greater than 30 min after diluting FeSSIF to FaSSIF, the largest particles (no.1, vesicles) had the highest contribution (zero angle scattering in the Guinier plots). Extended SANS data were estimated in the structural development with time resolution for all FaSSIF-C media with and without Fenofibrate. Due to the vast amount of data and figures, these results on nanoparticle structure will be presented elsewhere.

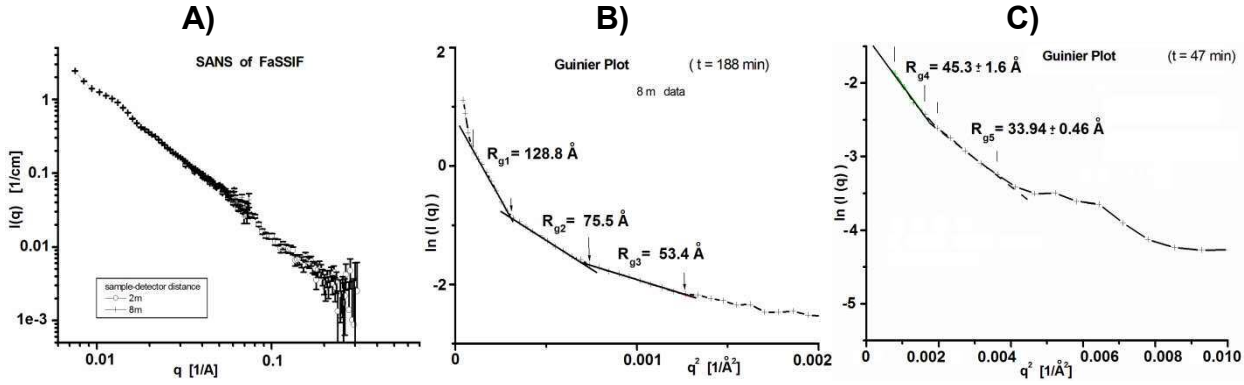

Fig.3.2-3: Detailed structure analysis (one individual sample experiment) of nanoparticles in gastrointestinal model fluid $FaSSIF_{mod6.5}$ by SANS: A) the SANS scattering profile appears as a sum of several particle contributions; the size analysis by Guinier plots of B) 8m data (3h old sample) and C) 2m data (47 min. old sample) indicate particles of different size in parallel.

3.2.4.2.2 Drug-Saturated Intestinal Model Fluids

3.2.4.2.2.1 Fenofibrate

The nanoparticles formed from bile acid, lecithin, cholesterol, and drugs were analyzed in a wide size regime (2 nm–5.6 µm) with DLS. Figure 3.2-4 shows an example of the resulting apparent particle size profiles for Fenofibrate in FaSSIF-10C (10% cholesterol) of one individual sample. The data were scaled yielding the volume contributions (= mass fraction) for massive particles as shown earlier that is, division of the crude data (DLS intensities) by r^3 as a rough estimate for a mixture of different particles: the profile depicts medium size particles (vesicles, d = 28.6 nm) as the main contribution (97.4%), a minor constituent (2.4%)

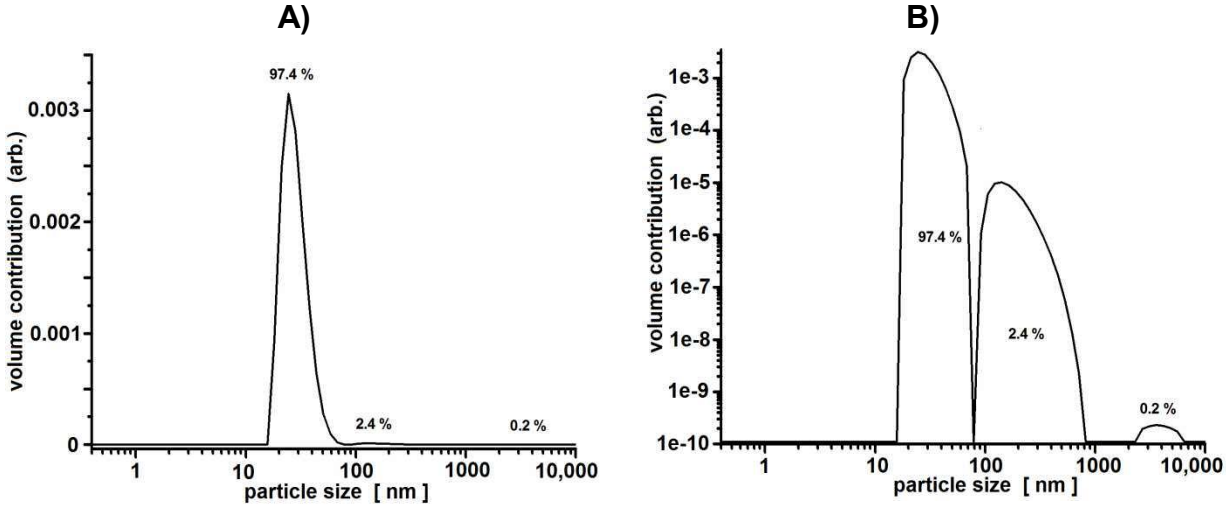

Fig.3.2-4: Particle size profiles of Fenofibrate in FaSSIF-10C (10% cholesterol) obtained by dynamic light scattering DLS in **A)** linear and **B)** logarithmic representation of the volume contribution (one individual sample experiment). The minor contributions are visible only in the unusual logarithmic plot.

of large particles (d = 282 nm), and traces (0.2%) of very large particles (4.768 µm) near the size detection limit of the used DLS instrument (5.6 µm). For the liposome part (peak 1), a scaling by 1/r2 (liposomes, plates)[3] resulted in the same particle size within the resolution of the method (10%).
The latter two minor components are visible only in the unusual logarithmic representation, chosen for Figure 3.2-4b. Thus, for the further 24 samples, a simplified representation was chosen in Figure 3.2-5, where the size of the major component (vesicles) is represented as a function of the cholesterol content in 2D-graph. Minor components are depicted as an asterisk with size and volume contribution in parenthesis, but out of the size scale; traces smaller than 1% were omitted.
The particle size in various intestinal model media containing Fenofibrate and cholesterol is shown in figure 3.2-5a. The main particles in all media (vesicles) depicted an average size between 44 nm to 25 nm. There was a general decrease in particle size in all media with increasing amount of cholesterol. In samples depicting a cholesterol content of at least 7 %, larger colloidal species (d > 200 nm) and big particles (> 1 µm) were observed (qualitatively). The dependence of the particle size of Fenofibrate-saturated FaSSIF-C on the cholesterol content appeared in two steps with a decrease at 0%-2% and a plateau from 4%-13%.

3.2.4.2.2.2 Carbamazepine

The particle size in various intestinal model media containing Carbamazepine and cholesterol is presented in Figure 3.2-5b. The main particles in the media (vesicles) had an average size between 64 nm to 32 nm. Between 2% and 4% cholesterol, a decrease in the particle size with increasing amount of cholesterol occurred. At 13 % cholesterol, the major particle size increased to 44 nm. In samples depicting a cholesterol content of at least 7 %, larger colloidal species (d > 400 nm) and big particles (> 1 µm) were observed. The particle size of Carbamazepine-saturated FaSSIF-C decreased with increasing cholesterol content.

3.2.4.2.2.3 Danazol

The particle size in various intestinal model media containing Danazol and cholesterol is shown in Figure 3.2-5c. The main particles in all media (vesicles) depicted an average size between 59 nm to 26 nm. There was a general decrease in particle size in all media with increasing amount of cholesterol. In samples with a cholesterol content of at least 7 %, larger colloidal species (d > 300 nm) and big particles (> 1 µm) were observed. The dependence of the particle size of FaSSIF-C containing Danazol on the cholesterol content developed in two steps. Between 7% and 13% cholesterol, a plateau in major particle size was observed.

3.2.4.2.2.4 Griseofulvin

The particle size in various intestinal model media containing Griseofulvin and cholesterol is presented in Figure 3.2-5d. The main particles in the media (vesicles) showed an average size between 58 nm to 30 nm. Between 2% and 7% cholesterol, a decrease in the particle size with

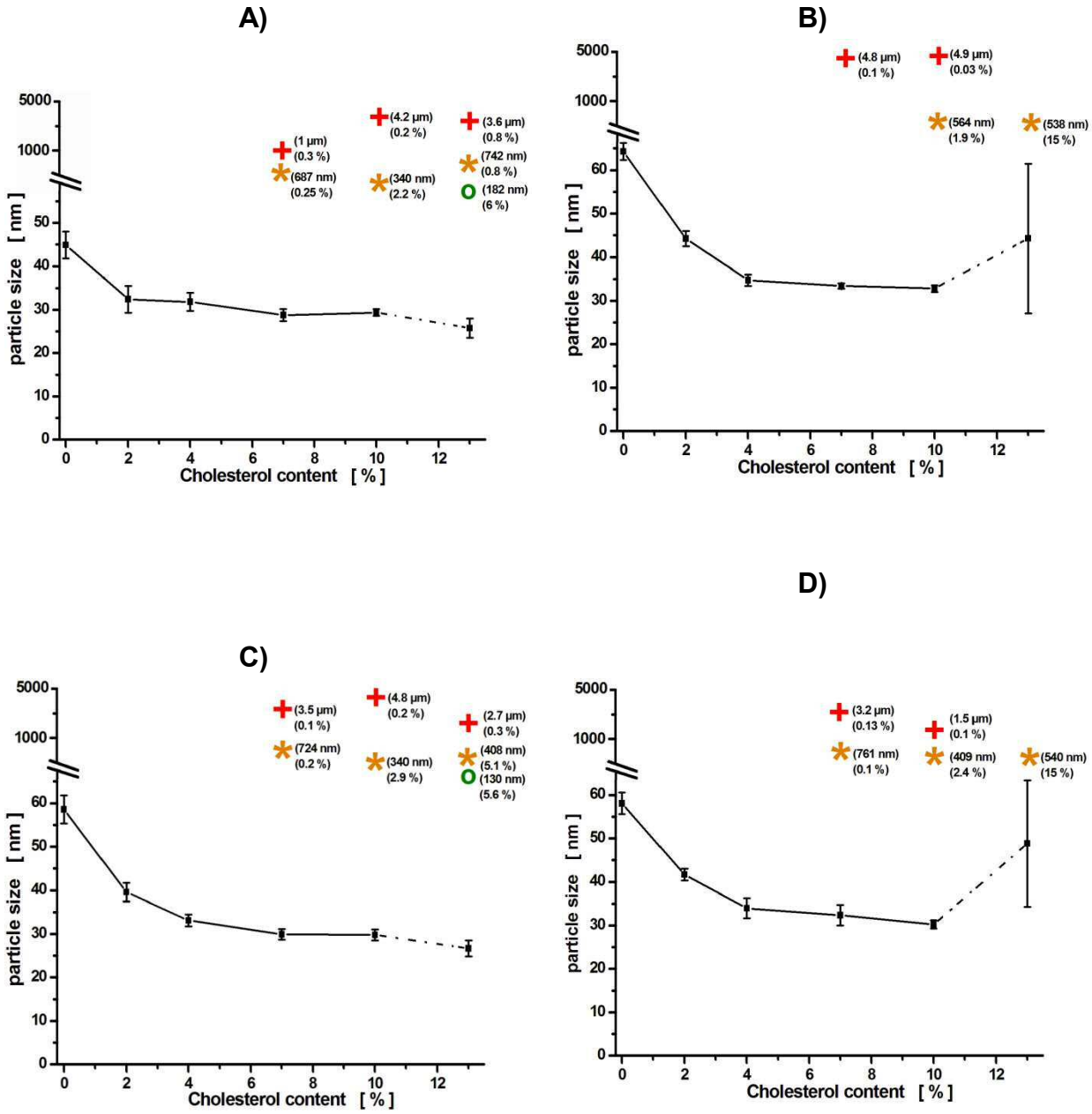

Fig.3.2-5: Average nanoparticle size (3 sample average) of gastrointestinal model fluids FaSSIF-C containing various amounts of cholesterol and **A)** Fenofibrate, **B)** Carbamazepine, **C)** Danazol and **D)** Griseofulvin. At high cholesterol content additional large particles appear as minor components, which are indicated as symbols off size scale (+, *, o).

increasing amount of cholesterol occurred. At 13 % cholesterol, the major particle size increased to 49 nm. In samples depicting a cholesterol content of at least 7%, larger colloidal species (d > 400 nm) and big particles (>1 µm) were observed. The particle size of Griseofulvin–saturated FaSSIF-C decreased with increasing cholesterol content.

3.2.4.3 Cytotoxicity Assay on Caco-2

The results of the cytotoxicity test of TM, $FaSSIF_{mod6.5}$ and FaSSIF-7C for 1-h incubation are shown in Figure 3.2-6. As compared to cell medium as control, the viability of the Caco-2 cells decreased by 20% with TM, but recovered to 94%-96% upon further addition of the

physiological bile components to TM. No significant difference is observed in results for cells treated with $FaSSIF_{mod6.5}$ and FaSSIF-7C. The viability of the cells was above 90% in $FaSSIF_{mod6.5}$ and FaSSIF-7C as compared with the negative control (culture medium).

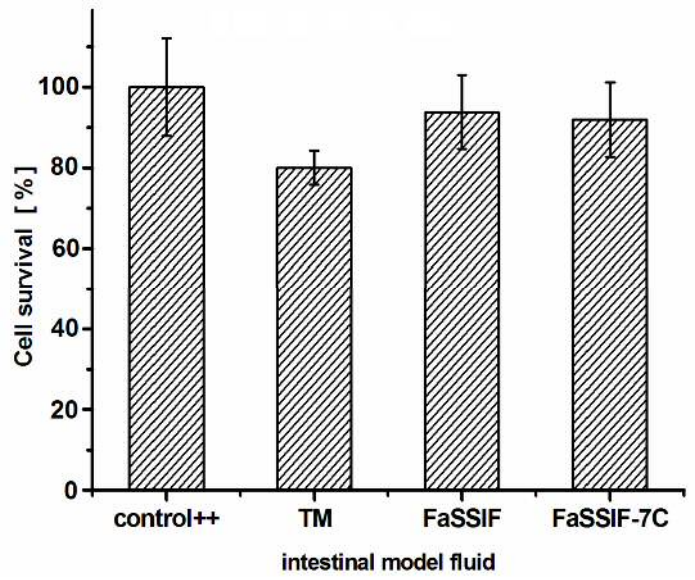

Fig.3.2-6: The biorelevant model fluid FaSSIF-7C and conventional $FaSSIF_{mod6.5}$ intestinal model fluids do not damage gut cells (Caco-2) upon incubation for 1h, while the bare transfer medium TM reduces the viability by 20%.

3.2.5. Discussion

In the current study, we have added cholesterol as a missing lipid entity in the intestinal model fluid FaSSIF-C in order to make it more similar to human intestinal fluids: FaSSIF-7C (7% cholesterol) modeled for healthy female, FaSSIF-10C (10% cholesterol) for healthy male, and FaSSIF-13C (13% cholesterol) for patients with diseases leading to cholesterol gall stones[37, 49]. This is relevant also to regional variations of the human bile composition, as the cholesterol content is different in Japan and northern Europe[167].

Lipophilic and amphiphilic vitamins and drugs form intermediate complexes with bile, lipids, and amphiphiles and their nanostructured assemblies in the gastrointestinal system[87]. Bile acids and lipids are capable to solubilize hydrophobic molecules by formation of mixed micelles and vesicles, for example, with cholesterol, fatty acids, monoglycerides, drugs, and vitamins[2, 39, 168]. Structure, dynamics, and interconversion of these nanoparticles and related liquid crystals have been intensely studied by biophysical methods[169-175]. The complex mixed particles, relevant for drug uptake, can be studied *in vitro* by time resolved and localizing methods of nanostructure research, for example, DLS and small angle scattering of x-rays and neutrons[3, 160, 161, 176]. Early studies of the intestinal bile micelle to vesicle conversion[159, 176]with rather concentrated solutions were improved by those using physiologically diluted systems. The low concentration of bile and lipid in the intestinal fluid and in $FaSSIF_{mod6.5}$, was with respect to the signal intensity compensated by deuterium solvent contrast in neutron scattering SANS[3]. The combination of DLS and SANS in twin or double beam experiments combined the wide range scale of DLS (10 nm to 50 µm with a projecting device), but at limited precision (10%-20%), with the highly precise results of neutron scattering SANS in a limited size window (1-500 nm).

The intestinal model fluids can be improved by addition of further amphiphilic materials. Kleberg et al.[155] showed that in FeSSIF with Fenofibrate, the rate and the total amount of lecithin, bile salt, oleic acid, and monoolein have an effect on the solubilization of the drug. Furthermore, the higher oil solubility of Fenofibrate shows that the solubilizing effect of the lecithin lipolysis products was greater than that of bile.
Cholesterol is a large flat hydrophobic molecule capable of vitamin and drug binding. In the gut, cholesterol is taken up at two regions (early jejunum and late ileum/colon). The enterohepatic circulation stabilizes the cholesterol pool in the body and enables the couptake of hydrophobic food entities, for example vitamins. In the human bile, cholesterol is solubilized by formation of mixed micelles with several bile acids and lecithin[30, 49-51]. In nanopharmacy and membrane sciences, liposomes from lecithin and cholesterol[171] are usual as transport and model particles, even after preparation with detergents[177]. Thus, a stability of lecithin-cholesterol-bile system can be assumed even for the chosen digestion model system.

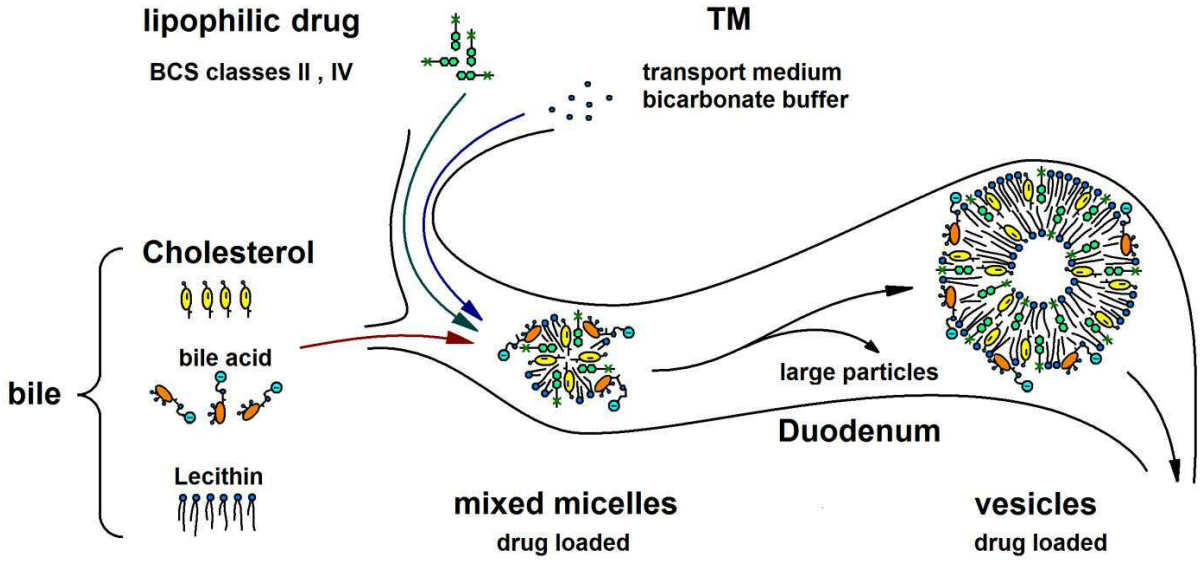

Fig.3.2-7: The nanoparticles in the simulated intestinal segment develop from micelles to liposomes, and some large particles in the presence of cholesterol. The drug solubility changes in partly parallel, which is an evidence for nano-intermediates.

By adding cholesterol in FaSSIF-C, the solubility data presented in this study show that cholesterol has a significant effect on the solubility of several example drugs in the medium. Additionally, the effect differed in several regimes of the cholesterol concentration for some drugs. The study was done near equilibrium (24 h) in order to separate the drug solubility from kinetic effects, which have to be investigated later. In parallel to the equilibrium drug solubility, the structure of the formed lipid-bile-drug nanoparticles (micelles, vesicles; Fig. 3.2-7) in the modelled duodenum varied with the cholesterol concentration. The observed cholesterol effects depend on the drug structure.
By our DLS experiments in general, a decrease of the nanoparticle size with increasing cholesterol concentration was detected. The average size of the transient intestinal vesicles

without drug (Fig. 3.2-2) decreased from 70 nm in $FaSSIF_{mod6.5}$ to 25 nm upon addition of cholesterol in FaSSIF-7C and FaSSIF-10C (representing healthy persons: female and male). At high cholesterol content (7%-13%), additional very large particles were detected. These are indicated as symbols at the top of the graphs (2, 5) with the tentative low mass fraction, which is preliminary because of the size detection limit of the used DLS device (<6 µm). This limit was significant for Carbamazepine and Griseofulvin in FaSSIF-13C (high error). We assume that the large particles correspond to cholesteric and discotic particles extensively studied in the literature earlier, for example, for human bile, cholesterol-lecithin vesicles and, high-density lipoproteins[160, 178].

The more detailed investigation by neutron scattering SANS indicated that even the drug-free model fluids were mixtures of several nanoparticles species (Fig. 3.2-3). By the size, the large particles (>20 nm in Fig. 3.2-3c) were assigned to vesicles (particles 1), whereas small particles in Figure 3.2-3c (<20 nm) were identified as micelles (particles 4, 5); intermediate-sized particles correspond to transient intermediates,[3] similar to the "bicelles" in the literature[160]. The "very big particles" seen in the DLS experiments (symbols, 200 nm to several micrometer size) were not visible in SANS, because of the low q-limit of the method and instrument.

The addition of the BCS class II drugs to the medium influences the particle size and structure. Additional to micelles and vesicles, large particles were observed in FaSSIF-7C, FaSSIF-10C, and FaSSIF-13C. They contained more than one intestinal nanoparticle entity of different size in parallel. The additional large particles may be cholesterol disks or related nanoparticles (Figs 3.2-2 and3.2-5).

Cholesterol in the medium increased the drug solubilization capacity for Fenofibrate in FaSSIF-C in a complex way. In case of FaSSIF-10C, a maximal solubilization effect (3.78-fold enhancement) of cholesterol as compared to $FaSSIF_{mod6.5}$ (bile acid and lecithin alone) was observed (Fig. 3.2-1a). In parallel to the cholesterol effect on drug solubility, the nanoparticle structure development was concentration dependent (Figs. 3.2-4 and 3.2-5a). Without cholesterol, the drug solubility in FaSSIF is low (16.45 µg/mL), whereas this is 56 times more than the value of 0.2912 µg/mL reported for water[94]. The solubility increase at moderate cholesterol content with FaSSIF-7C and FaSSIF-10C is an evidence for a strong drug-cholesterol interaction in parallel to a replacement of simple vesicles [phosphatidylcholine (PC)-TC-drug] by cholesterol containing vesicles (PC-cholesterol-TC-drug), whereas larger particles occur as additional component (Fig. 3.2-4). For high cholesterol content (13%, disease), the data are of limited significance because of possible separation problems and material exchange between the different particles. The secondary diminishing of the drug solubility in FaSSIF-13C correlates with the occurrence of several large particles (symbols in Fig. 3.2-5a, probably cholesteric particles).

For Carbamazepine, the solubility of the drug does not show a significant dependence on the cholesterol content. The solubility of the Carbamazepine in TM with an addition of 3 mM sodium TC (without cholesterol and lecithin) was about 419 µg/mL, whereas the drug is reported as a BCS-class II material. This shows a significant increase by the bile acid alone, as compared with the solubility of the Carbamazepine in water (236 µg/mL). This demonstrates why the presence of cholesterol and lecithin in the media does not show a significant effect on the solubilization of Carbamazepine. The higher solubility of Carbamazepine in the medium without lipids indicates that the solubilizing effect of the bile

acid alone is greater than that of lipids and thus dominant. The structure of the nanoparticles in the model media in the presence of Carbamazepine (Fig. 3.2-5b) depends in a similar way on the cholesterol content as in the presence of Fenofibrate (Fig. 3.2-5a). The larger cholesterol-free vesicles are first replaced by smaller cholesterol vesicles, whereas large particles occur at high cholesterol content (≥7%). This indicates that either Carbamazepine does not show a strong cholesterol interaction, or it is abolished by the stronger bile acid interaction, which also causes the enhanced drug solubility.

For Danazol and Griseofulvin, a general decrease in the solubility of the drug, up to a factor of two, with increasing amount of cholesterol in the medium was found (Figs. 3.2-1c and 3.2-1d). The major reduction occurs at low cholesterol content. The existence of cholesterol in the liposomal structure has a negative effect on solubility of these drugs, which could be interpreted as a competition of drug and cholesterol on the lecithin entity. The strong solubility decrease in the low cholesterol regime correlates with the replacement of the pure lecithin vesicles by mixed vesicles in the DLS results (Figs. 3.2-5c and 3.2-5d). This is an evidence for the cause of the higher solubility at low cholesterol content by drug embedding in the molecular-ordered membrane phase (lecithin:drug excess ~40). Thus, the solubility loss is interpreted as a structural phenomenon. The secondary solubility increase by 13% at high cholesterol content (<7 %) in the case of Griseofulvin (Fig. 3.2-1d) correlates with the occurrence of large particles (symbols in Fig. 3.2-5d, 540 nm size). The structure of these particles is unknown for drug-saturated systems. The structure of these complex systems should be investigated by further structural studies.

In the literature, Kleberg et al.[155] demonstrated for cholesterol-free system, that oleic acid and monoolein in the media have little effect on the solubility of the Danazol. Hence, the chemical structure of the lipid has an important effect on the solubility of drugs. Tanaka et al.[179] reports that in the lower jejunum, the *in vivo* solubility of Griseofulvin was about 1.5–2 times higher than that in the upper jejunum. The author explained this by the concentration of the bile acid in the upper jejunum, which was about twofold lower than in the lower jejunum. On the contrary, the concentration of phospholipids in upper jejunum is about 3.5 mM, but only 0.12 mM in lower jejunum, because of digestion and uptake.[179] Thus, the effect of the phospholipids on solubility of Griseofulvin may be quite small.

In addition to drug solubility and intestinal nanoparticle structure, the biocompatibility of the physiological adapted gastrointestinal model fluids FaSSIF-C was studied. The cytotoxicity of FaSSIF-7C was evaluated in Caco-2 cells upon a medium incubation for 1 h (Fig. 3.2-6). According to literature, FaSSIF containing up to 5 mM bile salts and up to 1.5 mM phospholipids (cell culture medium diluted FaSSIF) was compatible with Caco-2 cells[16]. Our results show that there is no significant difference in the viability of the cells treated with $FaSSIF_{mod6.5}$ and FaSSIF-7C. This demonstrates that the presence of the cholesterol in the media does not show a negative effect on the cytotoxicity of the Caco-2 cells. Thus, the new FaSSIF-C media are suitable for *in vivo – in vitro* correlation and uptake studies.

3.2.6 Conclusion

This study shows that the addition of cholesterol to the pH-stabilized intestinal model medium $FaSSIF_{mod6.5}$ yields a biocompatible and more physiologically adapted model fluid FaSSIF-C. FaSSIF-7C and FaSSIF-10C are equivalent to female and male human bile. The influence of

intestinal cholesterol in the solubility of several poor soluble or lipophilic drugs (BCS class II and IV) is demonstrated with four drugs as example.
The intestinal particle structure was studied with a combination of the complementary methods neutron and DLS. All media contained complex particle mixtures. For the drugs studied, the particle size of the vesicles in the media showed a decrease with increasing cholesterol concentration. Additional large particles were detected at high cholesterol concentration (≥ 10%) as minor component, which could be cholesterol-rich disks.
For Fenofibrate, an increasing cholesterol concentration changes the properties significantly. The drug solubility increased by a factor of about 4 by addition of 7%-10% cholesterol. In contrast, the solubility of Danazol decreased with increasing cholesterol concentration. Griseofulvin showed a decrease in solubility by a factor of two at moderate cholesterol concentration (<10%). The effect of cholesterol on the solubility of the Carbamazepine was not significant, which is caused by the high bile acid-induced solubility of this drug even in cholesterol-free FaSSIF. The observed cholesterol effects can be interpreted as drug dependent: as a drug-cholesterol interaction in the case of Fenofibrate, or as a competition on the lipid, as in the case of Danazol and Griseofulvin. The composition of the biorelevant media affects the solubilization capacity and particle size of the hydrophobic drugs (Fenofibrate, Danazol, Griseofulvin, and Carbamazepine) in parallel but different. Thus, the change in the particle size is not the reason for the solubility effects. As a consequence, cholesterol addition to intestinal models fluids, for example, FaSSIF-C, is recommended for further studies with hydrophobic drugs. A later comparison with results from a larger number of drugs will enable a resolution of the tentative drug structure-related mechanisms of cholesterol interaction and bioavailability.

3.2.7 Acknowledgement

We are thankful for the funding by the German ministry of science and education BMBF, grant 05KS7UMA; the Forschungszentrum Juelich FZJ, Juelich Centre of Neutron Science JCNS, outstation at the FRM2 reactor Munich Garching; and support by the Dr. Georg-Scheuing Stiftung, Mainz. The SANS investigation of this research project has been supported by the European Commission under the 7th Framework Programme through the 'Research Infrastructures' action of the 'Capacities' Programme (NMI3-II Grant number 283883). This work was contributed to the EU-FP7 OrBiTo project (http://www.imi.europa.eu/content) as side ground.

References

The references are included (re-numbered) in the general reference section (5) of this thesis.

3.3. Bifurcation of the Nanoparticle-Excipient mediated Drug Solubilization Pathways of oral Formulations in the Gastro-Intestinal model Fluid FaSSIF$_{mod6.5}$

Thomas Nawroth, Pooneh Khoshakhlagh, Philipp Buch, Raphael Johnson, Peter Langguth, Lars Schmueser, Nadja Hellmann, Heinz Decker, Noemi Kinga Szekely

International Journal of Pharmaceutics, submitted

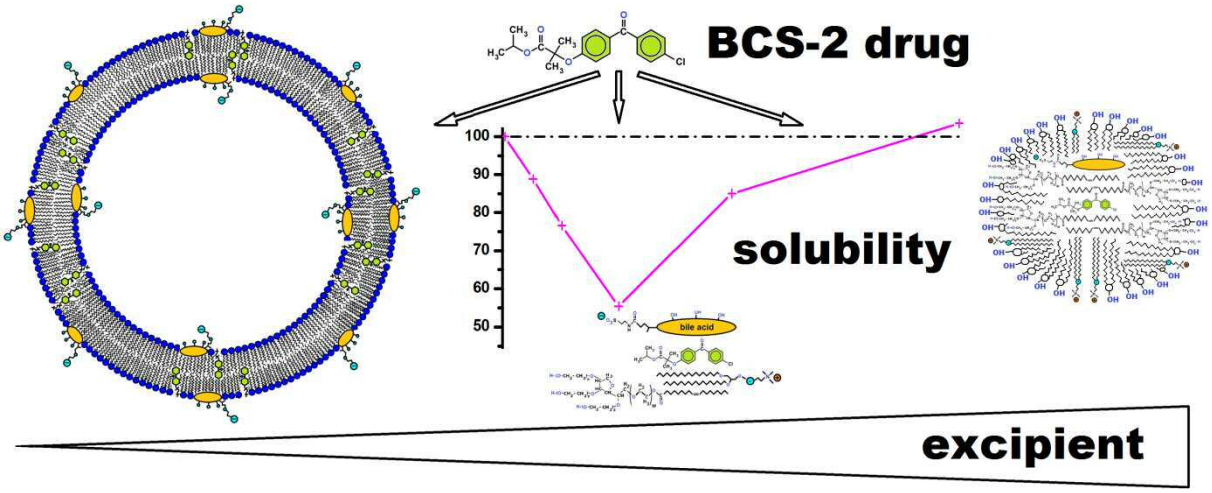

Fig.3-0: Excipient addition to intestinal model fluid FaSSIF$_{mod6.5}$ revealed for the hydrophobic drug Fenofibrate (BCS-2) a triple bifurcation of the solubilisation pathways and a drug solubility gap between the destruction of bile-lecithin liposomes and the formation of excipient rich micelles. The structures were investigated by quantitative dynamic light scattering DLS and neutron scattering SANS.

Key title: Bifurcation of excipient-drug nano-solubilization

Bifurcation of the Nanoparticle-Excipient mediated Drug Solubilization Pathways of oral Formulations in the Gastro-Intestinal Model Fluid $FaSSIF_{mod6.5}$

Thomas Nawroth[1], Pooneh Khoshakhlagh[1], Philipp Buch[1], Raphael Johnson[1], Peter Langguth[1], Lars Schmueser[2,3], Nadja Hellmann[2], Heinz Decker[2], Noemi Kinga Szekely[4]

Key title: Bifurcation of excipient-drug nano-solubilization

3.3.1. Abstract

Many new drugs show non-sufficient bioavailability and solubility, which is depicted by the BCS class 2-4. Drug embedding in lipid-detergent nanoparticles offers an opportunity for an improvement of the bioavailability of these difficult drugs. Such nanoparticles develop transiently from bile in the intestine, where they mix and restructure with food components or drug formulations.

By simulation experiments of the gastrointestinal system after bile secretion using FeSSIF and FaSSIF media, with and without drug, and additional detergents, we have investigated the occurrence of intermediate nanoparticles. The structures, micelles and liposomes, were observed with dynamic light scattering DLS and neutron small angle scattering SANS. The drug solubilization was correlated with the nanoparticle analysis. The quantitative tracing yielded the detergent and concentration dependence of three forms of soluble drug: in solution, solubilized in micelles and embedded in liposomes. The results indicated a bifurcation of the drug nanoparticle embedding into a liposomal and micellar branch, in parallel to the molecular resolved drug. An excess of detergents forced the pathway towards the micellar branch, but resulted in a breakdown of the well drug solubilizing liposomal phase. This indicates an opportunity of nanoparticle mediated drug uptake with lipid bilayers as an intermediate for a drug co-transport.

Key words: Excipients, drug carrier, biorelevant media, FaSSIF, DLS, SANS

Abbreviations:

BCS, biopharmaceutics classification system
cmc, critical micelle concentration
cmc_e, critical micelle concentration of added exipient
DLS, dynamic light scattering
Egg-PC, Egg-phosphatidylcholine
FeSSIF, fed state simulated intestinal fluid
FaSSIF, fasted state simulated intestinal fluid
$FeSSIF_{mod}$, fed state simulated intestinal fluid, bicarbonate-HEPES buffered, pH6.5
$FaSSIF_{mod}$, fasted state simulated intestinal fluid, bicarbonate-HEPES buffered, pH6.5
HBSS, Hank's buffered salt solution
HEPES, 4-(2-hydroxyethyl)-1-piperazineethanesulfonic acid
NP, nanoparticle
PSDi, particle size distribution by scattering intensity (DLS raw data)
PSDv, particle size distribution, particle volume scaled
SANS, small angle neutron scattering
Soy-PC, soybean phosphatidylcholine
TC, taurocholate
TM, transport medium

3.3.2 Introduction

Oral drug bioavailability is difficult for hydrophobic drugs, i.e. of the classes 2 and 4 of the Biopharmaceutics Classification System BCS[4, 10, 136, 144, 180] . Those materials can form uptake relevant intermediate complexes with lipidic nanoparticles, which develop from bile in the duodenum. The conditions in this part of the intestine are simulated in formulation development by the gastro-intestinal model fluids FeSSIF and FaSSIF[16, 26, 67, 69]which represent the situations of minimal bile dilution (fed state, FeSSIF), and average dilution (1:5) after gastric emptying after fluid intake (fasted state, FaSSIF).
The solubilization of hydrophobic drugs can be increased and accelerated by amphiphilic excipients in the formulation[138, 140, 181]. These may form intermediate mixed nanoparticles with drug, bile and food. An excipient induced drug solubilization is a first step in a formulation development with the aim of an increased bioavailability[157, 158, 181-183]. With hydrophobic drugs this is associated with a nanoparticle formation[3, 16, 137, 146].
In this study we describe the tracing of mixed nanoparticles from drug, excipients and bile by parallel drug solubilization study and dynamic light scattering DLS[3, 132, 162] with particle specific quantitative evaluation, and neutron small angle scattering SANS. With Fenofibrate as example of a hydrophobic drug of the BCS class 2 we found a bifurcation of the drug solubilisation and nanoparticle formation at simulated duodenal conditions upon administration of several amphiphilic excipients (detergents).

3.3.3 Material and Methods

3.3.3.1 Material

Egg *L-a*-lecithin 3-sn-phosphatidylcholin (Egg-PC, ≥99%) and sodium taurocholate hydrate (NaTC, ≥97%) were purchased from Sigma-Aldrich (Steinheim, Germany). HEPES was purchased from Merck. Glucose and methanol (p.A.) were purchased from Carl Roth. HBSS (Gibco14025) was purchased from Life Technologies (Paisley, UK).

3.3.3.2 Preparation of Transport medium

The transport medium (TM) was cell compatible buffer HBSS containing 4.167 mM $NaCO_3$ and 0.779 phosphate, supplemented with 19.45 mM glucose (final 25 mM) and 10 mM HEPES for pH stabilization[88] . The pH was adjusted to 6.5 with 0.1 M HCl. Finally the medium was sterile filtered (0.2 µm).

3.3.3.3 Preparation of $FeSSIF_{mod}$ and $FaSSIF_{mod}$

In this paper the model media $FeSSIF_{mod6.5}$ and $FaSSIF_{mod6.5}$ are abbreviated as $FeSSIF_{mod}$ and $FaSSIF_{mod}$ for easier nomenclature[88, 157, 158, 161, 182].
$FeSSIF_{mod}$: Into three separate tubes, 1.5 ml suspensions of 3.75mM of Egg-PC with 15mM Na-TC in TM were prepared. The suspensions were stirred about 15 minute at 37° C, and then agitated in an orbital shaker at 100 rpm for 1 day at 37°C, i.e. using the shake method[161].
$FaSSIF_{mod}$: To prepare the final solutions, $FaSSIF_{mod}$ dilutions of $FeSSIF_{mod}$ [157, 158, 161, 182]with transport medium TM (1:5 = FeSSIF:TM) were prepared manually in a short time (< 2 s), incubated unstirred at 37°C overnight (15h).

3.3.3.4 Preparation of drug saturated FaSSIF$_{mod}$

Aliquots (1.5 ml) of solution from section 2.3 were suspended in 2 ml white caps (Eppendorf) with an excess of micronized Fenofibrate (~ 1 mg) and incubated overnight (15h) at 37 °C upon shaking in an orbital shaker at 150 rpm. The non-resolved drug was removed by centrifugation (15,000 RPM, 10 min., 37°C, Eppendorf 5804R centrifuge). The supernatant analyzed by DLS; a part was diluted 1:1 with methanol and analysed for the drug concentration by UV-spectroscopy at 290 nm (lambda 20 photometer, Perkin Elmer). The light absorption of a drug free reference sample treated as above was subtracted. The concentration estimation was done with separate calibrating curves in FaSSIF containing the same excipient. All samples and experiments were done in triplicate (3 x 3).

3.3.3.5 Particle size estimation by Dynamic Light Scattering DLS

The particle size distributions were estimated by dynamic light scattering DLS using a Zetasizer Nano-ZS device, Malvern, Worcestershire, UK. The raw size distributions (by scattered light intensity; PSDi) were evaluated yielding volume contributions of micelles and liposomes as done in our previous investigation[3, 161]: For a component analysis (fig. 3.3-3, 3.3-5 – 3.3-7 and table 3.3-1) the raw intensity data were exported as text file with the Zetasizer Software V6.2, and scaled in Origin^{tm} 6.0, Northampton, MA, US after completing the radius values (the procedure and an example is shown in www.mpsd.de/DLS_dataexport_Malvern.html with the template "DLS_Malvern_d-template.txt"). Particles smaller than 20 nm were identified by size as micelles (massive), larger as liposomes. The raw intensity data were scaled to particle volume contributions c_{m3} (PSDv) for micelles (massive particles) as rough estimate by $1/r^3$ yielding the volume (~ mass) contribution using the Zetasizer Software V6.2 (Malvern Instruments Ltd.), for liposomes the scaling by $1/r^2$ yielding c_{m2} was done with Origin^{tm}. The relative micelle contribution to the nanoparticles[3] was calculated from the raw peak area of c_{m3} (PSDv) $c_1$as $P_m = 100\% * c_1 / (c_1 + c_2)$, while the liposome contribution was estimated from the raw peak area c_2 of c_{m3} (PSDv) and the particle size ratio as $P_l = c_1*(s_l/s_m)/ (c_1 + c_2)$ by the reverse scaling described in the text to fig.3.3-3.

3.3.3.6 Particle structure estimation by Neutron small angle scattering SANS

The precise structure estimation of the nanoparticles in the intestinal model fluid in a regime of <100 nm particle size was done with neutron small scattering SANS. The experiments were done with the Instrument KWS-2 at the FRM-II reactor using a cold neutron source beam at the Heinz Maier-Leibnitz Zentrum MLZ, Munich-Garching. The samples were prepared with 71 % D_2O-buffer for improving the contrast, but avoiding possible aggregation problems (at high D_2O content). The scattering experiments were done with neutrons of 0.453 nm wavelength at a sample-detector distance of 7.68 m. The momentum transfer q was estimated as $q = (4\pi/\lambda) \sin(\theta)$, where λ is the wavelength of the radiation and θ is half of the scattering angle. After normalization to beam intensity (monitor and subtraction of empty cuvette and buffer scattering), the scattering profiles were evaluated according to the Guinier approximation for small momentum transfer q[141], and by Kratky-Porod plot of the layer scaled intensity $I_d = I(q)*q^2$ yielding the span of the liposome membranes[142, 184]. The size s_l of

the liposomes was calculated from the radius of gyration R_g and the layer span d_l of phospholipid membranes as $s_l = 2 * R_g + d_l$ [142].

3.3.4 Results

The structure investigation of an intestinal model fluid containing an amphiphilic excipient upon the solubilization of the hydrophobic drug Fenofibrate (BCS class 2) by dynamic light scattering DLS is shown in fig.3.3-1 for a medium with 0.25% (w/v) Tween20 as example.

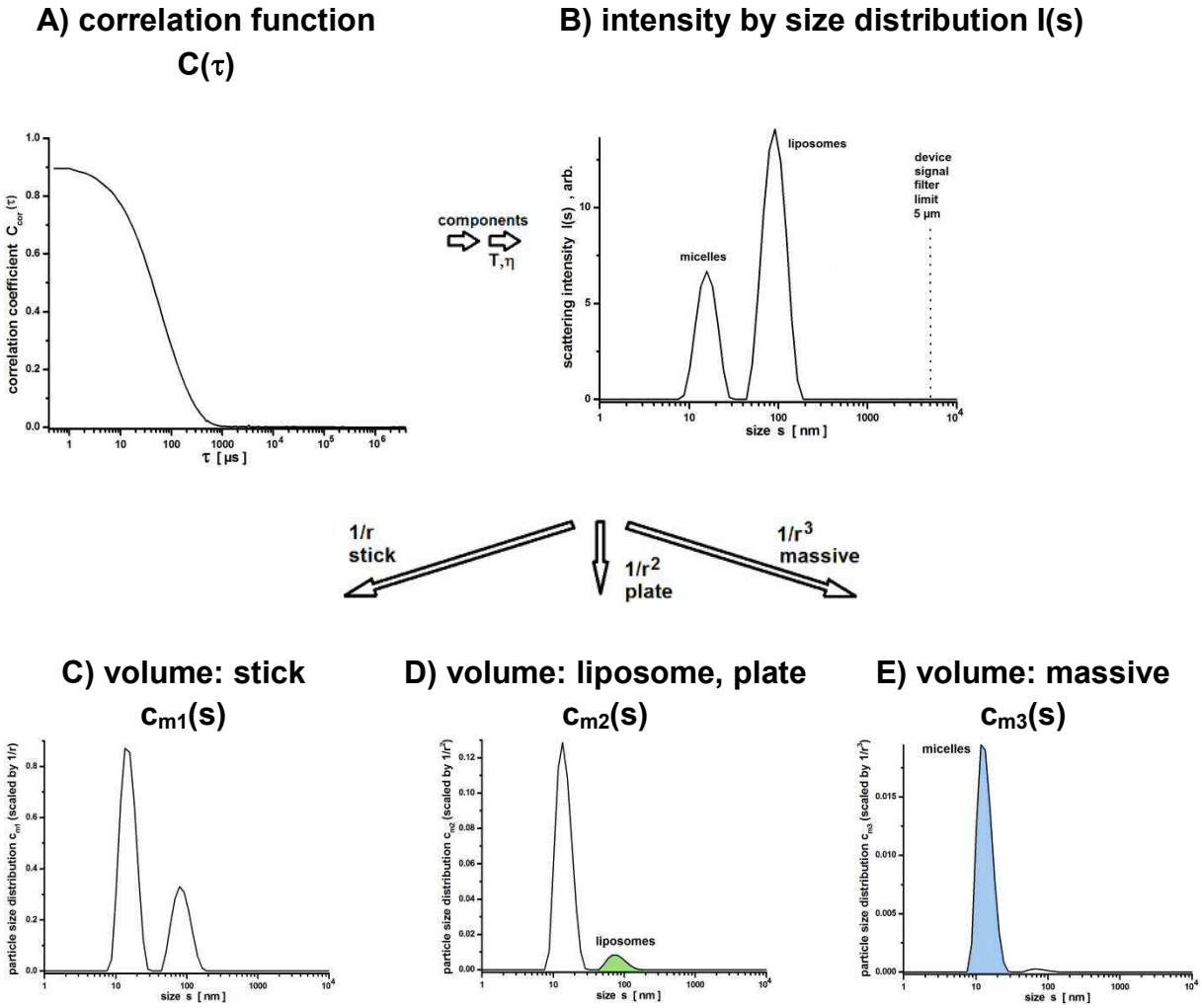

Fig.3.3-1: Structure investigation of Fenofibrate saturated $FaSSIF_{mod}$ containing 0.025% (w/v) Tween20 after 15h incubation by DLS and evaluation to particle size distributions PSD. From the scattering fluctuation signal the correlation function (A) is obtained by a correlator device, which yields the intensity particle size contributions I(s) (B, PSDi). The assignment to particle volume (mass) contributions needs assumptions of the particle shape, which may be a stick (C, $c_{m1}(s)$), plate or liposome (D, $c_{m2}(s)$), or a massive nanoparticle (E, $c_{m3}(s) \approx PSDv_3$).

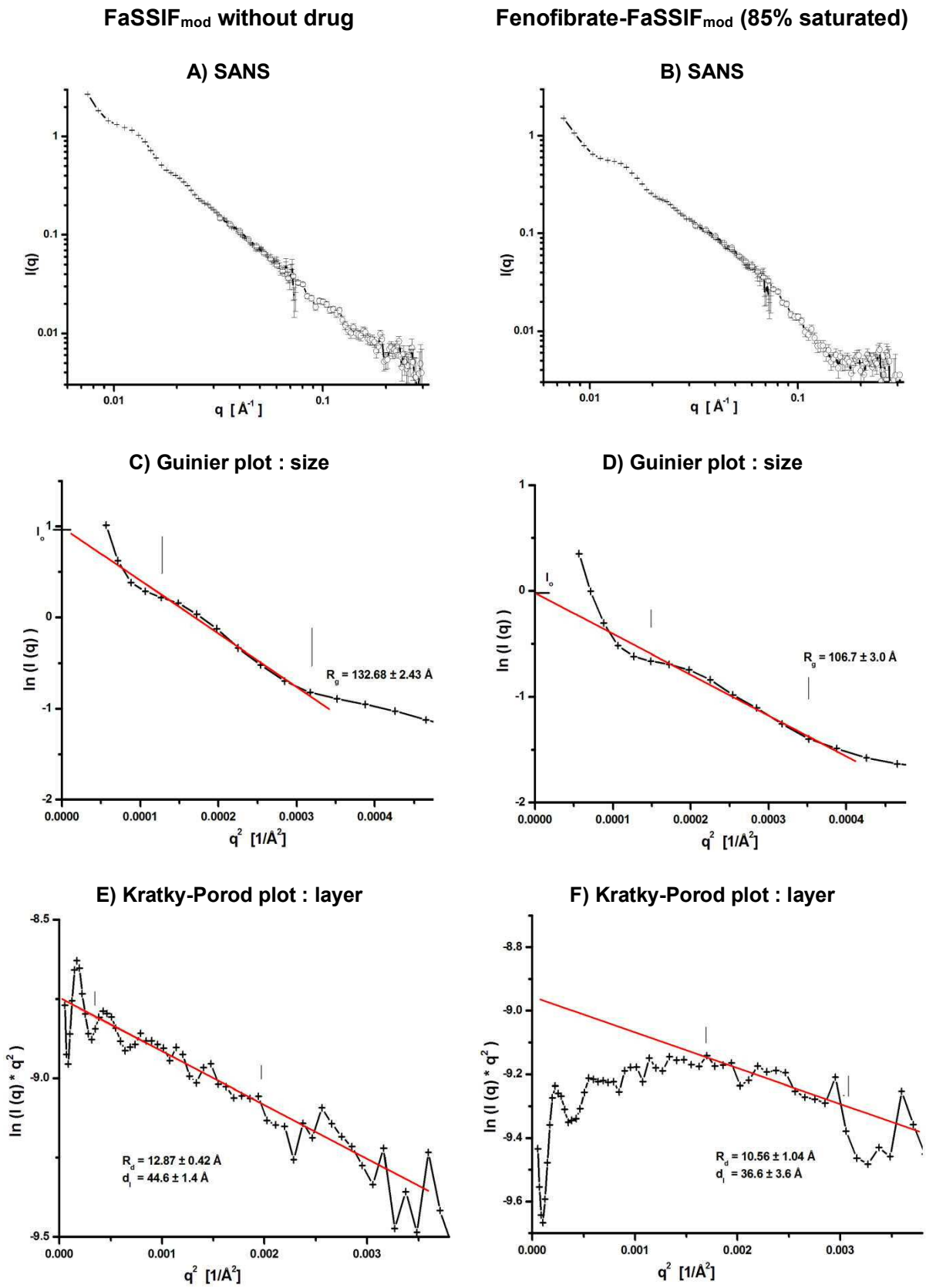

Fig.3.3-2: Neutron small angle scattering of 7 h old FaSSIF$_{mod}$ **left)** without drug and **right)** with 12 µg/ml Fenofibrate. The neutron small angle scattering SANS **(A,B)** is evaluated in **(C,D)** by Guinier plot yielding the size parameters radius of gyration R_g and zero angle scattering I_o, while (**E,F)** the layer thickness radius R_d and span d_l of the surface layer is obtained by the Kratky-Porod plot.

From the autocorrelation C(τ) of the intensity flickering caused by the Brownian motion (fig.3.3-1A) the scattering intensity distribution on the particle size I(s) is obtained (fig.3.3-1B) by component analysis and scaling with the parameters temperature T and the solution viscosity η[132, 162]. The further evaluation towards the volume related particle size distribution PSDv depends on the assumed particle structure and the resulting intensity scaling for either C) sticks by scaling to c_{m1} with 1/r, or D) liposomes and plates by scaling to c_{m2} with $1/r^2$, or D) massive particles and micelles by scaling to c_{m3} with$1/r^3$ [3, 162]. In the example the raw data (C) show two wide peaks at s_1 = 15.69 nm and s_2 = 91.28 nm. According to literature and previous investigations[3, 161] and the neutron investigation below (fig.3.3-2) particles smaller than 20 nm were identified as micelles, larger as liposomes, i.e. particles requiring different scaling rules. The compatibility of pure and Fenofibrate containing $FaSSIF_{mod}$ and the presence of liposomes in the intestinal model fluid solutions was shown by neutron small angle scattering SANS of specimens after 7 h incubation, as depicted in fig.3.3-2. The signal to background quality was improved by preparation of the samples in 71% D_2O (deuterium contrast variation). From the SANS profiles of A) of $FaSSIF_{mod}$ in 71% D_2O and B) $FaSSIF_{mod}$ containing 12µg/ml Fenofibrate (~ 85 % saturated) a size analysis was obtained by the Guinier plots in C,D), yielding a radius of gyration of R_g = 13.27 ± 0.24 nm for $FaSSIF_{mod}$ and 10.67 ± 0.3 nm for Fenofibrate-$FaSSIF_{mod}$. The surface layer was indicated by Kratky-Porod plots in E,F), which yielded for $FaSSIF_{mod}$ a membrane span radius R_d = 1.287 ± 0.042 nm and a layer span of $d_l = R_d*\sqrt{12}$ = 4.46 ± 0.14 nm. For Fenofibrate-$FaSSIF_{mod}$ a span radius R_d = 1.056 ± 0.104 nm and a layer span of d_l = 3.66 ± 0.36 nm was obtained. This shows the presence of liposomes depicting a size of $s = 2*R_g + d_l$ [142] of s = 31.0 ± 0.63 nm in $FaSSIF_{mod}$ and s = 25.0 ± 1.0 nm in Fenofibrate-$FaSSIF_{mod}$. The increase at the left side of the SANS signals (fig.3.3-2A, B) indicates the presence of some larger particles in both samples, which were not resolved because of the limited length (sample-detector distance) of the SANS instrument. The drug containing sample depicted some additional details (right end of fig. 3.3-2B, left half of fig. 3.3-2F), which will be studied later (local drug organization).

The combination of the methods DLS and SANS gave the scheme for the interpretation of the DLS data on a quantitative scale shown in fig. 3.3-3. The relative contributions of the particles, micelles and liposomes, can be obtained by two ways: A) directly by scaling of the intensity function I(s) as shown in fig. 3.3-1 and subsequent peak integration, or B) indirectly by peak integration of I(s) or a volume related particle size distribution, e.g. c_{m3}, and subsequent re-scaling of the peak integrals for those peaks related to another scaling rule. By Malvern Zetasizer software 6.20 the intensity function I(s), which is here named intensity related particle size distribution "PSDi", and the particle volume related function for massive particles c_{m3} [3], here named "PSDv", are available, both including an automatic integration of the three mostly dominant peaks. From the latter, the contributions of micelles (particles < 20 nm) were taken, while the contribution of liposomes were re-scaled by the relation of the particle sizes $f = r_{liposome}/r_{micelle}$, i.e. correction of the wrong scaling with $1/r^3$ by $1/r^2$ at a relative scale. A comparison of the peak rescaling with results of directly scaled DLS functions and integration with Origin© showed only negligible differences (< 10%, resolution of the DLS method).

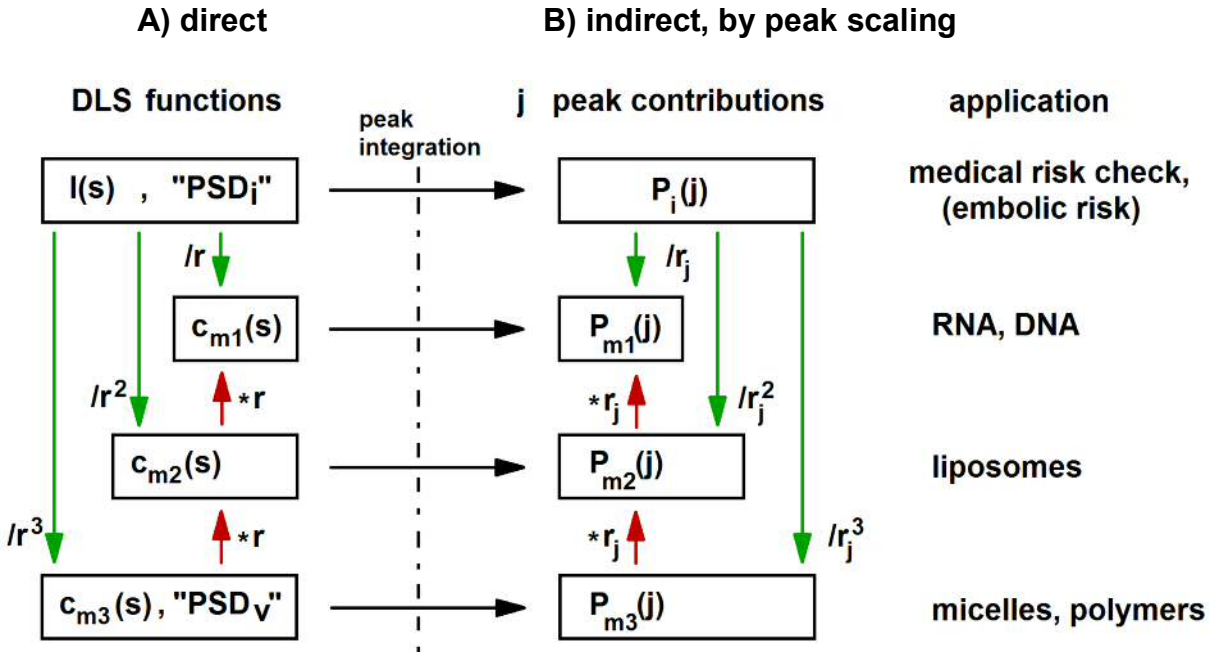

Fig.3.3-3: Evaluation sketch of the particle volume (mass) contribution of DLS for particle contributions of sticks ($P_{m1}(j)$), plates/ liposomes ($P_{m2}(j)$) and massive particles as micelles ($P_{m3}(j)$). The liposome contribution can be obtained directly ($\Rightarrow$) from $c_{m2}(s)$, or indirectly by reverse scaling by the particle radius r_j ($\Uparrow$) from the massive particle contributions $P_{m3}(j)$. With mixtures of liposomes and micelles, as present in $FaSSIF_{mod}$, the micelle peaks are obtained directly as $P_{m3}(j)$, the initially wrong liposome concentration by relative reverse scaling by $r_{liposome}/r_{micelle}$ to the same scale. The special nomenclature "PSDi" and "PSDv" refers to the Malvern DLS-software, which also delivers $r_j = s_j/2$, $P_i(j)$ and $P_{m3}(j)$.

The amphiphilic excipient effect on the solubilization of the hydrophobic drug Fenofibrate by the intestinal model fluid $FaSSIF_{mod}$ and the particle structure analysis is shown in fig. 3.3-4 for Tween20© at various concentrations. The drug solubilization (A), 14.15 µg/ml in pure $FaSSIF_{mod}$, first decreased until an excipient concentration of 0.05% (w/v). Then it increased up to a slight improvement (104%, 14.64 µg/ml) relative to $FaSSIF_{mod}$ at 0.2 % excipient (w/v), i.e. a drug solubility gap occurred between ~0.01 to 0.1 % excipient concentration, with a minimum of 7.83 µg/ml at 0.05 % excipient. The DLS investigation (fig. 3.3-4B-E) indicated a complex change from liposomes in Fenofibrate saturated $FaSSIF_{mod}$ to micelles in the excipient rich solutions. An example of the data treatment for 0.025% Tween20 is shown in fig. 3.3-4B-D: From the volume related particle size distribution (B, by the Malvern software), the peak contributions (areas) were estimated. The micelle data (fig. 3.3-4D) were taken as obtained, while the liposome content (fig. 3.3-4C) was re-scaled as shown above (indirect pathway in fig. 3.3-3). Finally the relative micelle contribution to the total nanoparticle concentration (upper curve in fig. 3.3-4D) was calculated as $c_{m,rel} = 100\% * c_1/(c_1 + c_2)$ from the absolute contribution c_1. The relative liposome contribution $c_{l,rel} = 100\% * c_2/(c_1 + c_2)$ was obtained from the absolute contribution c_2.The particle size analysis (peak centers in DLS) indicated, that the liposomes did not change in size significantly by the excipient addition, while the micelle changed over from large micelles in Fenofibrate saturated $FaSSIF_{mod}$ to small micelles in the excipient rich solution at $c_e \geq 0.05\%$ Tween20.

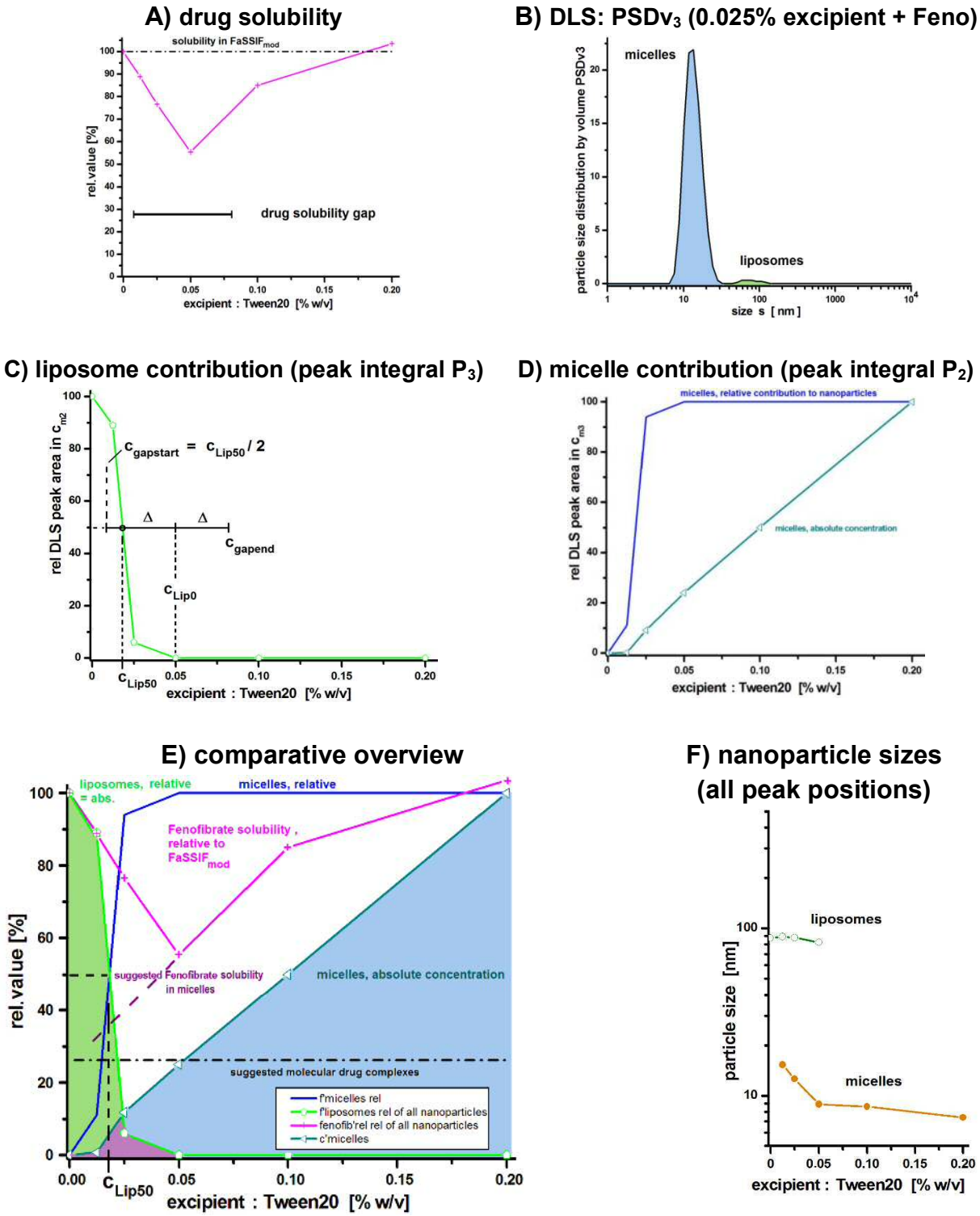

Fig.3.3-4: Development of Fenofibrate saturated FaSSIF$_{mod}$ at various excipient concentration of Tween20: **A)** the drug solubility (+) is compared with **B)** the DLS signals (0.025 % excipient w/v), which are evaluated for peaks of **C)** liposomes (>20 nm) as c_{m2} (P2) and **D)** for micelles (<20 nm) as c_{m3} (P3). The contributions are in **E)** combined in an overview of nanostructure and drug solubility. The micelle size **(F)** is in the coexistence range (0.0125 – 0.05%) larger as at excipient excess (≥ 0.05%). Traces: --+--: drug solubility; --o--: liposome contribution; ----: micelle contribution rel.; --◄--: absolute

For comparison, the DLS and drug solubility data were concluded in a comparative overview (fig. 3.3-4E), which is taken for data presentation of the further excipients. The results show a liposome destruction by a small detergent concentration which was calculated for 50% destruction as c_{Lip50} = 0.0183 %, and for complete destruction as c_{Lip0} = 0.05 % (w/v). The data are compared in table 3.3-1 with other excipients. The extrapolation of the right arm of the drug solubility to zero (dashed line in fig. 3.3-4E) results in a base drug solubility (dash-dot line in fig. 3.3-4E) which exceeds that in water and HBSS buffer. This, and the kink in the right arm of the solubility curve indicate the formation of molecular complexes of drug, bile and excipient, in parallel to the drug solubilized in liposomes (left) and excipient rich micelles (right).

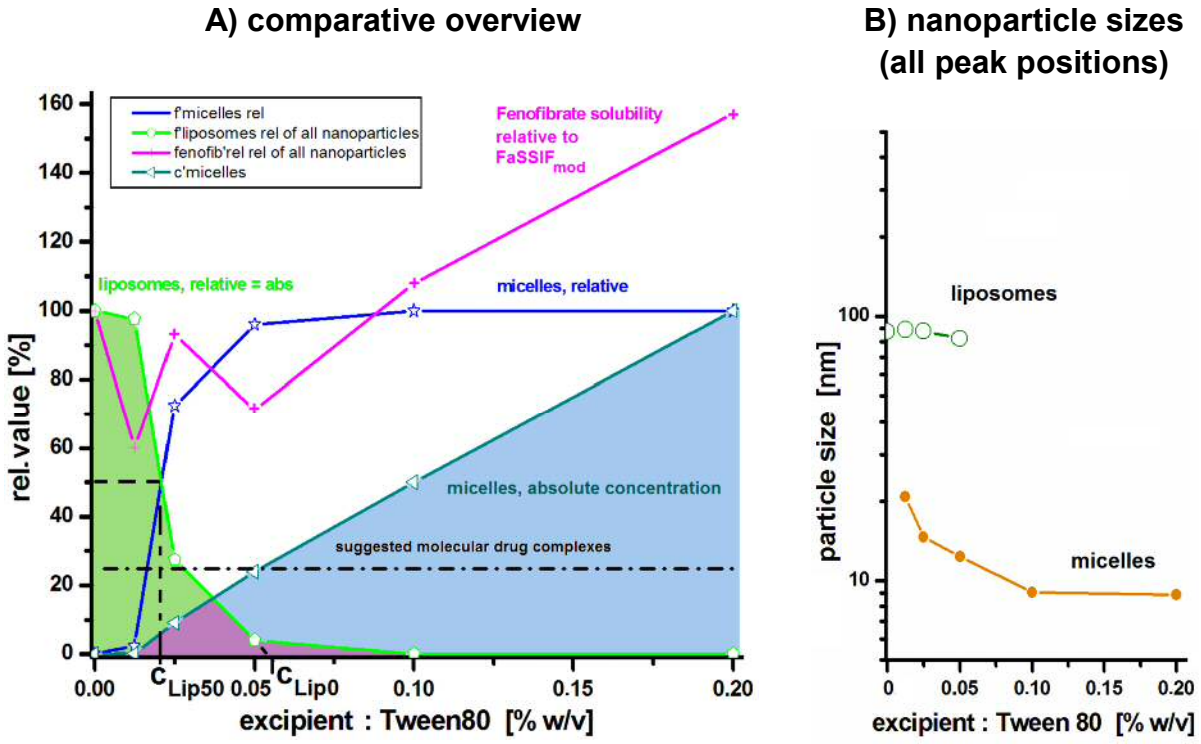

Fig.3.3-5: Development of Fenofibrate saturated $FaSSIF_{mod}$ at various excipient concentration of Tween80: The contributions are in **A)** combined in an overview of nanostructure and drug solubility. The micelle size **(B)** is in the coexistence range (0.0125 – 0.1 %) larger as at excipient excess (≥ 0.05%).

The amphiphilic excipient effect of Tween80© at various concentrations on the solubilization of Fenofibrate by the intestinal model fluid $FaSSIF_{mod}$ and the DLS particle structure analysis are shown in fig. 3.3-5. The comparative overview (A) depicts for the drug solubility a solubility gap between ~0.01 and 0.1 % (w/v) excipient, followed by an increase to 160 % relative drug solubility as compared to $FaSSIF_{mod}$. The results show in the gap region a liposome destructtion by a small detergent concentration which is compared in tab. 3.3-1 with other excipients. Tween80 as excipient resulted at 0.2% detergent in the best induced drug solubilization (22.25 µg/ml) of all studied excipients.

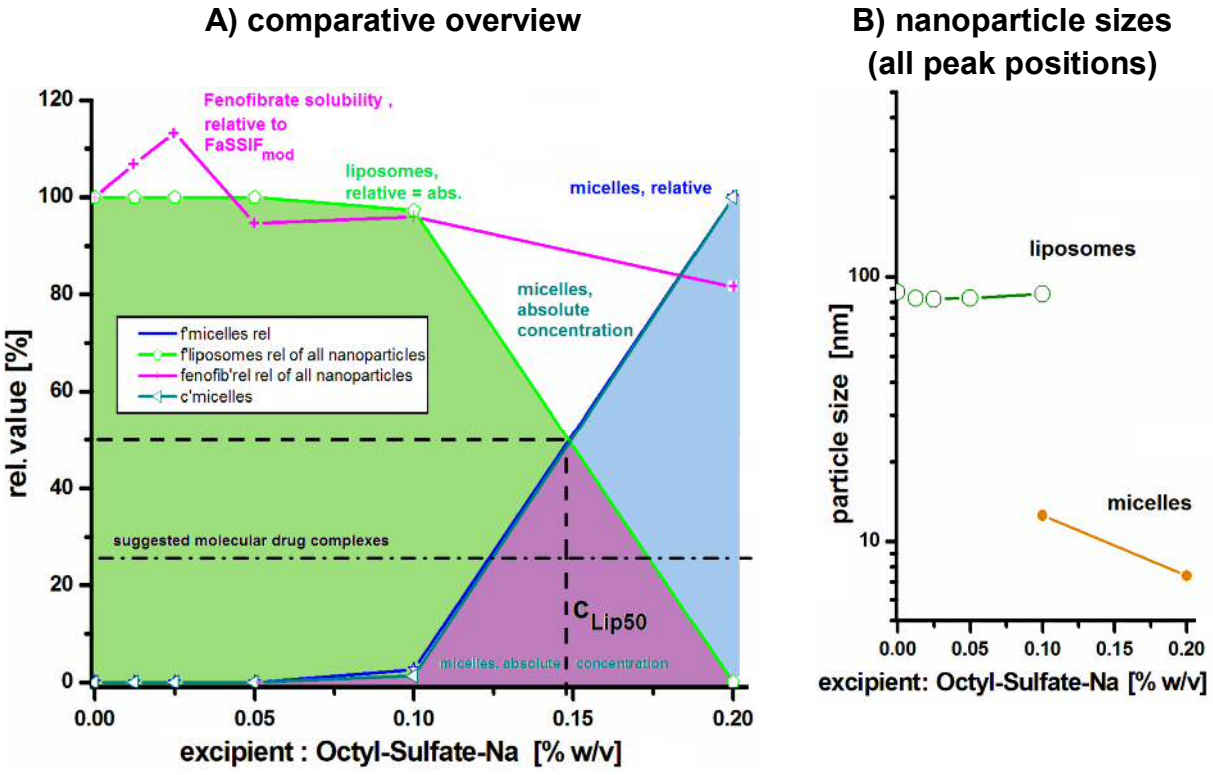

Fig.3.3-6: Development of Fenofibrate saturated $FaSSIF_{mod}$ at various excipient concentration of sodium-Octylsulfate: The drug solubility results and nanoparticle contributions from DLS are in combined in an overview.

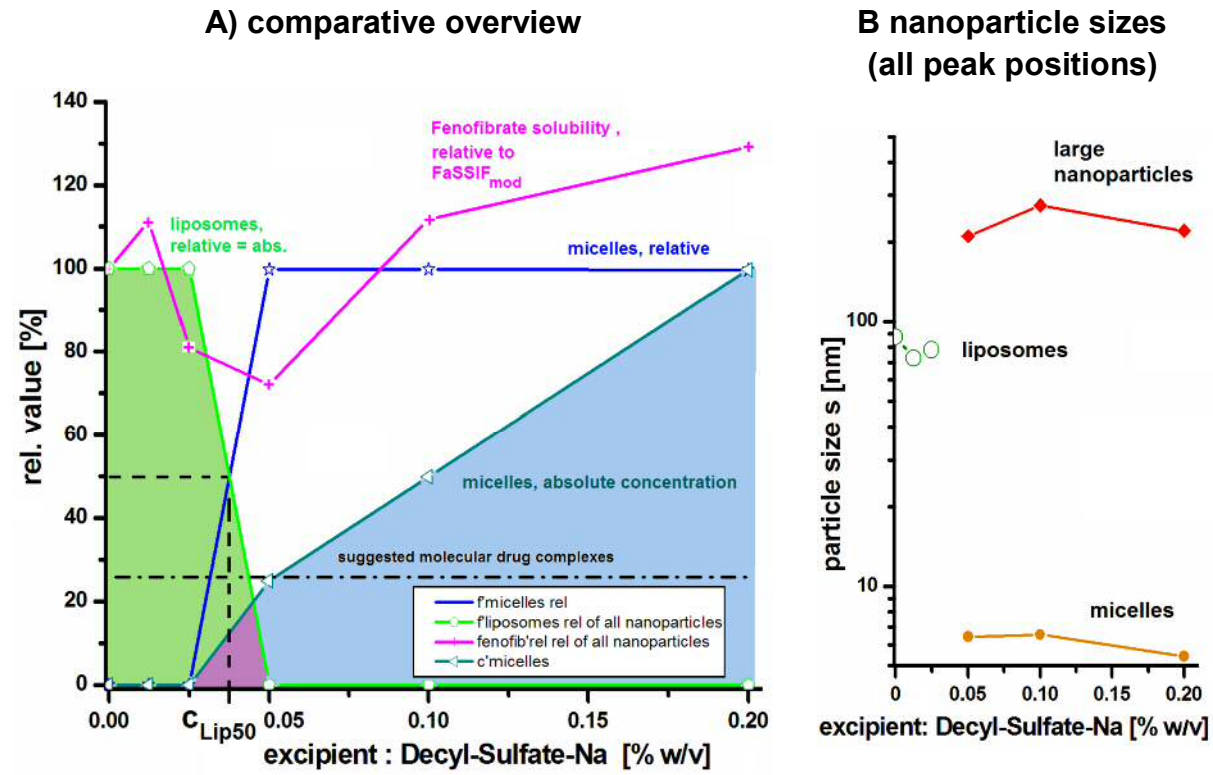

Fig.3.3-7: Development of Fenofibrate saturated $FaSSIF_{mod}$ at various excipient concentration of sodium-Decylsulfate: The drug solubility results and nanoparticle contributions from DLS are in combined in an overview.

The excipient effect of the ionic excipients octyl-sulfate sodium salt, and decyl-sulfate sodium salt at various concentrations on the solubilization of Fenofibrate by the intestinal model fluid $FaSSIF_{mod}$ and the DLS particle structure analysis is shown in fig. 3.3-6 and 3.3-7. The comparative overview (A) depicts for the drug solubility a solubility gap, followed by an increase to 130 % relative solubility as compared to $FaSSIF_{mod}$ in case of decyl-sulfate. Dodecyl-sulfate (SDS, not shown, the solubility data were published earlier[157, 158, 182]was very similar to decyl-sulfate.

Table.3.3-1: Table of liposome half loss c_{Lip50} and complete destruction c_{l100} concentrations in $FaSSIF_{mod}$ and the critical micelle concentration cmc_e (*) for some amphiphilic excipients for oral drug delivery. In the region $c_{Lip50}/2$ to $2c_{Lip0}$- c_{Lip50} the intestinal drug solubility is diminished because of a reduced nanoparticle content.

excipient amphiphilc	**cmc_e** (in H_2O)*		**liposome destruction parameters**		**→ solubility gap prediction**	
	[mM]	[% w/v]	**half** c_{Lip50} [%w/v]	**total** c_{Lip0} [%w/v]	**lower** $c_{gapstart}$ [%w/v]	**upper** c_{gapend} [%w/v]
Tween20	0.059	0.00724	0.0183	0.05	0.00915	0.0817
Tween80	0.012	0.00157	0.0212	0.1	0.0106	0.1788
Octyl-sulfat-Na	120	2.78724	0.148	0.2	0.074	0,252
Decyl-sulfat-Na	30	0.78099	0.0375	0.05	0.0187	0.0625
Dodecyl-sulfate-Na	8.3	0.23987	0.037	0.05	0.0185	0.063
Hexadecyl-sulfate-Na	0.6	0.02068	0.077	0.1	0.385	0.123
Octadecyl-sulfate-Na	0.2	0.07451	0.192	~ 0.4	0.096	~0.608
Cremophor EL	0.078	0.02	0.153	0.206	0.0765	0.259
Cremophor RH40	0.0488	0.039	(~ 0.35)**	(≥ 0.61)**	(0.175)**	0.87**
Poloxamer 188	~0.117	~0.105	no effect ≤ 0.2 %	no effect	no effect	no effect
Poloxamer 407	~0.076	~0.105	no effect ≤ 0.2 %	no effect	no effect	no effect

notes: *) the cmc_e is given for water; for $FaSSIF_{mod}$ it cannot be given as this already contains micelles and liposomes from bile acid and lecithin. Values in parenthesis () are extrapolated (c > 20 g/l).

The results show for all three alkyl-sulfates in the gap region a liposome destruction by a small detergent concentration which is compared in table 3.3-1 with six other excipients, where only the final results are presented.

The data on the drug solubility gap of excipient induced solubilization study of Fenofibrate in $FaSSIF_{mod}$ are compared in table3.3-1. This table compares the critical micelle concentration (cmc) with the observed liposome destruction parameters for half loss c_{Lip50} and complete liposome destruction c_{l100}. The drug solubility gap occurred with the studied excipients between

$\mathbf{c_{gapstart} = c_{Lip50}/2}$ **and** $\mathbf{c_{gapend} = c_{Lip50} + 2*(c_{Lip0} - c_{Lip50}) = 2*c_{Lip0} - c_{Lip50}}$.

**) extrapolated value

3.3.5 Discussion

The tracing of hydrophobic drugs and lipidic nanoparticles as intermediates of drug solubilization and possible uptake was done by a combination of drug dissolution study and nanoparticle structure investigation by dynamic light scattering DLS with particle specific quantitative evaluation, The DLS data and results (fig. 3.3-1) were scaled to particle volume contributions, which is equivalent to mass contributions at similar density, by structure case specific formalisms. According to the general scattering theory the scaling was in case of micelles as massive particles done by division by the third power of the particle radius r. In case of liposomes, the scaling was done by the second power of the particle radius, because of the constant span of the lipid bilayer, i.e. they show a two-dimensional volume increase with the particle size: a liposome is a spherical bent plate of constant span.

The structural equivalence of $FaSSIF_{mod}$ and the model fluid 85% saturated (12 µg/ml) with the hydrophibic drug Fenofibrate (BCS class 2) after 8 h development was shown by neutron small angle scattering SANS. The similar scattering profiles (fig. 3.3-2A,B) yielded by Guinier plots (fig. 3.3-2C,D) a size measure as radius of gyration R_g, which is for spheres (micelles) by $\sqrt{(5/3)}$ smaller than the particle radius r_j [141], but for liposomes equivalent to the membrane center radius r_m [142]. The existence of membranes and thus liposomes was proven by the linear range in the Kratky-Porod plots (fig. 3.3-2E,F), which yielded for pure and drug-loaded $FaSSIF_{mod}$ a membrane core span d_l of 4.4 nm and 3.6 nm respectively, which is similar to biomembranes in literature with the SANS method. The value is slightly smaller as that known for complete biological membranes (5 nm) because the SANS method is sensitive mainly for the hydrogen rich fatty acid core of the membranes, if no expensive deuterium contrast series is applied. Nevertheless those studies may resolve the tentative local drug organization in the samples, where an evidence is seen in the deviation between pure and drug media in fig. 3.3-2B (right end) and Fig. 3.3-4F (left half). A possible explanation is the formation of drug-rich domains.

With data from a comfortable DLS device with limited data access (Malvern Zetasizer©), the preliminary DLS peak integral results were re-scaled by the particle size (peak position r_j) with an equivalent result as with DLS function scaling (fig. 3.3-3). For the FeSSIF-FaSSIF system the existence of a structural development in time is partly known[3, 137, 140, 148, 161, 185].Thus the distinguishing between micelles (massive, scaling by $1/r^3$) and liposomes (plate-like, scaling by $1/r^2$) was done according to the particle size: a size $s < 20$ nm indicated indubitably micelles, while larger nanoparticle in the size range of $s = 20 \ldots 500$ nm were identified as liposomes. Very large particles, e.g. cochleate cylinders, cholesteric phases or

nanoparticle-protein complexes[186], occur only with special components or at high calcium concentration, but not in the investigated excipient-bile examples.
The comparative investigation of drug solubilization and nanoparticle formation at simulated late duodenal conditions indicated an excipient dependent bifurcation of the drug solubilization in $FaSSIF_{mod}$, here modelled by a 1:5 dilution of $FeSSIF_{mod}$ by the transfer medium TM containing a drug suspension resulting from gastric emptying and a pH-shift to pH6.5 in the first duodenum half[183]. This assumes a formulation disintegration in the stomach, or from a fast disintegrating enteric drug form.
At very low excipient concentration $c \leq cmc_e$ the simulated intestinal fluid developed to liposomes (~ 90 nm) from bile, which results in a partial solubilization of the hydrophobic drug, at sufficient long incubation time (15 h). This explains the observed, while low, Fenofibrate bioavailability with formulations without amphiphilic excipients.
An increasing excipient concentration resulted with the studied amphiphile excipients at moderate concentration in a breakdown of the native solubilization system liposomes and a drop of the drug solubility, probably after supersaturation[181]. This unfavorable effect is described by the typical liposome breakdown concentration c_{Lip50}, which differs for the excipients, but occurs at $c >$ the cmc_e.
At high excipient concentration a concentration dependent formation of excipient rich micelles is observed. The obviously contain the remaining bile acid and lipid from bile. With some excipients, Tween80 and to a lower extent with Tween20 and decyl-sulfate (or SDS), this is accompanied by an increased drug solubilisation[138, 140, 157, 158, 181, 182].

This is identified more precisely as a nano-solubilization, as the drug is in this regime included in excipient rich micelles. In the median excipient concentration region, between the bile-liposome destruction and the excipient rich micelle regime, an intermediate region was observed. Surprisingly the drug solubility exceeded in this region that in pure aqueous solutions (water, HBSS buffer), which indicates the partial formation of soluble molecular complexes from drug, bile and excipient. By the small size these were not detected by DLS, probably because of signal overwhelming by the parallel liposome and micelle signals.
The processes, summarized in fig. 3.3-9, indicate a triple bifurcation of the amphiphilic excipient dependent solubilization of hydrophobic drugs:

E_1: At low excipient concentration the drug is incorporated in mixed liposomes, the native solubilization agent, or an equivalent structure.

E_2: At moderate excipient concentration the liposomes are destroyed, but a minor amount of the drug is solubilized as molecular complexes of low size (invisible by DLS).

E_3: At high excipient concentration new micelles are formed from excipient, drug and bile (excipient rich micelles). These may result in an increased drug solubilization with a convenient excipient at sufficient concentration.

The findings explain why in some excipient studies a drug solubilization by excipients did not result in an increased bioavailability: If the drug is solubilized in the stomach by an excipient resulting in micelles of phase E3, it may happen that the further intestinal transport results in a dilution leading to the range E2. This would result in a drug oversaturation and precipitation[181]. The effect is indicated in the combined DLS-dissolution study as drug

solubility gap within the limits $c_{Lip50}/2$ and $c_{Lip50} + 2\Delta$ depicted in fig. 3.3-4C, where Δ is the excipient concentration difference of 50% loss c_{Lip50} and full destruction c_{Lip0} of the liposomes as established by DLS. The gap limits for the studied excipients and $FaSSIF_{mod}$ are summarized in tab. 3.3-1. In our study a favorable hydrophobic drug solubilization by excipient micelles was found for Tween80, and at lower extent for Tween20 and Decylsulfate, the corresponding improvement was earlier reported for dodecylsulfate SDS[157, 158, 182, 187]. Nevertheless all three nanoforms of excipient related drug solubilization may be successful, if the special formulations are optimized for their formation. An uptake over these nanoforms needs the preservation of the conditions during the intestinal transport to the drug specific uptake region in the intestine, and upon additional components, e.g. food. Thus this kind of studies will be continued including additional kinetics, food and lipid effects.

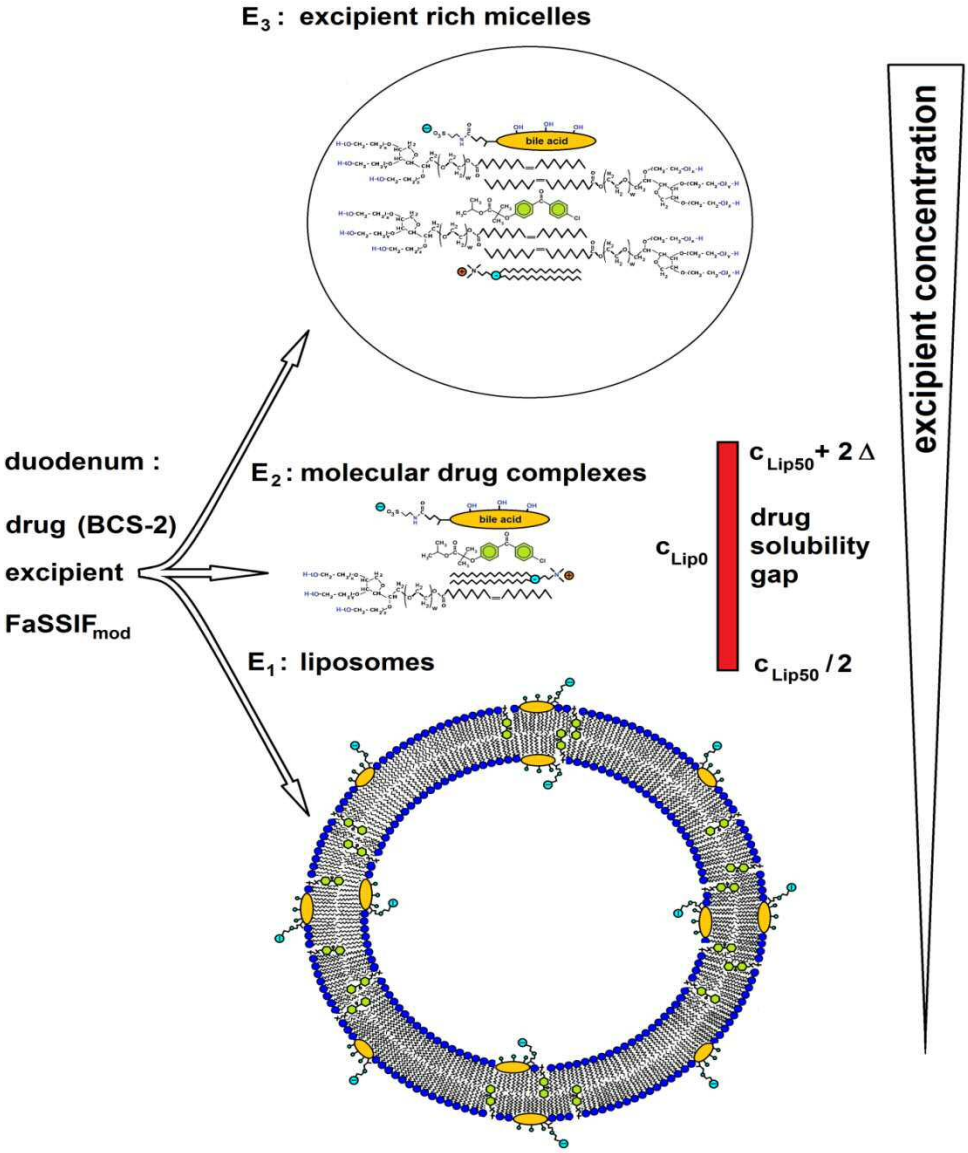

Fig.3.3-9: The hydrophobic drug Fenofibrate (BCS-2) and amphiphilic excipients were added to intestinal model fluid $FaSSIF_{mod}$. The combination of drug dissolution test, quantitative dynamic light scattering DLS and neutron scattering SANS revealed a bifurcation of the solubilisation pathways and a drug solubility gap between the destruction of bile liposomes and the formation of excipient rich micelles

3.3.6 Conclusion

By simulation experiments of the gastrointestinal system during bile secretion using FeSSIF and FaSSIF media, with and without drug and additional detergent formulations the occurrence of intermediate nanoparticles was investigated. The structures, micelles and liposomes, were observed with dynamic light scattering DLS and neutron small angle scattering SANS. The drug solubilization was investigated and correlated with the nanoparticle structure. The quantitative tracing yielded the excipient and concentration dependence of three forms of soluble drug: embedded in liposomes, in molecular complex solution, and solubilized in excipient rich micelles. The results indicated a bifurcation of the solubilisation and nanoparticle embedding of the drug into a liposomal and micellar branch, in parallel to the molecular resolved drug, i.e. three forms of soluble drug. An excess of excipients forced the pathway towards the excipient micellar branch, but first resulted in a breakdown of the well drug solubilizing liposomal phase implying a drug solubility gap between. This offers a fast test opportunity of nanoparticle mediated drug uptake with DLS detection of intermediates of the drug nano-transport.

3.3.7 Acknowledgments

We thank Ms. Simone Röber and Ute Hartung for excellent technical assistance. We are thankful for the funding by the German ministry of science and education BMBF, grant 05KS7UMA; the Forschungszentrum Jülich FZJ, Jülich Centre of Neutron Science JCNS, outstation at the FRM-II reactor Munich Garching; and support by the Dr. Georg-Scheuing Stiftung, Mainz. This work has received support from the Innovative Medicines Initiative Joint Undertaking (http://www.imi.europa.eu) under grant agreement n° 115369, resources of which are composed of financial contribution from the European Union's Seventh Framework Programme (FP7/2007-2013) and EFPIA companies' in kind contribution."

Conflict of interest: There are no financial or commercial conflicts of interest.

References

The references are included (re-numbered) in the general reference section (5) of this thesis.

3.4. Excipient effect on the colloidal structure and drug solubility in cholesterol containing biorelevant intestinal medium (FaSSIF-7C) with Fenofibrate

Pooneh Khoshakhlagh, Raphael Johnson, Lidija Krebs, Peter Langguth, Thomas Nawroth, Nadja Hellmann, Heinz Decker, Noemi Kinga Szekely

Johannes Gutenberg University, Pharmacy and Biochemistry Institute, Division Pharmaceutical Technology, Staudingerweg5, D-55099 Mainz, Germany

Johannes Gutenberg University, Molecular Biophysics Institute, Jakob Welder Weg 26, D-55128 Mainz, Germany

Forschungszentrum Jülich GmbH, Jülich Centre for Neutron Science (JCNS) at Heinz Maier-Leibnitz Zentrum (MLZ), Lichtenbergstraße 1, D-85747 Garching, Germany

J. Pharmaceutical Sciences, submitted (2015)

Excipient effect on the colloidal structure and drug solubility in cholesterol containing biorelevant intestinal medium (FaSSIF-7C) with Fenofibrate

Pooneh Khoshakhlagh[1], Raphael Johnson[1], Lidija Krebs[1], Peter Langguth[1], Thomas Nawroth[1], Nadja Hellmann[2], Heinz Decker[2], Noemi Kinga Szekely[3]

Pooneh Khoshakhlagh[1], Raphael Johnson[1], Peter Langguth[1], Thomas Nawroth[1], Lars Schmueser[2,3], Nadja Hellmann[3], Heinz Decker[3], Noemi Kinga Szekely[4]

1. Johannes Gutenberg University, Pharmacy and Biochemistry Institute, Division Pharmaceutical Technology, Staudingerweg5, D-55099 Mainz, Germany
2. Johannes Gutenberg University, Molecular Biophysics Institute, Jakob Welder Weg 26, D-55128 Mainz, Germany
3. Forschungszentrum Jülich GmbH, Jülich Centre for Neutron Science (JCNS) at Heinz Maier-Leibnitz Zentrum (MLZ), Lichtenbergstraße 1, D-85747 Garching, Germany

3.4.1. Abstract

Surfactants are excipients that are commonly used in drug formulations for increasing the solubility of lipophilic drugs by nanoparticle structure formation. These nanostructures interact with colloidal structures of bile and food in the intestine. This study investigated the effect of Tween 80, Tween 20, decyl sulfate and dodecyl sulfate as model surfactants on the solubility of Fenofibrate in the cholesterol containing biorelevant medium, FaSSIF-7C. The structural development investigated with dynamic light and small angle neutron scattering revealed mixed micelles and liposomes. Surfactant at high concentration destroyed the liposome structure and increased the formation of surfactant rich micelles, which depend on the surfactant. The data showed that the solubility of Fenofibrate improved by a factor of four with the highest concentration of Tween 80 to a two-fold reduction with the maximum concentration of Tween 20. An intermediate solubility gap was observed at low concentrations of the surfactants. At moderate surfactant concentration the membrane stabilizing effect of cholesterol resulted in the formation of detergent enriched excipient-cholesterol-lecithin liposomes depicting a high solubilization capacity of the hydrophobic drug. At high detergent, these liposomes were destroyed and replaced by detergent rich mixed micelles of case selective drug solubility. The observation can serve as a key for formulations of poorly soluble drugs (BCS-II, IV) included in artificial lecithin-cholesterol nanoparticles.

Keywords: Surfactant, Biorelevant media, drug solubility, DLS, SANS, FaSSIF

Corresponding author:
PD. Dr. Thomas Nawroth
Department of Pharmaceutical Technology
Institute of Pharmacy and Biochemistry
Staudingerweg 5
D-55099 Mainz
Tel.: 0(049) 6131 - 3923416
Fax.: 0(049) 6131 – 3925021
Email: nawroth@uni-mainz.de

Abbreviations:

BCS, biopharmaceutics classification system
DLS, dynamic light scattering
FaSSIF-7C, fasted state simulated intestinal fluid, 7% w/v cholesterol
FeSSIF-7C, fed state simulated intestinal fluid, 7% w/v cholesterol
HBSS, Hank's buffered salt solution
HEPES, 4-(2-hydroxyethyl)-1-piperazineethanesulfonic acid
PC, phosphatidylcholine
SANS, small angle neutron scattering
TC, taurocholate
TM, transport medium

3.4.2 Introduction

In the gastrointestinal system, drug absorption is a complex interaction between the drug, its formulation (excipients), and the contents of the gastrointestinal (GI) tract[188, 189]. The solubility of the drug in the GI fluids and its permeability through lipophilic membranes are important parameters that impede a drug's bioavailability[16, 190]. Thus, for the prediction of in vivo dissolution and solubility, biorelevant media such as FeSSIF and FaSSIF have been designed. The composition of the traditional FeSSIF and FaSSIF was phosphatidylcholine (PC) and taurocholic acid (TC) to mimic bile micelles in the small intestine[16, 67, 69, 108]. These media have been improved to make them more similar to the body condition by variation of the amount and type of lecithin, osmolality and buffer capacity[16, 66, 69, 83, 87]. In $FeSSIF_{mod6.5}$ and $FaSSIF_{mod6.5}$, cell compatible buffer HBSS supplemented with glucose and HEPES was added to improve the buffer capacity[88]. In addition to bile salts and phospholipids, cholesterol is found in human intestinal fluids. Cholesterol is however, completely missing in most biorelevant media[2, 24, 48]. In our previous study we have introduced cholesterol containing biorelevant media (FaSSIF-C), similar to the human physiological situation. For healthy persons, a cholesterol content of 7 % of the total amphiphiles (FaSSIF-7C) is suggested[191], which can serve as a minimum cholesterol model for media simulation of female persons. For male and diseased persons 10% (FaSSIF-10C) and 13% (FaSSIF-13C) are recommended. The effect of this medium was studied on the solubility and nanoparticle structure development of some poor water soluble drugs.

Drug development of poorly water soluble drugs incorporate amphiphiles such as surfactants to improve drug solubilisation in dosage forms and also to enhance drug dissolution and absorption[60, 192-198]. Chemical structure of the surfactant, chemical structure of the drug, temperature, pH and ionic strength show effect on the function of surfactants in solubilizing drugs[199, 200]. Kleberg et al. reported[16] in their review that the presence of amphiphiles in the gastrointestinal fluids increases the solubility of many of these hydrophobic drugs by reducing the surface tension of gastrointestinal fluids, thereby improving the initial wetting of compounds. Intestinal amphiphiles are known to form mixed micelles and other colloid structures that solubilize compounds and hence increase their solubility. The effect of the interaction of these mixed micelles and colloids with additional amphiphiles in drug formulations have not been investigated structurally in literature. The study of surfactant effect in this new medium was necessary to have a better grasp of the influence of this type of excipients in combination with cholesterol. The *in vitro* influence of surfactants on colloidal structure of the intestinal model fluid, and their effect on drug solubilization is studied by dynamic light scattering (DLS) and neutron small angle scattering (SANS) using Fenofibrate as a lipophilic model drug (BCS- II).

3.4.3. Materials and Methods

3.4.3.1. Materials

Cholesterol, Egg-lecithin (99%) and sodium taurocholate hydrate (≥97%) were purchased from Sigma- Aldrich (Steinheim, Germany). Fenofibrate was obtained from Labochim, Hamburg. HEPES was obtained from Merck, Darmstadt. HBSS (Gibco 14025) was purchased from Life Technologies, Darmstadt. Glucose, sodium dodecyl sulfate and chloroform (HPLC grade) were delivered by Carl Roth, Karlsruhe. Tween 20 and Tween 80 were purchased from

Haasrode, Belgium and Fagron, Barsbüttel, Germany respectively. Sodium n-decyl sulfate was a product of Alfa Aesar, Karlsruhe, Germany.

3.4.3.2. Intestinal model media preparation and drug solubility study

The transport medium (TM) was prepared from cell compatible bicarbonate buffer HBSS (final 25 mM Glucose, 10 mM HEPES, pH 6.5) as described earlier[88] . FeSSIF-7C was prepared by the sequential film method[161, 191]. The solution was incubated overnight at 37^{0}C for equilibration. To prepare the final solution (FaSSIF-7C), FeSSIF-7C was diluted 1:5 with transport medium.

Various concentrations of surfactants (0.005%, 0.01%, 0.03%, 0.1% and 0.3% w/v) were added to the intestinal model media. Excess amount of the Fenofibrate was added to each tube. The solutions were allowed to equilibrate for 24h at 37^{0}C, 35% speed in a shaking water-bath (Köttermann, Haenigsen, Germany). After double centrifugation the drug content was analyzed photometrically as described earlier[191]. All experiments were done in triplicate.

3.4.3.3. Particle size estimation by Dynamic Light Scattering DLS

The particle size distributions were measured after centrifugation of the samples by dynamic light scattering (DLS) using a Zetasizer Nano-ZS device, Malvern, Worcestershire, UK. All samples were measured in triplicate at 37°C. The raw intensity data were exported and evaluated using Origin7.0 (Northampton, MA) as done in our previous investigation[3, 161]. Particles smaller than 20 nm were identified by size as micelles (massive) and larger ones as liposomes[198]. For micelles the mass/volume contributions were obtained from the $1/r^3$ scaled distribution C_{m3}, (Malvern software: PSD-v). For liposomes the mass/volume contributions were obtained from the $1/r^2$ scaled distribution C_{m2} as shown earlier[198].

3.4.3.4. Particle structure estimation by Neutron Small Angle Scattering SANS

The nanoparticle structure was investigated by neutron small scattering (SANS) in a regime of <100 nm. The Instrument KWS-2 at the FRM-II reactor at the Heinz Maier-Leibnitz Zentrum MLZ, Munich-Garching was used with neutrons of 0.453 nm wavelength at sample-detector distances of 1.8 and 8 m. For improved contrast the samples were prepared with 71 % D_2O-buffer. The momentum transfer $q = (4\pi / \lambda) \sin(\Theta)$, was calculated from the wavelength of the radiation λ and the half scattering angle Θ. For the particle size analysis the scattering profiles were estimated according to the Guinier approximation yielding the radius of gyration R_g. The liposome size $s_l = 2 * R_g + d_l$ was calculated with the lipid membrane span d_l as described earlier[142]. For comparable conditions during the colloid structure development[161] the FaSSIF-7C samples were prepared from FeSSIF-7C and transfer medium TM by mixing (1:5) with a stopped flow device (Biologique SFX20m, Grenoble, France). The data were taken in a time frame of 20 minutes after the dilution shot.

3.4.4. Results

3.4.4.1 Micelle to liposome conversion detection by DLS

The colloidal structure of FaSSIF-7C containing 0.03% (w/v) and 0.3% (w/v) Tween 80 without drug (24 pre-incubated) was investigated by DLS. Intensity raw data PSDi, and data evaluated for liposome and micelle contributions are represented in Fig. 3.4-1. The size profiles for 0.03% Tween 80 (Fig. 3.4-1A) showed liposomes with an average particle size s_{av} = 77.4 nm, while the most frequent particle size was s_{max} = 67.8 nm. FaSSIF-7C containing

0.3% Tween 80 revealed mostly (99.85%) micelles with an average particle size of s_{av} =8.3 nm, and a most frequent size of s_{max} = 9.5 nm. A trace of liposomes with 86 nm size was detected in 0.3% Tween 80.

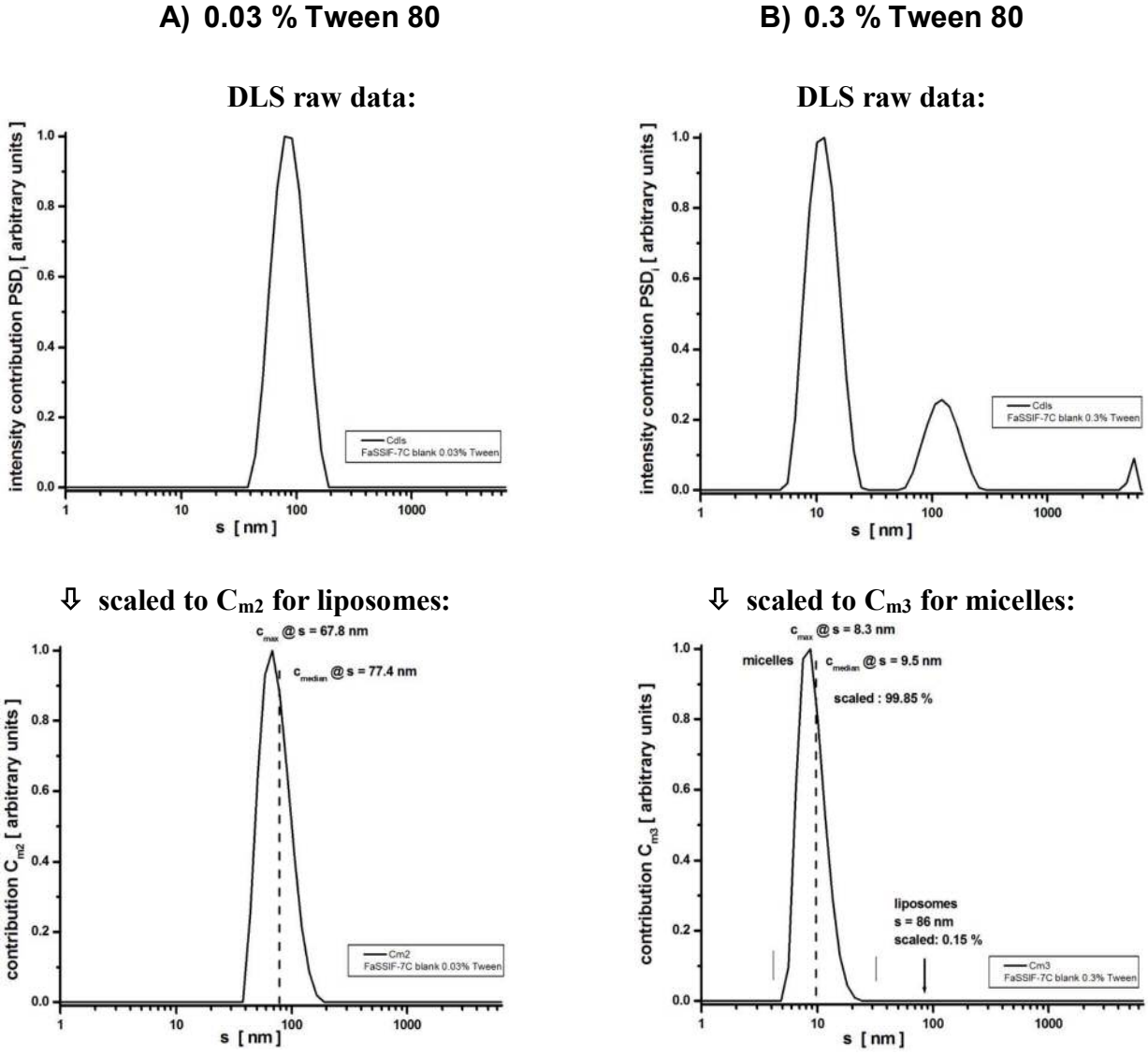

Fig. 3.4-1: Particle size distribution of FaSSIF-7C containing **(A)** 0.03%(w/v), and **(B)** 0.3%(w/v) Tween 80, 24h after preparation estimated by DLS as intensity data, and after evaluation to the volume(mass) contributions for liposomes C_{m2} and massive particles C_{m3} (micelles).

Figure 3.4-2 shows the DLS particle analysis of Fenofibrate saturated FaSSIF-7C containing 0.03% and 0.3% Tween 80, after 24h of preparation. The intensity raw data PSDi were treated for liposome (C_{m2}) and micelle (C_{m3}) contributions. In FaSSIF-7C with 0.03% SDS, the calculated average size s_{av} = 58.8 nm and most frequent size of s_{max} = 68.7 nm indicated liposomes. At 0.3% SDS micelles were the main component of the medium, while about 0.9% liposomes with particle size of 106 nm was detected as a minor component. The average particle size of micelles was s_{av} = 9.8 nm, with a most frequent size of s_{max} = 8.7 nm.

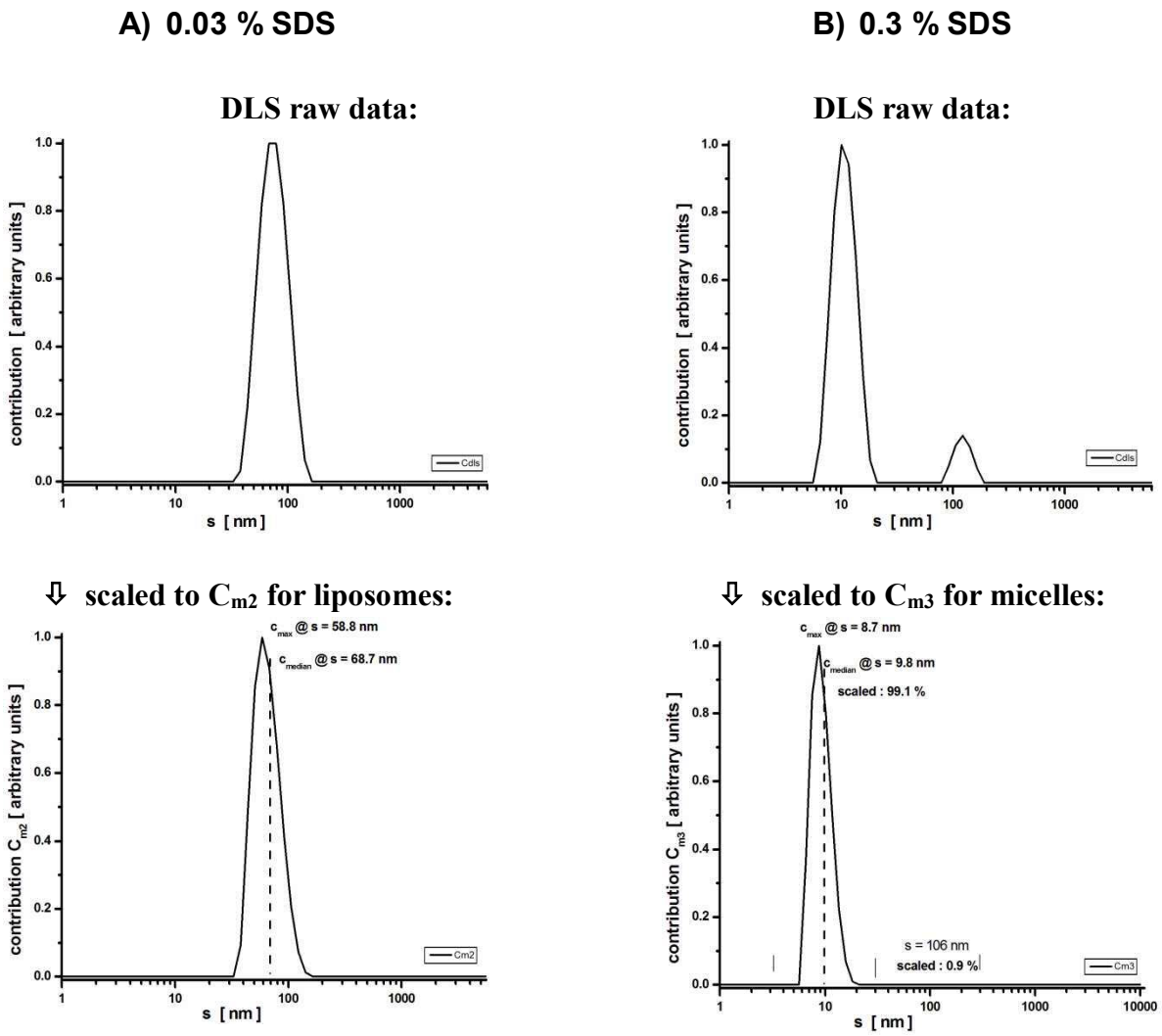

Fig. 3.4-2: Particle size distribution of Fenofibrate saturated FaSSIF-7C containing **(A)** 0.03%(w/v), and **(B**) 0.3%(w/v) SDS, 24h after preparation estimated by DLS as intensity data. They were further evaluated to the volume (mass) contribution for liposomes C_{m2} and massive particles C_{m3} (micelles).

3.4.4.2 Micelle structure investigation by SANS

The nanoparticle structure investigation of FaSSIF-7C in 71% D_2O buffer 20 minutes after preparation from FeSSIF-7C without excipient and drug by SANS is shown in Fig. 3.4-3: (A) as scattering profile and (B) as size analysis by Guinier plot at low q. The results indicated a mixture of two particle populations with R_{g1} = 14.529 nm ± 0.07 nm and R_{g2} = 5. 91 nm ± 0.12 nm, which were identified as liposomes and micelles, respectively. The liposome size was calculated as $s= 2*R_g + d_l$ = 34.1 ± 0.2 nm using a membrane span of d_l = 5 nm [23]. The size of the minor contribution of bile-lecithin micelles was calculated as $s = 2*R_g\sqrt{(5/3)}$ = 15.26 ± 0.36 nm assuming a spherical structure.

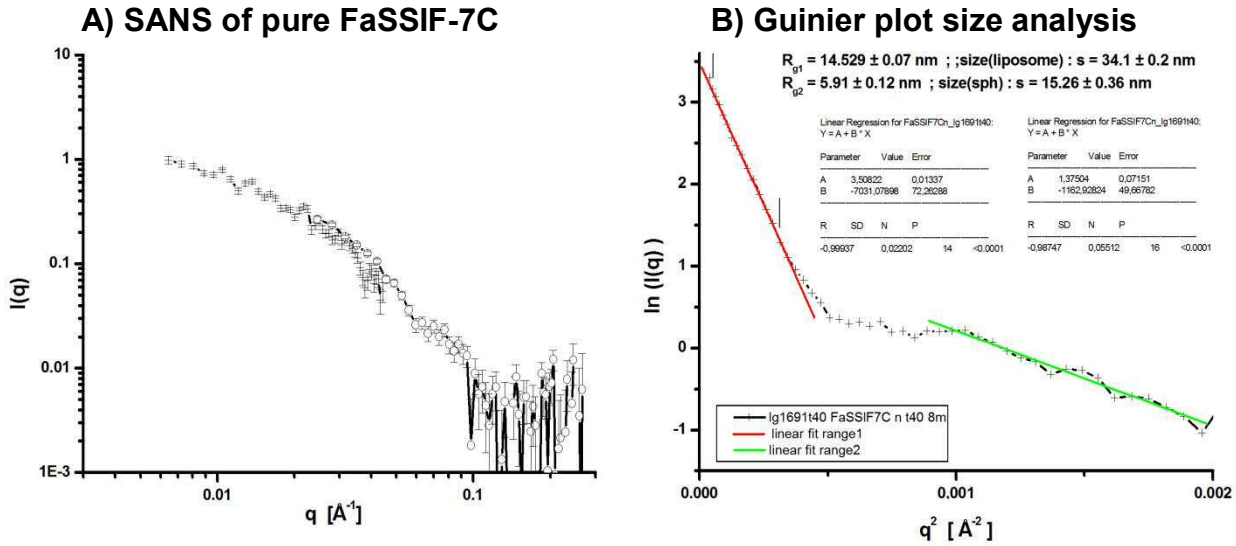

Fig. 3.4-3: Structure investigation of FaSSIF-7C in 71% D_2O buffer 20 min after preparation from FeSSIF-7C without excipient or drug addition: **A)** the SANS profile shows two contributions, and **B)** the Guinier representation indicates large particles, interpreted as liposomes of 34 nm size, and residual bile-lecithin micelles of 15.26 nm size.

The nanoparticle structure of the 20 minutes old FaSSIF-7C containing 0.03% and 0.3% Tween 80 in 71% D_2O buffer by SANS is shown in Fig. 3.4-4. (A) and (B) are scattering profiles and (C) and (D) are size analysis by Guinier plots. Figure 3.4-4A indicated mostly liposome scattering at low q (<0.04 $Å^{-1}$), while at high detergent concentration (Fig. 3.4-4B) mostly micelle scattering was detected. The radius of gyration of these component were estimated as R_g = 3.19 nm ± 0.05 nm and R_g = 3.142 nm ± 0.055 nm for medium containing 0.03% and 0.3% Tween80 respectively. Assuming a spherical structure, particles sizes of s = 8.24± 0.14 nm for 0.03% Tween 80 and s = 8.11±0.14 nm for 0.3% Tween 80 were calculated after scaling.

Figure 3.4-5 shows the nanoparticle structure determination of the 20 minutes old FaSSIF-7C containing 0.03% and 0.3% SDS in 71% D_2O buffer by SANS. (A) and (B) are scattering profiles, and (C) and (D) are size analysis by Guinier plots. Figure 3.4-5A showed some additional liposome scattering at low q (<0.03 $Å^{-1}$), whereas at high detergent concentration (Fig. 3.4-5B) only the micelle scattering was identified. The radius of gyration of these components R_g = 2.89 nm ± 0.059 nm and R_g = 1.933 nm ± 0.018 nm for medium containing 0.03% and 0.3% SDS respectively, were estimated. The size of mixed micelles after scaling for spherical structure of s = 7.48 ± 0.15 nm for 0.03% SDS and s = 4.99 ± 0.05 nm for 0.3% SDS was calculated.

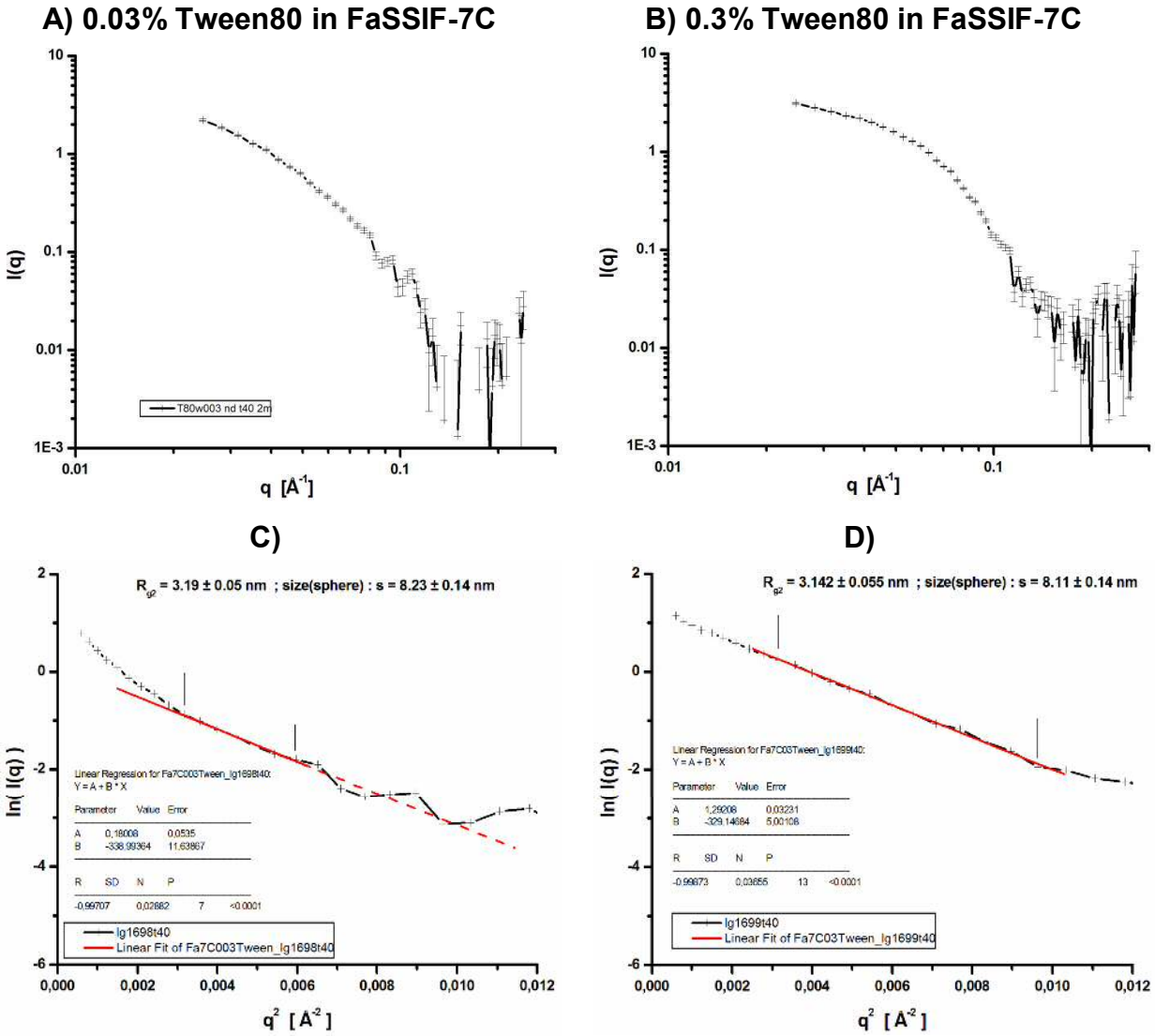

Fig. 3.4-4: Structure investigation of micelles in FaSSIF-7C in 71% D_2O buffer 20 min after preparation from FeSSIF-7C containing 0.03% (A,C) and 0.3% (B,D) Tween 80. The SANS profile at low detergent (A) consists of mostly liposomes scattering at low q (<0.04 $Å^{-1}$), while at high detergent (B) the micelle scattering was detected. The corresponding Guinier plots (C, D) indicate a mixed micelle particle size, which is nearly identical (s = 8.23 and 8.11 nm) for both detergent concentrations.

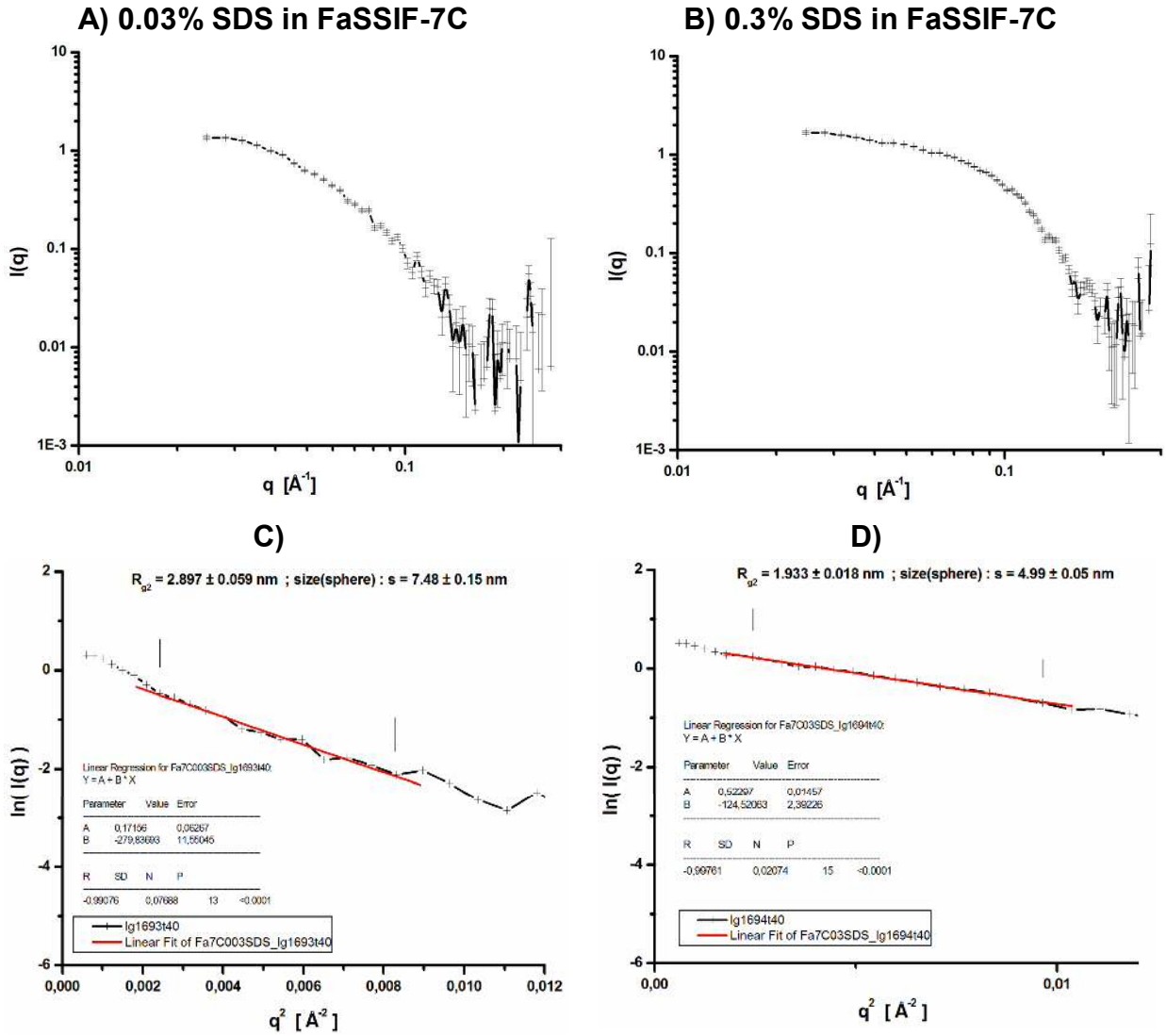

Fig. 3.4-5: Structure investigation of micelles in FaSSIF-7C in 71% D_2O buffer 20 min after preparation from FeSSIF-7C containing 0.03% (A,C) and 0.3% (B,D) SDS. The SANS profile at low detergent (A) consists of some liposome scattering at low q (<0.03 $Å^{-1}$), while at high detergent concentration (B) the micelle scattering was predominant. The corresponding Guinier plots (C, D) indicate a detergent concentration dependence of the mixed micelle particles, which are s = 7.48 ± 0.15 nm at 0.03 % SDS, and 4.99 ± 0.05 nm for 0.3% SDS.

3.4.4.3 Excipient effect on nanostructure and drug solubility

The effect of Tween 80 at different concentrations on the solubility of Fenofibrate in the intestinal model fluid FaSSIF-7C and DLS particle structure analysis are shown in figure 3.4-6. The solubility profile shows that this surfactant has a marked effect on the drug's solubility. At the lowest excipient concentration (0.005%) the solubility showed a decrease by a factor of 0.17 (solubility gap). By increasing the amount of the surfactant, there was a general increase in solubility of Fenofibrate. At 0.01% w/v, solubility increased by a factor of 1.83 and at 0.03% w/v concentration, the enhancement factor was 1.28 as compared to Tween 80-free medium. The solubility of the drug increased by a factor of up to 4.18 at high Tween 80

content (0.3% w/v). The DLS investigation indicated that the main particle contribution are liposomes in the medium up to 0.1% w/v excipient. An increase in surfactant concentration up to 0.3% w/v resulted in micelles in the medium. In media without drug (blank) but containing Tween 80, the particle size profile was the same as media with Fenofibrate. With DLS micelles were only detectable at 0.3 % excipient.

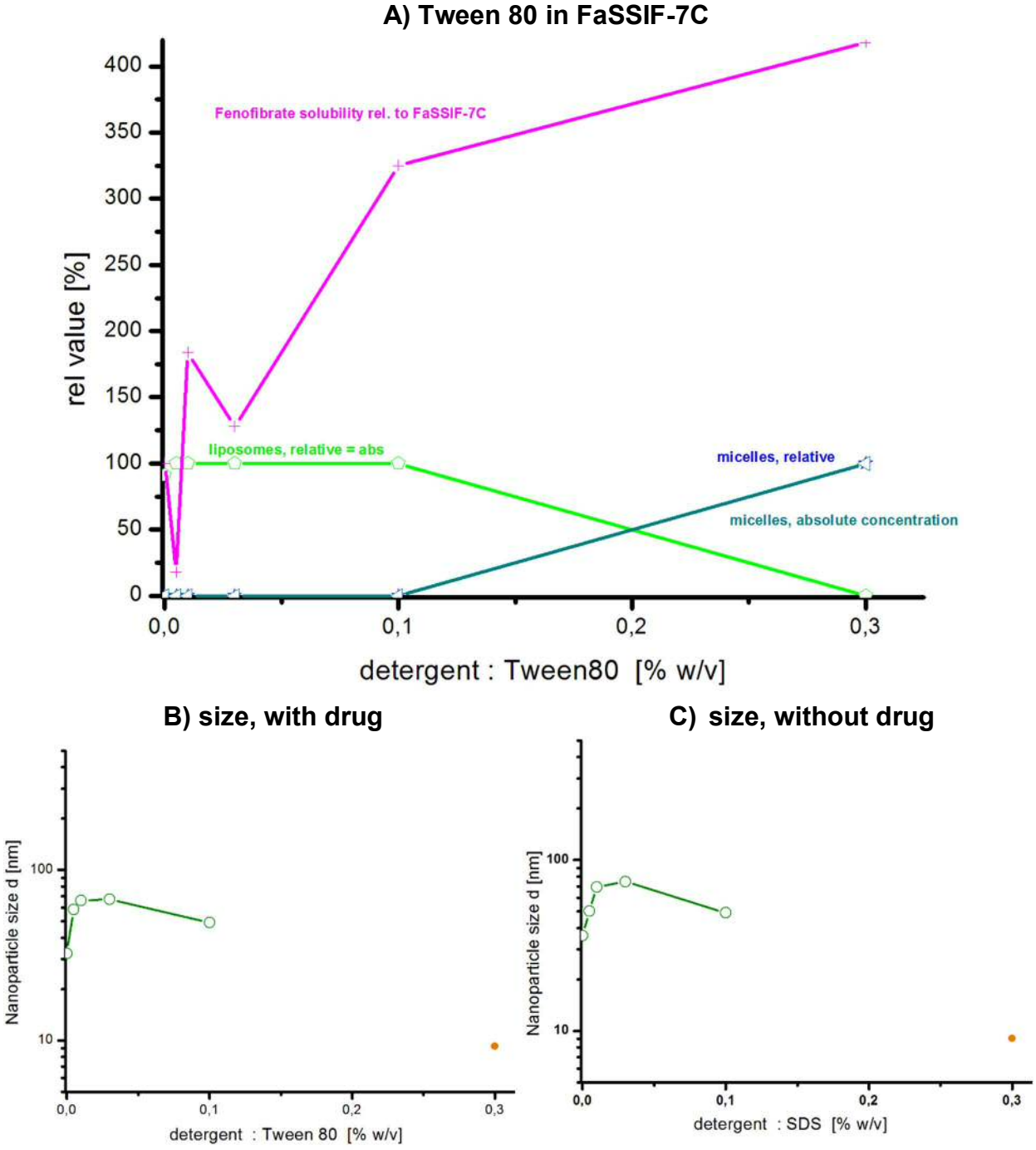

Fig. 3.4-6: (A) Nanostructure and saturation solubility of Fenofibrate in FaSSIF-7C at different concentrations of Tween 80, **(B)** the range of particle size in media with Fenofibrate and **(C)** the range of particle size in media without Fenofibrate.

A) Tween 20 in FaSSIF-7C+ Fenofibrate

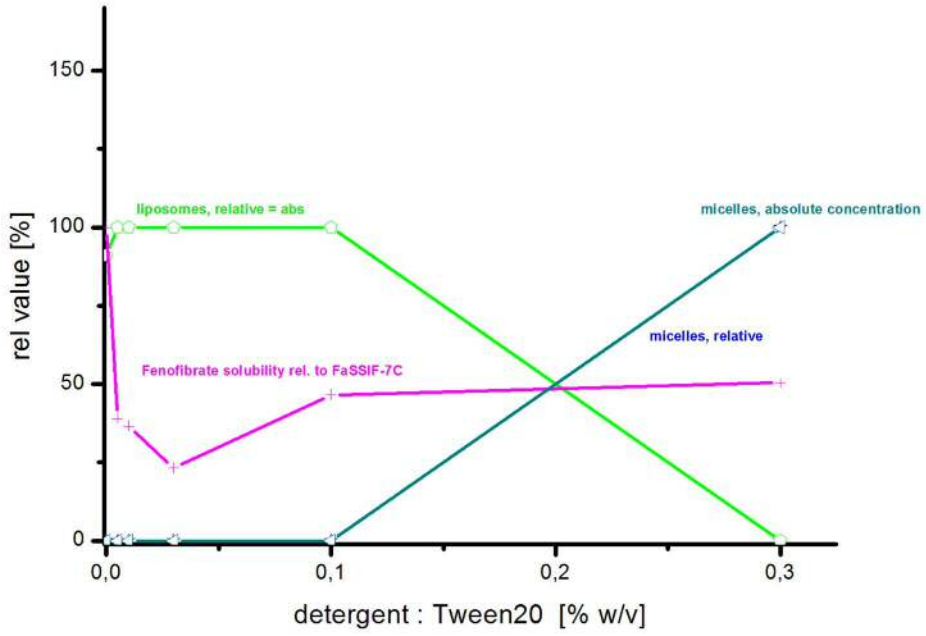

B) size, with drug

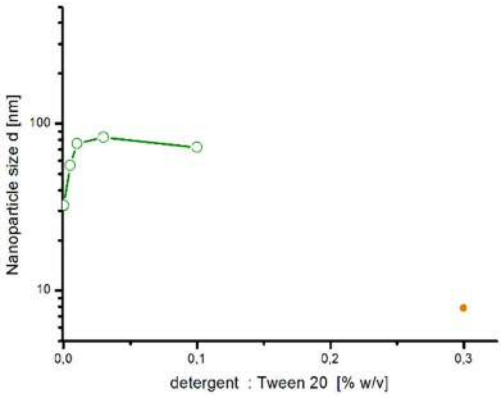

Fig. 3.4-7: (A) Nanostructure and the solubility of Fenofibrate in FaSSIF-7C at different concentrations of Tween 20. **(B)** the range of particle size in media with Fenofibrate and **(C)** nanoparticle structure development of FaSSIF-7C at various concentrations of Tween 20 in media without drug.

Tween 20 in FaSSIF-7C, blank

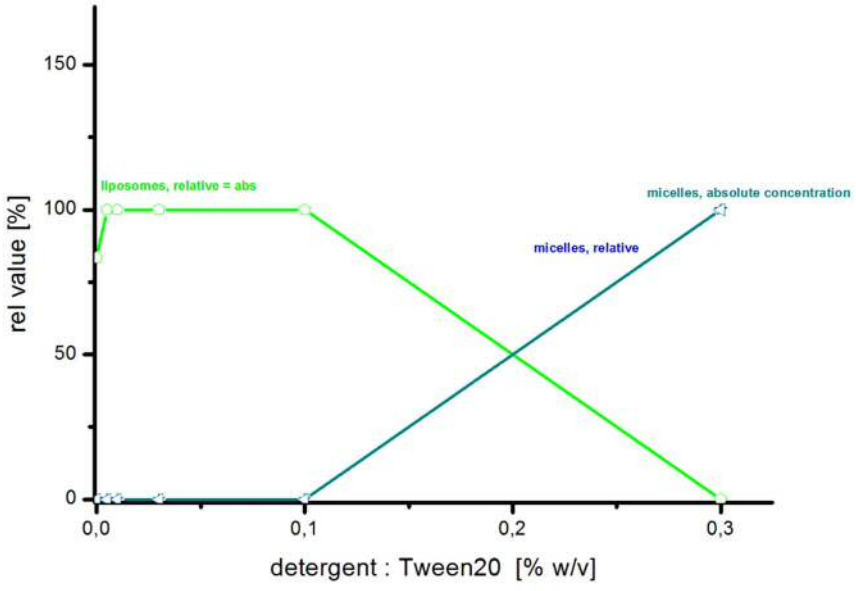

Figure 3.4-7 represents the solubility of Fenofibrate and the particle structure development in FaSSIF-7C at various concentrations of Tween 20. The excipient induced an initial reduction in the solubility of the drug up to 0.03 % w/v. At 0.03% w/v excipient concentration the solubility was reduced to 11.44 µg/ml. Thereafter the solubility increased by a factor of two at Tween 20 concentrations of 0.1 and 0.3% w/v. Liposomes were identified as the main colloidal component in the medium up to 0.1 % w/v excipient. Micelles were predominant at 0.3 % w/v (Fig3.4-7 C, B).

A) Decyl sulfate in FaSSIF-7C, blank

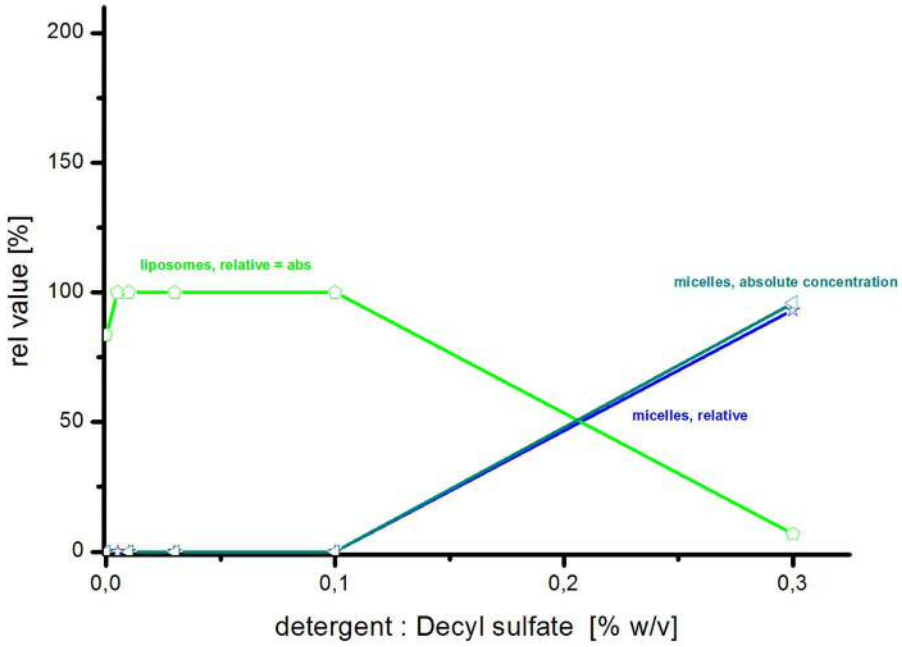

B) Decyl sulfate in FaSSIF-7C + Fenofibrate

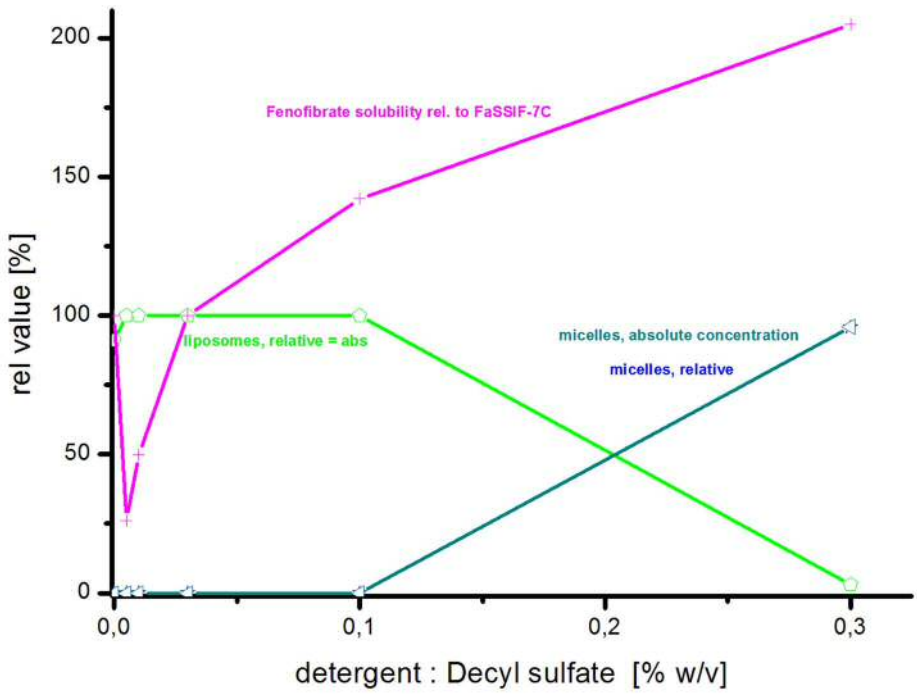

Fig. 3.4-8: (A) Nanoparticle structure development of FaSSIF-7C at various concentrations of sodium n-decyl sulfate in media without drug and **(B)** shows nanostructure and the solubility of Fenofibrate in FaSSIF-7C at different concentrations of sodium n-decyl sulfate.

Figure 3.4-8 depicts the solubility profile of Fenofibrate in FaSSIF-7C and colloid structure of FaSSIF-7C with increasing additions of sodium n-decyl sulfate. The solubility of the Fenofibrate was first reduced by a factor of up to 0.26 at 0.005 % w/v excipient (solubility gap). A concentration dependent increase was observed with higher surfactant concentrations. At high sodium n-decyl sulfate content (0. 3 % w/v) the solubility improved by a factor of 2.05.

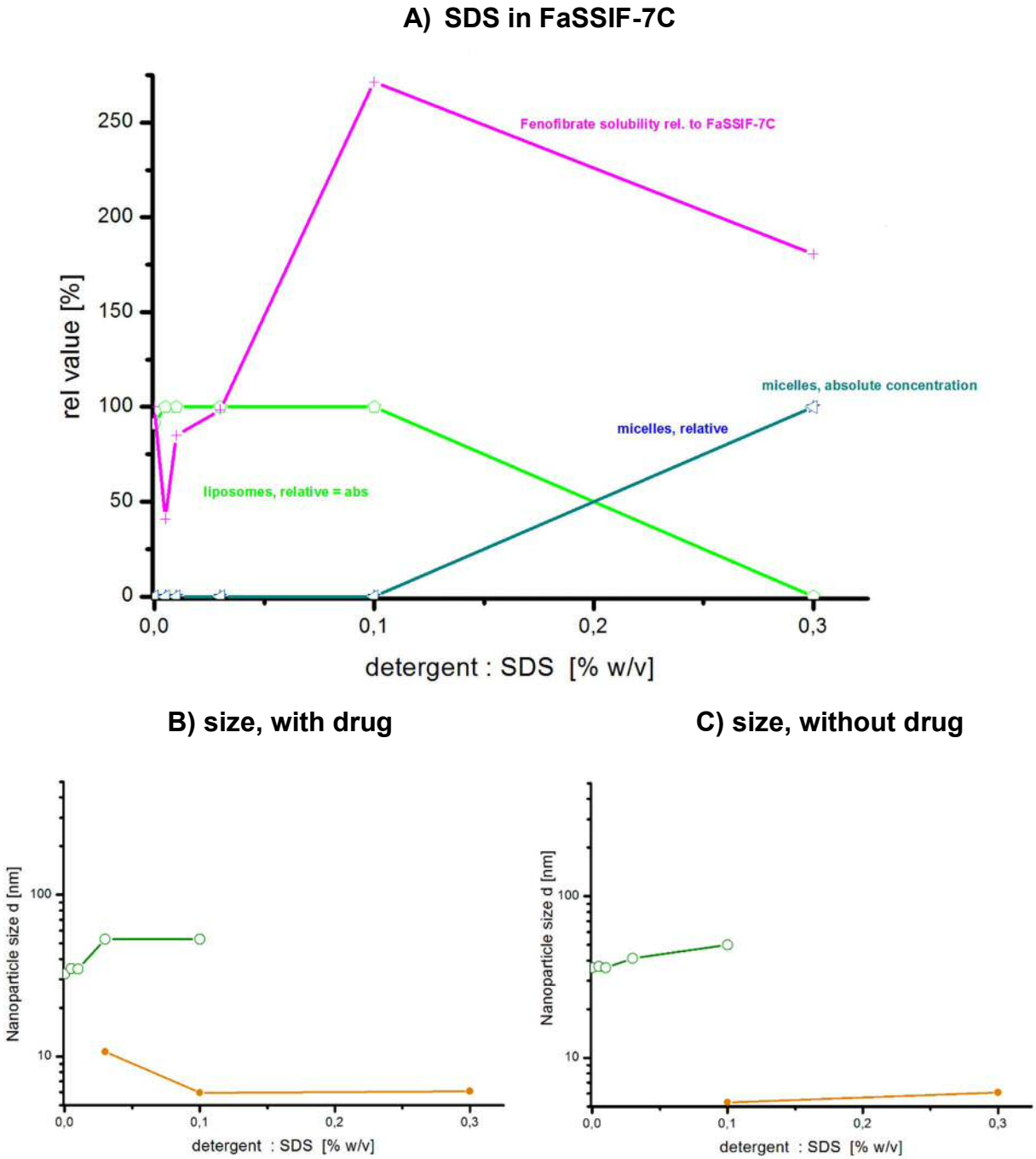

Fig. 3.4-9. (A) Nanostructure and the saturation solubility of Fenofibrate in FaSSIF-7C at different concentration of sodium dodecyl sulfate, **(B)** the range of particle size in media with Fenofibrate and **(C)** the range of particle size in media without Fenofibrate.

The effect of sodium dodecyl sulfate (SDS) on the colloid structure and hydrophobic drug solubility in FaSSIF-7C is presented in figure 3.4-9. The solubility of Fenofibrate increased after an initial dip at 0.005% w/v concentration to a peak at 0.1%, followed by a drop at high

excipient concentration (0.3%). There was an increase by a factor of 2.7 and 1.8 at concentrations of 0.1% w/v and 0.3% w/v respectively. The structure analysis by DLS showed a particle size decrease with increasing concentration of the surfactant in the medium with and without the drug. Majority of the particles in the medium were micelles at 0.3%w/v (Fig. 3.4-9C, B).It was only with SDS that micelles were detectable with DLS at surfactant concentrations lower than 0.3% in FaSSIF-7C.

3.4.5. Discussion

The composition of the fluids in human intestine influences the nanoparticle structures, solubility and dissolution of poorly soluble drugs[155]. In cholesterol free $FaSSIF_{mod6.5}$, data showed that the solubility of drugs and the nanostructure development are affected by surfactant structure, type and concentration[198]. The inclusion of cholesterol in FaSSIF-C mimics the physiological environment of the duodenum and human bile. FaSSIF-7C, FaSSIF-10C and FaSSIF-13C represent models for female, male, and diseased persons[191] respectively. The model FaSSIF-7C can be used as a general model fluid for the simulation of the duodenal environment. This medium uses cholesterol at a minimum level. Thus it was chosen for the study of surfactant effects in this new medium. The surfactants employed are non-ionic (Tween 20 and Tween 80) and anionic (sodium decyl sulfate and sodium dodecyl sulfate). The effect of these amphiphiles in FaSSIF-7C with the hydrophobic drug (Fenofibrate) was investigated by a combination of drug solubility study and nanoparticle structure determination with dynamic light scattering DLS and neutron scattering. This was to evaluate the drug solubility in relation to colloid structure. DLS investigation was done with particle specific quantitative evaluation of the nanoparticle contributions as shown in our pervious study [198].

In the previous work the DLS data showed that in both drug free FaSSIF-7C and Fenofibrate saturated medium, the main particles were vesicles and some big particles as minor component after development from initial bile-lecithin micelles for >10 min. [191]. In this study the micelles of FaSSIF-7C with and without surfactant excipients were investigated more precisely with SANS. To make it more comparable to human bile with influx of excipient micelles, the SANS experiments were done in a stopped flow setup after 20 min development. The results indicate that the blank FaSSIF-7C medium is a mixture of two nanoparticle species; liposomes (34 nm) and residual bile-lecithin micelles of 15.26 nm size, which are not seen well by DLS. This finding is consistent with the earlier investigation of the cholesterol free medium $FaSSIF_{mod6.5}$, which also depicted a co-existence of liposomes and bile-micelles[3, 161]. The micelle structure investigation by DLS of the FaSSIF-7C containing Tween 80 and SDS (not shown) showed liposomes in the medium at low surfactant content(0.03% w/v), but micelles at high concentration (0.3%).

The more detailed SANS investigation of the micelle contribution at short detector distance (1.8 m) indicated additional the liposomes by the increased intensity at lowest q in the Guinier plots (Fig. 3.4-4C, 3.4-5C). By increasing the concentration of the Tween 80 and SDS to 0.3% micelles were detected as the major particles. The size of these micelles were different for Tween 80 (s = 8.11 nm) and SDS (4.99 nm). This may be due to anionic nature of SDS. A further difference between Tween and SDS in FaSSIF-7C was the micelle size dependence on the surfactant concentration. With the non-charged Tween 80 the mixed detergent-bile-lecithin micelles at low concentration (s = 8.23 nm) were similar to that at high surfactant

concentration (s = 8.11 nm), while the mixed micelle size changed with increasing SDS content from s =7.48 to a size of s = 4.99 nm of the detergent-rich micelles. These results show that surfactants change the properties of bile-lecithin micelles even at low concentration (0.03 %), while with the charged detergent a further structure rearrangement occurs at high surfactant concentration. These findings are probably relevant for the bioavailability of hydrophobic drugs, as the intermediate mixed micelles could serve as a drug transport nanoparticle intermediates in the intestine.

In the solubility-structure study (Fig. 3.4-6 to 3.4-9), the solubility of the hydrophobic test drug Fenofibrate (BCS class II) was compared to the content and size of the intermediate nanoparticles, liposomes and micelle, at high detergent concentration (0.3% w/v). The solubility patterns for Tween 80 and Tween 20 (Fig. 3.4-6 and 3.4-7) were similar, showing an initial drug solubility decrease (gap) at low surfactant concentration (0.005 - 0.03 % w/v). However, the solubility of the drug increased with increasing surfactant concentrations of 0.1 and 0.3 % w/v for Tween 80 whilst that for Tween 20 showed a plateau effect. This is in confirmation with Ong and Manoukian who reported that the solubility of Timbosone acetate in nonionic solution increased with increasing length of hydrophobic tail of the surfactant[200]. Thus Tween 80 with a longer chain length of the hydrophobic tail was able to solubilize Fenofibrate to a greater extent than the Tween 20[201].

The solubility patterns for decyl sulfate and dodecyl sulfate (SDS) (Fig. 3.4-8 and 3.4-9) depicted some similarity, showing an initial drug solubility decrease (gap) at low surfactant concentration (0.005 - 0.01 % w/v). At moderate surfactant concentration (~ 0.1 % w/v) the drug solubility increased tremendously due to the fact that the cholesterol-lecithin liposomes were the major nanostructure. Micelles were present but was difficult to detect by DLS due to the strong scattering of the liposomes. At high detergent concentration the drug in SDS decreased but the amount was higher than that of the decyl sulfate. In parallel the liposomes were destroyed by the detergent and replaced by mixed micelles, which were detected by DLS. The drug was obviously incorporated into liposomes from the excipient-cholesterol-lecithin mixture at the moderate surfactant concentration and into the detergent-rich mixed micelles at high surfactant concentration.

In the earlier study of the surfactants effect in $FaSSIF_{mod6.5}$ three regimes of nanostructured particles that correlated with the solubilization of Fenofibrate was detected: bile-lecithin liposomes without detergent, drug-detergent complexes at moderate concentration, and excipient-rich micelles at high surfactant content[202, 203]. At low excipient concentration the liposomes were destroyed, and only a minor amount of the drug was solubilized as molecular complexes of low size. In the current study a drug solubility gap was observed at low surfactant concentration as before, but the cholesterol addition revealed a stabilization of the liposome phase, which is consistent with the general stabilization of biological membranes by cholesterol[204, 205]. The change of the liposome structure was indicated by a slight size increase in the DLS analysis. For pharmaceutical application this has the consequence that a novel species occurs: detergent enriched liposomes at moderate surfactant concentration, which depict an enhanced drug solubilization capacity. At high surfactant concentration these are destroyed as in the case of the cholesterol free systems[198]. If the drug solubilization power of these is higher, then a further increase is observed, as in case of Tween 80 and decyl sulfate. If this is not the case, a secondary breakdown of the drug solubilization at high detergent is observed, as with SDS. This indicates that the existence of the drug solubilizing detergent

enriched liposomes is as a result of their stabilization by cholesterol. This finding could be used as a recipe for future formulations of BCS-II drugs by incorporating them in artificial lecithin-cholesterol nanoparticles.

3.4.6 Conclusion

The study has revealed that addition of surfactants to a cholesterol containing biorelevant medium (FaSSIF-7C) changes the colloidal structures and the solubility of the poorly soluble drug Fenofibrate (BCS-II). The interaction is concentration and surfactant type dependent.
At low concentration all detergents reduced the solubility of the Fenofibrate, i.e. a solubility gap occurred. At moderate surfactant concentration the membrane stabilizing effect of cholesterol resulted in the formation of detergent enriched excipient-cholesterol-lecithin liposomes depicting a high solubilization capacity of the hydrophobic drug. At high detergent, these liposomes were destroyed and replaced by detergent rich mixed micelles of case selective drug solubility. The observation could be used as a recipe for formulations of poorly soluble drugs (BCS-II, IV) by including them in artificial lecithin-cholesterol nanoparticles.

3.4.7 Acknowledgement

We are thankful for the funding from the German ministry of science and education BMBF, grant 05KS7UMA; the Forschungszentrum Jülich FZJ, Jülich Centre of Neutron Science JCNS, outstation at the FRM-II reactor Munich Garching; and support by the Dr. Georg-Scheuing Stiftung, Mainz. The SANS investigation of this research project has been supported by the European Commission under the 7th Framework Programme through the 'Research Infrastructures' action of the 'Capacities' Programme, NMI3-II Grant number 283883. This work has received support from the Innovative Medicines Initiative Joint Undertaking (http://www.imi.europa.eu) under grant agreement n° 115369, resources of which are composed of financial contribution from the European Union's Seventh Framework Programme (FP7/2007-2013) and EFPIA companies' in kind contribution."

Conflict of interest: There are no financial or commercial conflicts of interest.

References

The references are included (re-numbered) in the general reference section (5) of this thesis.

4. General discussion

The use of intestinal biorelevant media such as FeSSIF and FaSSIF with physiologically based modeling approaches help to better predict and understand intestinal drug absorption[1, 16]. Different methods and compositions have been used for the preparation of these artificial intestinal fluids[206]. In this work different methods of preparing $FeSSIF_{mod}$ and $FaSSIF_{mod}$, pH stabilized intestinal fluids, from several phospholipids were investigated (chapter 3.1). The methods of preparation included the shake method, bile-film method and sequential-film method .The shake method is convenient and less costly since it does not involve any organic solvent. With this method the components are mixed up in the media and shaking for a period of time. By the shake method reproducibility and preparation of homogenous mixture of lipids is low and lipid hydrolysis can occur upon shaking for a long time at 37°C. Film methods are appropriate for the preparation of a homogenous lipid mixture and avoid the hydrolysis during preparation. In the bile-film-method, lipids and bile acid are dissolved in methanol and chloroform and after evaporation of the solvent, transport medium (TM) is added. In this method, methanol is necessary for the solubilization of the bile acid, and for complete evaporation about 4-5 hours is needed. Though preparation is faster than the shake method, spilling and delay in evaporation are disadvantages of this method. These problems are however solved in the sequential-film method. By this method, sodium taurocholate is omitted from the film preparation part and a solution of that in TM is added to the lipid film. With film methods the $FeSSIF_{mod6.5}$ is ready after 2 hours of adding the TM and it can be stored frozen at (-20ºC).

Phospholipids and bile salts are the main components of the small intestinal model fluids. Different types of bile acids (for instance, sodium taurocholate and taurodeoxycholic acid) and phospholipids (such as POPC, DOPC, Soy-PC, and Egg-PC) are used for the preparation of small intestinal media. Soy-PC and Egg-PC are the most abundantly used of them[16]. However, semisynthetic DOPC and POPC are used for precise physicochemical and biochemical studies. In this work the effect of different types of lecithin such as DOPC, POPC and Egg-PC using these different methods of preparation was investigated. The particle size of these methods was very important in this investigation. Previous investigations indicated that in fed state condition small mixed bile salt-lipid micelles are formed. The results showed that in $FeSSIF_{mod6.5}$ a particle size of about 5nm was detected. The preparation methods and the lipid type do not have a significant effect on the particle size.

Nawroth et al.[3] investigated the structure development of $FeSSIF_{mod}$ to $FaSSIF_{mod}$ by dilution of FeSSIF with TM by a ratio of 1:5.This was done by time-resolved dynamic light scattering.

The results showed that in fasted state predominantly large liposomes are created from micelles of the $FeSSIF_{mod}$. In most pharmaceutical studies FeSSIF is diluted by a factor of 5 to obtain FaSSIF. However, this dilution rate may vary with food and fluid intake. These data led us to hypothesize that various water content relevant for oral drug administration could have an effect on the structure of biorelevant systems and these structural changes could be time dependent. Subsequently, to mimic the physiological condition of the second part of the duodenum, $FeSSIF_{mod}$ from the different types of lipids prepared with the various methods was diluted with TM and the effect of particle size with time (10min -24h) was investigated. Different dilution rates from 1:3 to 1:10 were applied to simulate different physiological conditions presented by food and fluid intake. Additionally, the nanoparticle structure in $FaSSIF_{mod}$ (dilution 1:5) containing Egg-PC was studied by dynamic light scattering (DLS) and small angle scattering with best contrast using neutrons. The size detection limit of SANS was < 100 nm (because of the low q-limit of the method and instrument), whereas the size detection limit of the used DLS device is <6µm with the Malvern instrument. Distinguishing between micelles and liposomes was done according to the particle size, and particles larger than 20 nm were identified as liposome. The neutron scattering investigation indicated that there is a mixture of several particle populations; liposomes and large micelles. The presence of liposomes was confirmed with SANS by the lamellar structure with a membrane span of d_l = 5.5nm. By DLS investigation, the major contribution of the nanoparticles was identified as liposomes. The time resolved investigation indicated that liposomes are formed in a slow process during 20 min to hours at all dilutions greater than 1:3. With Egg□PC, the lipid of human bile, the liposome concentration led to a constant plateau after two hours, while the main part was already formed in the transit time through the second part of the duodenum *in vivo* (between 10 min and one hour). With DOPC and POPC the liposome formation continued up to one day. The liposome formation kinetics indicated that the concentration of these particles strongly depends on the time, dilution rate and to a lesser extent on the $FeSSIF_{mod}$ preparation method. For simplicity the dilution 1:5 was used for further investigations.

The development of the nanostructures as a result of the interaction of the drugs with the biorelevant media is as depicted figure 4-1.

The more detailed investigation of the $FaSSIF_{mod}$ was conducted with SANS. The radius of gyration Rg[141] which refers to the geometric averaged distance of the scatters from the center of the object was estimated. Radius of gyration is by $\sqrt{(5/3)}$ smaller than the particle radius r_j

in micelles. R_g is for liposomes equivalent to the membrane center radius r_m[142]. The membrane span and hence the size of liposomes were estimated with the aid of Kratky-Porod plots. The results revealed a mixture of nanoparticles in $FaSSIF_{mod}$.

The traditional model media FeSSIF and FaSSIF and improved forms of them until now have some missing components. The composition of these media must mimic exactly what is *in vivo*. In human intestinal media, in addition to phospholipids and bile salts, free fatty acid (as lipolysis product of lecithin) and low concentration of cholesterol have been detected[2, 154, 207-209]. The cholesterol content is reported to be about 7% in female, and 10% in male persons with reference to the amount of total amphiphiles. These amounts show an increase in some diseases. For instance in gall stone the amount could be up to 13%.

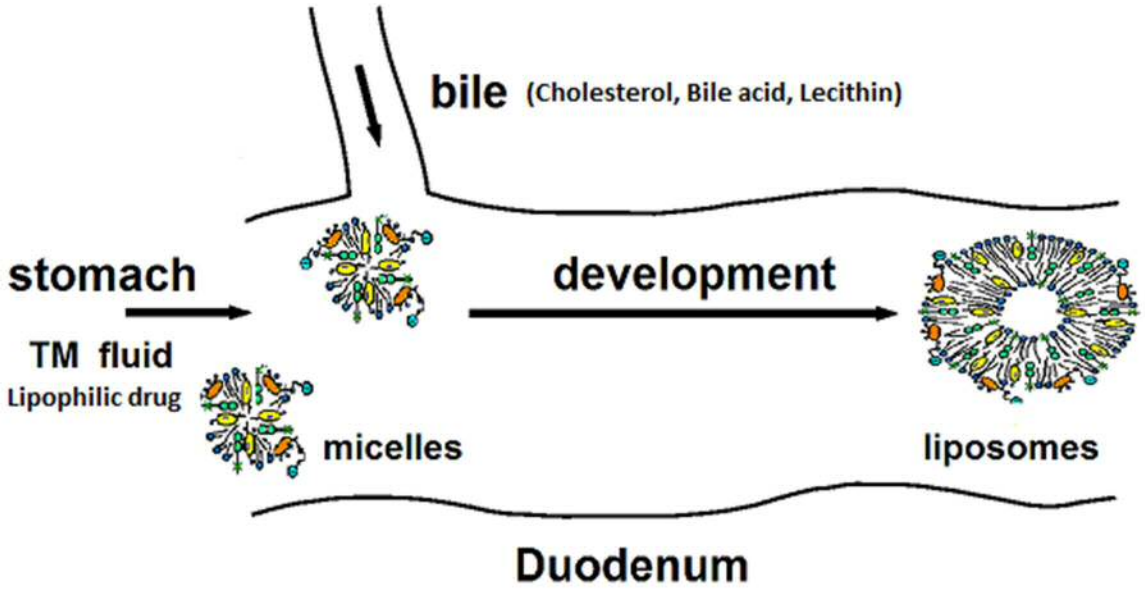

Fig. 4-1. Proposed scheme of the development of the duodenal nanoparticles from bile.

Cholesterol and phospholipids are insoluble in an aqueous medium. In the human bile they become solubilized by formation of a bilayer structures (e.g. mixed micelles or vesicles) with bile salts. A supersaturation of cholesterol can occur when either too much cholesterol or insufficient bile salt and lecithin are secreted[52, 53]. Extra cholesterol will form vesicles (ie, spherical bilayers of cholesterol and phospholipid, without bile salts) or cholesterol crystal[52].

To have a more realistic prediction of oral drug bioavailability based on the human intestinal fluids composition, new biorelevant media were developed (chapter 3.2). Cholesterol was added as missing component[21] to $FaSSIF_{mod}$ (dilution 1:5) to make this medium more similar to the physiological composition : FaSSIF-7C (7% cholesterol) modeled for healthy females, FaSSIF-10C (10% cholesterol) for healthy males, and FaSSIF-13C (13% cholesterol) for patients with diseases leading to cholesterol gall stones. This variation is also related to differences in the cholesterol content between different races[167]. In these media the solubility of some poorly soluble drugs from BCS class II and nanoparticle structures were studied and the results compared with $FaSSIF_{mod}$. The equilibrium solubility data indicated that cholesterol has a significant effect on the solubility of the model drugs in the medium and this effect varied with the cholesterol concentration for some of the drugs. In addition, the nanostructure development in the modeled media also varied with the cholesterol concentration. These cholesterol effects are influenced by the chemical structure of the drug.

By the DLS investigation, a general decrease of the particle size from $FaSSIF_{mod}$ to high cholesterol content in either drug free or drug saturated media was observed. The main particles were liposomes in all media. At high cholesterol content (7%-13%) additional large particles were detected that can be cholesterol disk or related nanoparticles. The detection of the large particles were preliminary because of the limitation of the used Malvern DLS device (<6µm).The structure of these complex system should be investigated by further structural studies.

The SANS investigation of blank FaSSIF-7C, 20 minutes after preparation indicated that this medium was a mixture of micelles and liposomes but the micelles were not detected by DLS (Fig.3.4-3).

The solubility study of Fenofibrate in the model fluid with different concentrations of cholesterol showed an increase in drug solubility. At low cholesterol concentration (2%) only small effect was observed. In FaSSIF-7C and FaSSIF-10C maximum enhancement of the solubility occurred that can be attributed to a specific drug-cholesterol interaction upon replacement of simple liposomes (PC-TC-drug) by cholesterol containing liposomes (PC-Chol-TC-drug). FaSSIF-13C showed a little decrease winch correlated with the occurrence of large particles.

The solubility of Carbamazepine in FaSSIF-C does not show a significant dependence on cholesterol content. This drug shows a higher solubility in the medium without lipid but containing 3mM sodium taurocholate. This reveals that the solubilizing effect of the bile acid alone is greater than that of lipids and thus dominant. The structure of the nanoparticles in

these model media in the presence of the Carbamazepine depends in a similar manner, on the cholesterol content as in case of Fenofibrate. By this drug, the larger cholesterol free vesicles were replaced by smaller cholesterol containing vesicles. However, large particles occurred at high cholesterol content. These data may be interpreted either by a weak interaction of Carbamazepine with cholesterol or this is eliminated by a stronger bile acid interaction with cholesterol.

For Danazol and Griseofulvin, existence of cholesterol in the media caused a negative effect on solubility of these drugs which could be considered as a competition of drug and cholesterol on the lecithin entity. For these drugs the major reduction occurred at low cholesterol content and a general decrease in the solubility of the drugs up to a factor of two was detected. This behavior is correlated with the replacement of the pure lecithin vesicles by mixed vesicles and the solubility reduction can be a structural phenomenon. In medium with 13% cholesterol the solubility of Griseofulvin was enhanced which correlated with the occurrence of large particles.

The compatibility of biorelevant media with cell cultures and excised tissue is an important factor for permeability assessment. The cytotoxicity of FaSSIF-7C was evaluated in Caco-2 cells by MTT test[135]. No significant difference in the viability of the cells treated with $FaSSIF_{mod}6.5$ and FaSSIF-7C was observed. This showed that the presence of the cholesterol in the media did not show a negative effect on the cytotoxicity of the Caco-2 cells. Thus this medium can be used for the Caco-2 system to evaluate the uptake of drugs and for *in vivo – in vitro* correlation studies.

A pharmaceutical drug product consists of the active ingredient and excipients to enhance dissolution and bioavailability[1, 210, 211]. These excipients from the drug formulation can interact with colloidal phases in biorelevant media. The nanoparticle–surfactant mediated drug solubilization pathways of drug formulation in the $FaSSIF_{mod}$ and FaSSIF-7C were investigated (chapter 3.3 and 3.4). For this aim a combination of drug solubility study and nanoparticle structure investigation by dynamic light scattering DLS with particle specific quantitative evaluation was done. The DLS data were scaled to particle volume contributions. According to general scattering theory the raw intensity of scattering is divided by the third power of the particle radius in case of micelles. A liposome is a spherical bent plate of constant span and in this case the raw intensity is divided by second power of the particle radius. The Malvern Zetasizer device assumes all particles as spherical structure (micelles), so for liposomes there is the need to rescale intensity data by division of the raw intensity

(PSD_i) by second power of the particle radius (Fig. 3.3-3), or by multiplying the overscaled distribution (PSD_r) by r.

The effect of Tween 20 and Tween 80 in the solubilization of the Fenofibrate in the intestinal model fluid $FaSSIF_{mod}$ and the particle structure analysis showed that the drug solubilization in pure $FaSSIF_{mod}$ decreased until an excipient concentration of 0.05%. There was a slight improvement relative to $FaSSIF_{mod}$ at 0.2 % excipient to 104% in the case of Tween 20. Tween 80 increased the solubility by 160%. Thus it was a favorable excipient for Fenofibrate as a maximum effective synergism at 0.2% detergent concentration was observed. The effect of the ionic decyl sulfate at various concentrations showed a reduction at low surfactant concentration. After that, drug solubility increased to 130% relative to $FaSSIF_{mod}$, which was similar to SDS data in the previous work[157, 182]. It can be inferred that a solubility gap is created between the lower and higher concentrations of the surfactants.

The DLS investigation revealed the change from liposomes to micelles in the excipient rich solution seen in this study. At very low excipient concentration (concentration below cmc) the simulated intestinal fluid developed liposomes from bile and the drug was incorporated in mixed liposomes. An increasing excipients concentration resulted in a breakdown of liposomes and a decrease in the drug solubility occured. This breakdown happened at concentration higher than the cmc which is different for each excipient. The drug solubility was higher in this region than in pure aqueous solutions (water, HBSS buffer), which indicates the partial formation of soluble molecular complexes from drug, bile and excipient. At high excipient concentration new micelles are formed from excipient, drug and bile. These excipient rich micelles resulted in increasing the drug solubilization. Data from more investigations in some amphiphilic excipients in $FaSSIF_{mod6.5}$ showed that this gap occurs between $c_{Lip50}/2$ and (c_{Lip50}+ 2*(c_{Lip0}- c_{Lip50})) (chapter 3.3). However, some surfactants like poloxamer do not destroy the liposome structure and they solubilized the drug by their micellar structure. These data explain why in some excipient studies a drug solubilization by excipients did not cause an increase in bioavailability.

The FaSSIF- 7C results showed that by increasing the concentration of the surfactants the nanoparticles changed from liposomes to micelles as in the case of cholesterol free medium. However, surfactants at higher concentration destroy the liposome structure in spite of the general stabilization of the membranes by cholesterol.

The nanoparticle study with DLS and SANS of FaSSIF-7C containing Tween 80 and SDS showed a co-existence of liposomes and micelles at low concentration of the surfactants. However, the predominant particles in the media were liposomes. At high concentration of

these two surfactants micelles were detected as the major particles. The size of these micelles were different for SDS (4.99 nm) and Tween 80 (8.11 nm).This difference can be as a result of the ionic nature of the SDS.

The drug solubility pattern of Tween 80 and Tween 20 in FaSSIF-7C showed a similar decrease at low surfactant concentration. However, in the case of Tween 80 an increase in drug solubility was observed while that for Tween 20 showed a decrease. The drug solubility effect of decyl sulfate on Fenofibrate was similar to dodecyl sulfate. The solubility of Fenofibrate decreased at first and at moderate surfactant concentration increased because of the detergent rich cholesterol-lecithin liposomes. By increasing the concentration of the SDS and decyl sulfate the liposomes were replaced by detergent rich micelles. In the case of SDS a reduction of the drug solubility was observed which shows that the solubility of Fenofibrate is higher in liposome rich detergent than micellar structure in FaSSIF-7C.

These finding led to the conclusion that to mimic duodenal condition we need to update our knowledge about the physiology of the body. Choosing the correct composition and dilution rate are necessary for this simulation. Moreover, to have a good oral bioavailability of the drug the interaction of the excipients in the formulation with body components should be considered. Additionally, the cholesterol enriched liposomes which depict an enhancement of the drug solubility can be used for pharmaceutical application. This offers membrane containing formulations as a novel perspective in oral drug delivery.

5. Summary

Biorelevant model media mimic the gastrointestinal conditions before and after meal. FaSSIF and FeSSIF were introduced to reflect not only the pH and buffer capacity of the small intestine but also include physiological surfactant species. These media have been improved for bioavailability study in drug development over the years (FaSSIF-V2 and FaSSIF$_{mod6.5}$). Nevertheless, a physiological component to mimic the real physiological conditions is missing. Moreover, only one dilution rate (1:5) is considered for the conversion of FeSSIF to FaSSIF, while, also other ratios can occur during drug administration. The aim of this thesis was therefore to simulation of the second part of the duodenum more closely to the *in vivo* condition for better prediction of drug absorption.

To study the effect of the dilution rate and time in the small intestine, the development of the nanoparticles in the gastrointestinal fluid FaSSIF$_{mod6.5}$ at various time and water content relevant for oral drug administration was investigated. This was to show the effect of the different volumes of water (fluids) administered with drugs. The results show that the size of the nanoparticle strongly depended on the dilution rate and the passage time.

The human intestinal fluid contains cholesterol which is missing in all previous biorelevant media. Therefore a biocompatible and more physiological model fluid, FaSSIF-C, was developed. The cholesterol content of FaSSIF-7C is equivalent to healthy female, FaSSIF-10C to healthy male person and FaSSIF-13C for some disease states. The particle structure investigation with dynamic light scattering (DLS) and small angle neutron scattering (SANS) showed that the particle size of the vesicles decreased with increasing cholesterol concentration. At high cholesterol concentration additional large particles were detected, which could be cholesterol- rich disks. The solubility of some BCS class II drugs (Fenofibrate, Griseofulvin, Carbamazepine, Danazol) in these new media showed that the solubility varied widely with the cholesterol content and this effect was drug specific.

Furthermore, the effect of some surfactants used in pharmaceutical formulations on the colloidal structure and solubility of Fenofibrate in FaSSIF$_{mod6.5}$ and FaSSIF-7C indicated a change and this change was concentration dependent. In the case of FaSSIF$_{mod6.5}$ the results showed a bifurcation of the solubilization pathways, and a drug solubility gap was observed between the destruction of the native bile liposomes and the formation of excipient rich micelles. In FaSSIF-7C, surfactants at higher concentration destroyed the liposomes in spite of the general stabilization of the membranes by cholesterol.

The results presented in this thesis concluded that the presence of cholesterol as a missing component of human intestinal fluid in biorelevant model media is important and can help to

better predict the behavior of poorly soluble drugs *in vivo*. Different dilution rates have effect on nanoparticle structure. Formulation surfactants influence the solubility of drugs in biorelevant media and this effect is also concentration and surfactant type dependent.

6. Zusammenfassung

Biorelevante Medien sind entwickelt worden, um die Bedingungen im Magen-Darm-Trakt vor und nach der Mahlzeit zu imitieren. Mit FaSSIF und FeSSIF wurden Medien eingeführt, die nicht nur die pH- und Puffer-Kapazität des Dünndarms widerspiegeln, sondern auch Lipid und physiologische Tensid-Arten enthalten. Diese Medien (FaSSIF-V2 und $FaSSIF_{mod6.5}$) wurden für Bioverfügbarkeitstudien in der Medikamentenentwicklung im Laufe der Jahre kontinuierlich weiterentwickelt. Dennoch sind die auf dem Markt verfügbaren Medien immer noch nicht in der Lage, die realen physiologischen Bedingungen zu simulieren. In der jetzigen Zusammensetzung sind nicht alle Kompetenten enthalten, welche natürlicher Weise im Duodenum vorkommen. Darüber hinaus wird nur eine 1:5 Verdünnung von FeSSIF zu FaSSIF angenommen, die individuelle Wasserzufuhr bei Medikamentengabe wird hierdurch jedoch nur eingeschränkt simuliert, obwohl diese von Patient zu Patient schwanken kann.
Ziel dieser Dissertation war die Verbesserung der Vorhersage der Auflösung und Absorption lipophiler Arzneistoffe durch Simulation der Bedingungen im zweiten Teil des Zwölffingerdarms mit neuen biorelevanten Medien, sowie unter Einwirkung zusätzlicher Detergention als Wirkstoffträger.
Um den Effekt der Verdünnungsrate und Zeit im Dünndarm zu untersuchen, wurde die Entwicklung der Nanopartikel in der Magen-Darm-Flüssigkeit $FaSSIF_{mod6.5}$ zu verschiedenen Zeitpunkten und Wassergehalten untersucht. Dafür wurden kinetische Studien an verschieden konzentrierten Modellmedien nach Verdünnungssprung untersucht. Das Modell entspricht der Vermischung der Gallenflüssigkeit mit dem Darminhalt bei variablem Volumen. Die Ergebnisse zeigen, dass Art und Grö*ß*e der Nanopartikel stark von Verdünnung und Einirkungszeit abhängen.

Die menschliche Darmflüssigkeit enthält Cholesterin, welches in allen früheren Modellmedien fehlt. Daher wurden biokompatible und physiologische Modellflüssigkeiten, FaSSIF-C, entwickelt. Der Cholesteringehalt von FaSSIF - 7C entspricht der Gallenflüssigkeit einer gesunden Frau, FaSSIF - 10C der einer gesunden männlichen Person und FaSSIF - 13C der in einigen Krankheitszuständen. Die intestinale Teilchen-Struktur-Untersuchung mit dynamische Lichtstreuung (DLS) und *Neutronen-Kleinwinkelstreuun*g (SANS) ergab, dass die Korngröße von Vesikeln mit zunehmender Cholesterin-Konzentration abnahm. Zu hohe Cholesterin-Konzentration bewirkte zusätzlich sehr große Partikel, welche vermutlich aus Cholesterin-reichen “Disks“ bestehen. Die Löslichkeiten einiger BCS Klasse II Wirkstoffe (Fenofibrat, Griseofulvin, Carbamazepin, Danazol) in diesen neuen Medien zeigten, dass die

Löslichkeit in unterschiedlicher Weise mit der Cholesteringehalt zusammen hing und dieser Effekt selektiv für die Droge war.

Darüber hinaus wurde die Wirkung von einigen Tensiden auf die kolloidale Struktur und Löslichkeit von Fenofibrat in $FaSSIF_{mod6.5}$ und FaSSIF -7C untersucht. Struktur und Löslichkeit waren Tensid- und Konzentrations-abhängig. Im Falle von $FaSSIF_{mod6.5}$ zeigten die Ergebnisse eine dreifache Verzweigung der Lösungswege. Im Bereich mittlerer Tensidkonzentration wurde eine Löslichkeitslücke der Droge zwischen der Zerstörung der Galle-Liposomen und der Bildung von Tensid-reichen Mizellen beobachtet. In FaSSIF - 7C, zerstörten Tenside in höherer Konzentration die Liposomenstruktur trotz der allgemeinen Stabilisierung der Membranen durch Cholesterin.

Die in dieser Arbeit vorgestellten Ergebnisse ergeben, dass die Anwesenheit von Cholesterin als eine fehlende Komponente der menschlichen Darmflüssigkeit in biorelevanten Medien wichtig ist und dazu beitragen kann, das *in vivo* Verhalten schwerlöslicher Arzneistoffe im Körper besser vorhersagen zu können. Der Verdünnungsgrad hat einen Einfluss auf die Nanopartikel-Struktur und Tenside beeinflussen die Löslichkeit von Medikamenten in biorelevanten Medien: Dieser Effekt ist sowohl von der Konzentration das Tensids abhängig, als auch dessen Typ.

7. References

1. Bergstrom, C. A. S.; Holm, R.; Jorgensen, S. A.; Andersson, S. B. E.; Artursson, P.; Beato, S.; Borde, A.; Box, K.; Brewster, M.; Dressman, J.; Feng, K. I.; Halbert, G.; Kostewicz, E.; McAllister, M.; Muenster, U.; Thinnes, J.; Taylor, R.; Mullertz, A. Early pharmaceutical profiling to predict oral drug absorption: Current status and unmet needs. *Eur J Pharm Sci* **2014,** *57*, 173-199.
2. Fuchs, A.; Dressman, J. B. Composition and physicochemical properties of fasted-state human duodenal and jejunal fluid: a critical evaluation of the available data. *J Pharm Sci* **2014,** *103*, (11), 3398-411.
3. Nawroth, T.; Buch, P.; Buch, K.; Langguth, P.; Schweins, R. Liposome Formation from Bile Salt-Lipid Micelles in the Digestion and Drug Delivery Model FaSSIF(mod) Estimated by Combined Time-Resolved Neutron and Dynamic Light Scattering. *Mol Pharmaceut* **2011,** *8*, (6), 2162-2172.
4. Söderlind, E.; Dressman, J. B., Physiology of oral drug absorption. In *oral drug absorption prediction and assessment*, second ed.; Dressman, J. B.; Reppas, C. Informa healthcare: New York,London **2010,** pp 1-20.
5. Koziolek, M.; Gorke, K.; Neumann, M.; Garbacz, G.; Weitschies, W. Development of a bio-relevant dissolution test device simulating mechanical aspects present in the fed stomach. *Eur J Pharm Sci* **2014,** *57*, 250-256.
6. Weaver, L. T.; Austin, S.; Cole, T. J. Small Intestinal Length - a Factor Essential for Gut Adaptation. *Gut* **1991,** *32*, (11), 1321-1323.
7. DeSesso, J. M.; Jacobson, C. F. Anatomical and physiological parameters affecting gastrointestinal absorption in humans and rats. *Food and chemical toxicology : an international journal published for the British Industrial Biological Research Association* **2001,** *39*, (3), 209-28.
8. Akbar, N. S.; Nadeem, S. Simulation of peristaltic flow of chyme in small intestine for couple stress fluid. *Meccanica* **2014,** *49*, (2), 325-334.
9. Davis, S. S.; Hardy, J. G.; Fara, J. W. Transit of Pharmaceutical Dosage Forms through the Small-Intestine. *Gut* **1986,** *27*, (8), 886-892.
10. Sugano, K., *Biopharmaceutics Modeling and Simulations*. ed.; John Wiley & Sons, Inc: United States of America **2012,** pp 1,8,129,151,155,170,179,181,183,185,189,206,225.
11. Minekus, M.; Alminger, M.; Alvito, P.; Ballance, S.; Bohn, T.; Bourlieu, C.; Carriere, F.; Boutrou, R.; Corredig, M.; Dupont, D.; Dufour, C.; Egger, L.; Golding, M.; Karakaya, S.; Kirkhus, B.; Le Feunteun, S.; Lesmes, U.; Macierzanka, A.; Mackie, A.; Marze, S.; McClements, D. J.; Menard, O.; Recio, I.; Santos, C. N.; Singh, R. P.; Vegarud, G. E.; Wickham, M. S. J.; Weitschies, W.; Brodkorb, A. A standardised static in vitro digestion method suitable for food - an international consensus. *Food Funct* **2014,** *5*, (6), 1113-1124.
12. Koziolek, M.; Grimm, M.; Garbacz, G.; Kuehn, J. P.; Weitschies, W. Intragastric Volume Changes after Intake of a High-Caloric, High-Fat Standard Breakfast in Healthy Human Subjects Investigated by MRI. *Mol Pharmaceut* **2014,** *11*, (5), 1632-1639.
13. Schulze, K. Imaging and modelling of digestion in the stomach and the duodenum. *Neurogastroenterology and motility : the official journal of the European Gastrointestinal Motility Society* **2006,** *18*, (3), 172-183.
14. Marciani, L.; Young, P.; Wright, J.; Moore, R.; Coleman, N.; Gowland, P. A.; Spiller, R. C. Antral motility measurements by magnetic resonance imaging. *Neurogastroenterology and motility : the official journal of the European Gastrointestinal Motility Society* **2001,** *13*, (5), 511-518.
15. Hellstrom, P. M.; Gryback, P.; Jacobsson, H. The physiology of gastric emptying. *Best practice & research. Clinical anaesthesiology* **2006,** *20*, (3), 397-407.

16. Kleberg, K.; Jacobsen, J.; Mullertz, A. Characterising the behaviour of poorly water soluble drugs in the intestine: application of biorelevant media for solubility, dissolution and transport studies. *J Pharm Pharmacol* **2010,** *62*, (11), 1656-1668.
17. Pritchard, S. E.; Marciani, L.; Garsed, K. C.; Hoad, C. L.; Thongborisute, W.; Roberts, E.; Gowland, P. A.; Spiller, R. C. Fasting and postprandial volumes of the undisturbed colon: normal values and changes in diarrhea-predominant irritable bowel syndrome measured using serial MRI. *Neurogastroent Motil* **2014,** *26*, (1), 124-130.
18. Pedersen, P. B.; Vilmann, P.; Bar-Shalom, D.; Mullertz, A.; Baldursdottir, S. Characterization of fasted human gastric fluid for relevant rheological parameters and gastric lipase activities. *Eur J Pharm Biopharm* **2013,** *85*, (3), 958-965.
19. Kalantzi, L.; Goumas, K.; Kalioras, V.; Abrahamsson, B.; Dressman, J. B.; Reppas, C. Characterization of the human upper gastrointestinal contents under conditions simulating bioavailability/bioequivalence studies. *Pharmaceut Res* **2006,** *23*, (1), 165-176.
20. Dressman, J. B.; Berardi, R. R.; Dermentzoglou, L. C.; Russell, T. L.; Schmaltz, S. P.; Barnett, J. L.; Jarvenpaa, K. M. Upper Gastrointestinal (Gi) Ph in Young, Healthy-Men and Women. *Pharmaceut Res* **1990,** *7*, (7), 756-761.
21. Psachoulias, D.; Vertzoni, M.; Goumas, K.; Kalioras, V.; Beato, S.; Butler, J.; Reppas, C. Precipitation in and Supersaturation of Contents of the Upper Small Intestine After Administration of Two Weak Bases to Fasted Adults. *Pharmaceut Res* **2011,** *28*, (12), 3145-3158.
22. de la Cruz Moreno, M. P.; Oth, M.; Deferme, S.; Lammert, F.; Tack, J.; Dressman, J.; Augustijns, P. Characterization of fasted-state human intestinal fluids collected from duodenum and jejunum. *J Pharm Pharmacol* **2006,** *58*, (8), 1079-1089.
23. Clarysse, S.; Brouwers, J.; Tack, J.; Annaert, P.; Augustijns, P. Intestinal drug solubility estimation based on simulated intestinal fluids: Comparison with solubility in human intestinal fluids. *Eur J Pharm Sci* **2011,** *43*, (4), 260-269.
24. Persson, E. M.; Gustafsson, A. S.; Carlsson, A. S.; Nilsson, R. G.; Knutson, L.; Forsell, P.; Hanisch, G.; Lennernas, H.; Abrahamsson, B. The effects of food on the dissolution of poorly soluble drugs in human and in model small intestinal fluids. *Pharmaceut Res* **2005,** *22*, (12), 2141-2151.
25. Abrahamsson, B.; Pal, A.; Sjoberg, M.; Carlsson, M.; Laurell, E.; Brasseur, J. G. A novel in vitro and numerical analysis of shear-induced drug release from extended-release tablets in the fed stomach. *Pharmaceut Res* **2005,** *22*, (8), 1215-1226.
26. Clarysse, S.; Psachoulias, D.; Brouwers, J.; Tack, J.; Annaert, P.; Duchateau, G.; Reppas, C.; Augustijns, P. Postprandial Changes in Solubilizing Capacity of Human Intestinal Fluids for BCS Class II Drugs. *Pharmaceut Res* **2009,** *26*, (6), 1456-1466.
27. Mudie, D. M.; Amidon, G. L.; Amidon, G. E. Physiological Parameters for Oral Delivery and in Vitro Testing. *Mol Pharmaceut* **2010,** *7*, (5), 1388-1405.
28. Hall, G. a., *Textbook of Medical Physiology*. ed.; Saunders Elsevier: U.S. **2011,** pp 784
29. Barrett, K. E., Ganong's review of medical physiology. In ed. McGraw-Hill Medical: New York **2012,** pp 512.
30. Marschall, H. U.; Einarsson, C. Gallstone disease. *J Intern Med* **2007,** *261*, (6), 529-542.
31. Hofmann, A. F. The Function of Bile Salts in Fat Absorption. The Solvent Properties of Dilute Micellar Solutions of Conjugated Bile Salts. *The Biochemical journal* **1963,** *89*, 57-68.
32. Jandacek, R. J.; Tso, P. Factors affecting the storage and excretion of toxic lipophilic xenobiotics. *Lipids* **2001,** *36*, (12), 1289-1305.
33. Shaffer, E. A. Review article: control of gall-bladder motor function. *Aliment Pharm Ther* **2000,** *14*, 2-8.

34. Ghibellini, G.; Leslie, E. M.; Brouwer, K. L. R. Methods to evaluate biliary excretion of drugs in humans: an Updated Review. *Mol Pharm.* **2006,** *3*, (3), 198-211.
35. Diakidou, A.; Vertzoni, M.; Goumas, K.; Soderlind, E.; Abrahamsson, B.; Dressman, J.; Reppas, C. Characterization of the Contents of Ascending Colon to Which Drugs are Exposed After Oral Administration to Healthy Adults. *Pharmaceut Res* **2009,** *26*, (9), 2141-2151.
36. Meier, Y.; Eloranta, J. J.; Darimont, J.; Ismair, M. G.; Hiller, C.; Fried, M.; Kullak-Ublick, G. A.; Vavricka, S. R. Regional distribution of solute carrier mRNA expression along the human intestinal tract. *Drug Metab Dispos* **2007,** *35*, (4), 590-594.
37. Fisher, M. M.; Yousef, I. M. Sex differences in the bile acid composition of human bile: studies in patients with and without gallstones. *CMAJ* **1973,** *109*, (3), 190-193.
38. Vlahcevic, Z. R.; Heuman, D. M.; Hylemon, P. B. Regulation of Bile-Acid Synthesis. *Hepatology* **1991,** *13*, (3), 590-600.
39. Mukhopadhyay, S.; Maitra, U. Chemistry and biology of bile acids. *Curr Sci India* **2004,** *87*, (12), 1666-1683.
40. Narain, P. K.; DeMaria, E. J.; Heuman, D. M. Lecithin protects against plasma membrane disruption by bile salts. *J Surg Res* **1998,** *78*, (2), 131-136.
41. Brouwers, J.; Tack, J.; Lammert, F.; Augustijns, P. Intraluminal drug and formulation behavior and integration in in vitro permeability estimation: a case study with amprenavir. *J Pharm Sci* **2006,** *95*, (2), 372-83.
42. Annaert, P.; Brouwers, J.; Bijnens, A.; Lammert, F.; Tack, J.; Augustijns, P. Ex vivo permeability experiments in excised rat intestinal tissue and in vitro solubility measurements in aspirated human intestinal fluids support age-dependent oral drug absorption. *Eur J Pharm Sci* **2010,** *39*, (1-3), 15-22.
43. Holmstock, N.; De Bruyn, T.; Bevernage, J.; Annaert, P.; Mols, R.; Tack, J.; Augustijns, P. Exploring food effects on indinavir absorption with human intestinal fluids in the mouse intestine. *Eur J Pharm Sci* **2013,** *49*, (1), 27-32.
44. Bevernage, J.; Brouwers, J.; Clarysse, S.; Vertzoni, M.; Tack, J.; Annaert, P.; Augustijns, P. Drug Supersaturation in Simulated and Human Intestinal Fluids Representing Different Nutritional States. *J Pharm Sci* **2010,** *99*, (11), 4525-4534.
45. Pearson, R. H. The Molecular-Structure of Lecithin Dihydrate. *Fed Proc* **1980,** *39*, (6), 1833-1833.
46. Small, D. M. The physical chemistry of lipids: from alkanes to phospholipids. *Plenum Press: New York* **1986**.
47. Heikkila, T.; Karjalainen, M.; Ojala, K.; Partola, K.; Lammert, F.; Augustijns, P.; Urtti, A.; Yliperttula, M.; Peltonen, L.; Hirvonen, J. Equilibrium drug solubility measurements in 96-well plates reveal similar drug solubilities in phosphate buffer pH 6.8 and human intestinal fluid. *Int J Pharm* **2011,** *405*, (1-2), 132-136.
48. Kossena, G. A.; Charman, W. N.; Wilson, C. G.; O'Mahony, B.; Lindsay, B.; Hempenstall, J. M.; Davison, C. L.; Crowley, P. J.; Porter, C. J. H. Low dose lipid formulations: Effects on gastric emptying and biliary secretion. *Pharmaceut Res* **2007,** *24*, (11), 2084-2096.
49. Admirand, W. H.; Small, D. M. The physicochemical basis of cholesterol gallstone formation in man. *The Journal of clinical investigation* **1968,** *47*, (5), 1043-52.
50. Stahlberg, D.; Reihner, E.; Angelin, B.; Einarsson, K. Interruption of the Enterohepatic Circulation of Bile-Acids Stimulates the Esterification Rate of Cholesterol in Human Liver. *Journal of lipid research* **1991,** *32*, (9), 1409-1415.
51. Schulthess, G.; Compassi, S.; Boffelli, D.; Werder, M.; Weber, F. E.; Hauser, H. A comparative study of sterol absorption in different small-intestinal brush border membrane models. *Journal of lipid research* **1996,** *37*, (11), 2405-2419.

52. Somjen, G. J.; Gilat, T. Contribution of vesicular and micellar carriers to cholesterol transport in human bile. *Journal of lipid research* **1985,** *26*, (6), 699-704.
53. Wang, D. Q. H.; Cohen, D. E.; Carey, M. C. Biliary lipids and cholesterol gallstone disease. *Journal of lipid research* **2009,** *50*, S406-S411.
54. Hao, W.L.; Lee, Y.K. Microflora of the gastrointestinal tract: a review. *Methods Mol Biol.* **2004,** 268,491-502.
55. Larhed, A. W.; Artursson, P.; Grasjo, J.; Bjork, E. Diffusion of drugs in native and purified gastrointestinal mucus. *J Pharm Sci* **1997,** *86*, (6), 660-665.
56. Brouwers, J.; Deferme, S.; Annaert, P.; Augustijns, P., Permeability measurement. In *oral drug absorption prediction and assessment*, second ed.; Dressman, J. B.; Reppas, C. Informa healthcare: New York,London **2010,** pp 168-205.
57. Back, D. J.; Rogers, S. M. Review: first-pass metabolism by the gastrointestinal mucosa. *Aliment Pharmacol Ther* **1987,** *1*, (5), 339-57.
58. Ungell, A. B., Drug Transport Mechanisms Across the Intestinal Epithelium. In *oral drug absorption prediction and assessment*, ed.; Dressman, J. reppas. B. Informa healthcare: New York,London **2010,** pp 21-40.
59. Zakeri-Milani, P.; Valizadeh, H. Intestinal transporters: enhanced absorption through P-glycoprotein-related drug interactions. *Expert Opin Drug Met* **2014,** *10*, (6), 859-871.
60. Seedher, N.; Kanojia, M. Micellar solubilization of some poorly soluble antidiabetic drugs: A technical note. *Aaps Pharmscitech* **2008,** *9*, (2), 431-436.
61. Brouwers, J.; Brewster, M. E.; Augustijns, P. Supersaturating Drug Delivery Systems: The Answer to Solubility-Limited Oral Bioavailability? *J Pharm Sci* **2009,** *98*, (8), 2549-2572.
62. Horter, D.; Dressman, J. B. Influence of physicochemical properties on dissolution of drugs in the gastrointestinal tract. *Adv Drug Deliver Rev* **2001,** *46*, (1-3), 75-87.
63. Yang, B.; Lowe, J. P.; Schweins, R.; Edler, K. J. Small Angle Neutron Scattering Studies on the Internal Structure of Poly(lactide-co-glycolide)-block-poly(ethylene glycol) Nanoparticles as Drug Delivery Vehicles. *Biomacromolecules* **2015,** *16*, (2), 457-464.
64. Wyatt, P. J. Light-Scattering and the Absolute Characterization of Macromolecules. *Anal Chim Acta* **1993,** *272*, (1), 1-40.
65. Zhao, Y. H.; Abraham, M. H.; Le, J.; Hersey, A.; Luscombe, C. N.; Beck, G.; Sherborne, B.; Cooper, I. Rate-limited steps of human oral absorption and QSAR studies. *Pharm Res* **2002,** *19*, (10), 1446-57.
66. Fotaki, N.; Vertzoni, M. Biorelevant dissolution methods and their applications in in vitro-in vivocorrelations for oral formulations. *The Open Drug Delivery* **2010,** *4*, 2-13.
67. Galia, E.; Nicolaides, E.; Horter, D.; Lobenberg, R.; Reppas, C.; Dressman, J. B. Evaluation of various dissolution media for predicting in vivo performance of class I and II drugs. *Pharmaceut Res* **1998,** *15*, (5), 698-705.
68. Dressman, J. B.; Vertzoni, M.; Goumas, K.; Reppas, C. Estimating drug solubility in the gastrointestinal tract. *Adv Drug Deliv Rev.* **2007,** *59*, (7), 591-602.
69. Jantratid, E.; Janssen, N.; Reppas, C.; Dressman, J. B. Dissolution media simulating conditions in the proximal human gastrointestinal tract: An update. *Pharmaceut Res* **2008,** *25*, (7), 1663-1676.
70. Nicolaides, E.; Symillides, M.; Dressman, J. B.; Reppas, C. Biorelevant dissolution testing to predict the plasma profile of lipophilic drugs after oral administration. *Pharmaceut Res* **2001,** *18*, (3), 380-388.
71. Leigh, M.; Kloefer, B.; Schaich, M. Comparison of the Solubility and Dissolution of Drugs in Fasted- State Biorelevant Media (FaSSIF and FaSSIF-V2). *Dissolut Technol* **2013,** *20*, (3), 44-50.

72. Ingels, F.; Deferme, S.; Destexhe, E.; Oth, M.; Van den Mooter, G.; Augustijns, P. Simulated intestinal fluid as transport medium in the Caco-2 cell culture model. *Int J Pharm* **2002,** *232*, (1-2), 183-192.
73. Lakeram, M.; Lockley, D. J.; Pendlington, R.; Forbes, B. Optimisation of the Caco-2 permeability assay using experimental design methodology. *Pharmaceut Res* **2008,** *25*, (7), 1544-1551.
74. Lind, M. L.; Jacobsen, J.; Holm, R.; Mullertz, A. Development of simulated intestinal fluids containing nutrients as transport media in the Caco-2 cell culture model: Assessment of cell viability, monolayer integrity and transport of a poorly aqueous soluble drug and a substrate of efflux mechanisms. *Eur J Pharm Sci* **2007,** *32*, (4-5), 261-270.
75. Patel, N.; Forbes, B.; Eskola, S.; Murray, J. Use of simulated intestinal fluids with Caco-2 cells in rat ileum. *Drug Dev Ind Pharm* **2006,** *32*, (2), 151-161.
76. Fossati, L.; Dechaume, R.; Hardillier, E.; Chevillon, D.; Prevost, C.; Bolze, S.; Maubon, N. Use of simulated intestinal fluid for Caco-2 permeability assay of lipophilic drugs. *Int J Pharm* **2008,** *360*, (1-2), 148-155.
77. Tippin, T. K.; Thakker, D. R. Biorelevant refinement of the Caco-2 cell culture model to assess efficacy of paracellular permeability enhancers. *J Pharm Sci* **2008,** *97*, (5), 1977-1992.
78. Galia, E.; Horton, J.; Dressman, J. B. Albendazole generics - A comparative in vitro study. *Pharmaceut Res* **1999,** *16*, (12), 1871-1875.
79. Dressman, J. B.; Amidon, G. L.; Reppas, C.; Shah, V. P. Dissolution testing as a prognostic tool for oral drug absorption: Immediate release dosage forms. *Pharmaceut Res* **1998,** *15*, (1), 11-22.
80. Aburub, A.; Risley, D. S.; Mishra, D. A critical evaluation of fasted state simulating gastric fluid (FaSSGF) that contains sodium lauryl sulfate and proposal of a modified recipe. *Int J Pharm* **2008,** *347*, (1-2), 16-22.
81. Vertzoni, M.; Dressman, J.; Butler, J.; Hempenstall, J.; Reppas, C. Simulation of fasting gastric conditions and its importance for the in vivo dissolution of lipophilic compounds. *Eur J Pharm Biopharm* **2005,** *60*, (3), 413-417.
82. Russell, T. L.; Berardi, R. R.; Barnett, J. L.; Dermentzoglou, L. C.; Jarvenpaa, K. M.; Schmaltz, S. P.; Dressman, J. B. Upper gastrointestinal pH in seventy-nine healthy, elderly, North American men and women. *Pharm Res* **1993,** *10*, (2), 187-196.
83. Klein, S. The Use of Biorelevant Dissolution Media to Forecast the In Vivo Performance of a Drug. *Aaps J* **2010,** *12*, (3), 397-406.
84. Nicolaides, E.; Galia, E.; Efthymiopoulos, C.; Dressman, J. B.; Reppas, C. Forecasting the in vivo performance of four low solubility drugs from their in vitro dissolution data. *Pharmaceut Res* **1999,** *16*, (12), 1876-1882.
85. Ashby, L. J.; Beezer, A. E.; Buckton, G. In vitro dissolution testing of oral controlled release preparations in the presence of artificial foodstuffs. I. Exploration of alternative methodology: microcalorimetry. *Int J Pharm* **1989,** *51*, (3), 245-251.
86. Macheras, P.; Koupparis, M.; Tsaprounis, C. Drug Dissolution Studies in Milk Using the Automated Flow-Injection Serial Dynamic Dialysis Technique. *Int J Pharm* **1986,** *33*, (1-3), 125-136.
87. McNamara, D. P.; Whitney, K. M.; Goss, S. L. Use of a physiologic bicarbonate buffer system for dissolution characterization of ionizable drugs. *Pharmaceut Res* **2003,** *20*, (10), 1641-1646.
88. Kataoka, M.; Masaoka, Y.; Sakuma, S.; Yamashita, S. Effect of food intake on the oral absorption of poorly water-soluble drugs: In vitro assessment of drug dissolution and permeation assay system. *J Pharm Sci* **2006,** *95*, (9), 2051-2061.
89. Vertzoni, M.; Fotaki, N.; Kostewicz, E.; Stippler, E.; Leuner, C.; Nicolaides, E.; Dressman, J.; Reppas, C. Dissolution media simulating the intralumenal composition of the

small intestine: physiological issues and practical aspects. *J Pharm Pharmacol* **2004,** *56*, (4), 453-462.
90. Fatouros, D. G.; Mullertz, A. In vitro lipid digestion models in design of drug delivery systems for enhancing oral bioavailability. *Expert Opin Drug Met* **2008,** *4*, (1), 65-76.
91. Fotaki, N.; Symillides, M.; Reppas, C. In vitro versus canine data for predicting input profiles of isosorbide-5-mononitrate from oral extended release products on a confidence interval basis. *Eur J Pharm Sci* **2005,** *24*, (1), 115-122.
92. Chapman, M. J. Pharmacology of Fenofibrate. *Am J Med* **1987,** *83*, (5B), 21-25.
93. Sunitha Reddy, M.; Mahammad FAzal ulHaq, S.; Apte, S. S. solubility enhancement of Fenofibrate,A BCS class II drug, by self emulsifying drug delivery systems *IRJP* **2011,** *2*, (11), 173-177.
94. Granero, G. E.; Ramachandran, C.; Amidon, G. L. Dissolution and solubility behavior of fenofibrate in sodium lauryl sulfate solutions. *Drug Dev Ind Pharm* **2005,** *31*, (9), 917-922.
95. Vogt, M.; Kunath, K.; Dressman, J. B. Dissolution enhancement of fenofibrate by micronization, cogrinding and spray-drying: comparison with commercial preparations. *Eur J Pharm Biopharm* **2008,** *68*, (2), 283-288.
96. Illingworth, D. R. Management of Hyperlipidemia - Goals for the Prevention of Atherosclerosis. *Clin Invest Med* **1990,** *13*, (4), 211-218.
97. Packard, C. J. Overview of fenofibrate. *Eur Heart J* **1998,** *19*, A62-A65.
98. Adkins, J. C.; Faulds, D. Micronised fenofi brate: a review of its pharmacodynamic properties and clinical effi cacy in the management of dyslipidaemia. *drugs* **1997,** *54*, (4), 615-633.
99. Kersten , S.; Desvergne, B.; Wahli, W. Roles of PPARs in health and disease. *Nature* **2000,** *405*, (6785), 421 -424.
100. Balfour , J. A.; McTavish, D.; Heel, R. C. Fenofi brate. A review of its pharmacodynamic and pharmacokinetic properties and therapeutic use in dyslipidaemia. *drugs* **1990,** *40*, (2), 260 -290.
101. Filippatos, T.; Milionis, H. J. Treatment of hyperlipidaemia with fenofi brate and related fibrates. *Expert Opin. Investig. Drugs* **2008,** *17*, (10), 1599-1613.
102. Najib, J. Fenofi brate in the treatment of dyslipidemia: a review of the data as they relate to the new suprabioavailable tablet formulation. *Clin Ther* **2002,** *24*, (12), 2022 -2050.
103. Weil, A.; Caldwell, J.; Strolin-Benedetti, M. The metabolism and disposition of fenofibrate in rat, guinea pig, and dog. *Drug Metab Dispos* **1988,** *16*, (2), 302-309.
104. Keating, G. M.; Ormrod, D. Micronised fenofi brate: an updated review of its clinical efficacy in the management of dyslipidaemia. *Drugs* **2002,** *62*, (13), 1909 -1944.
105. Guichard, J. P.; Blouquin, P.; Qing, Y. A new formulation of fenofi brate:suprabioavailable tablets. *Curr Med Res Opin* **2000,** *16*, (2), 134 -138.
106. Barbieri, R. L.; Canick, J. A.; Ryan, K. J. Danazol inhibits steroidogenesis in the rat testis in vitro. *Endocrinology* **1977,** *101*, (6), 1676-82.
107. Mithani, S. D.; Bakatselou, V.; TenHoor, C. N.; Dressman, J. B. Estimation of the increase in solubility of drugs as a function of bile salt concentration. *Pharm Res* **1996,** *13*, (1), 163-167.
108. Dressman, J. B.; Reppas, C. In vitro-in vivo correlations for lipophilic, poorly water-soluble drugs. *Eur J Pharm Sci* **2000,** *11*, S73-S80.
109. Hoffman, B. L.; Schorge , J. O.; Schaffer , J. I.; Halvorson , L. M.; Bradshaw, K. D.; Cunningham, F. G.; Calver , L. E., Endometriosis. In *Williams Gynecology*, 2ed ed.; McGraw-Hill Medical: New York **2012,** pp 294.
110. Potts, G. O.; Schane, H. P.; Edelson, J. Pharmacology and Pharmacokinetics of Danazol. *Drugs* **1980,** *19*, (5), 321-330.

111. Forbes, K. L.; Dowsett, M.; Rose, G. L.; Mudge, J. E.; Jeffcoate, S. L. Dosage-Related Effects of Danazol on Sex-Hormone Binding Globulin and Free and Total Androgen Levels. *Clin Endocrinol* **1986,** *25*, (5), 597-605.
112. Barbieri, R. L.; Ryan, K. J. Danazol - Endocrine Pharmacology and Therapeutic Applications. *Am J Obstet Gynecol* **1981,** *141*, (4), 453-463.
113. http://www.malvern.com.
114. Bazil, C. W.; Pedley, T. A. Clinical pharmacology of antiepileptic drugs. *Clinical neuropharmacology* **2003,** *26*, (1), 38-52.
115. Mansuri, S. M.; Raval, J. D.; Girdhar, A. O.; Gandhi, T. P. A study of some pharmacological actions of Carbamazepine and Sodium valproate *Ind. J. Physiol. Pharmac.* **1984,** *28*, (4), 315-318.
116. Patel, M. V.; Patel, D. S.; Patel, N. U.; Patel, K. N.; Patel, P. A. Solubility enhancement of Carbamazepine by using various solubility enhancement techniques *JCPS* **2014,** *1* (1), 2321-8630.
117. Pandey, A.; Rath, B. Improved Physicochemical Characteristics of Amorphous Drug Solid Dispersions. *RJPBCS* **2012** *3*, (2), 844-849.
118. Vajda, F. J.; Eadie, M. J. The clinical pharmacology of traditional antiepileptic drugs. *Epileptic disorders : international epilepsy journal with videotape* **2014,** *16*, (4), 395-408.
119. Albani, F.; Riva, R.; Baruzzi, A. Carbamazepine clinical pharmacology: A review. *Pharmacopsychiatry* **1995,** *28*, (6), 235-244.
120. Carruthers , S. G.; Hoffman , B.; Melmon , K.; Nierenberg, D.; L. Melmon , K.; Hoffman, B. B.; Carruthers, G.; Nierenberg, D. W., *Melmon and Morrelli's Clinical Pharmacology*. 4th ed.; MacGraw-Hill: New York **2000,** pp 483,628,498.
121. Ekbom, K. A.; Westerberg, C. E. Carbamazepine in glossopharyngeal neuralgia. *Archives of neurology* **1966,** *14*, (6), 595-6.
122. Kim, S. H.; Han, K. R.; Kim do, W.; Lee, J. W.; Park, K. B.; Lee, J. Y.; Kim, C. Severe pain attack associated with neurocardiogenic syncope induced by glossopharyngeal neuralgia: successful treatment with carbamazepine and a permanent pacemaker -a case report. *The Korean journal of pain* **2010,** *23*, (3), 215-218.
123. Bertilsson, L.; Tomson, T. Clinical Pharmacokinetics and Pharmacological Effects of Carbamazepine and Carbamazepine-10,11-Epoxide - an Update. *Clinical pharmacokinetics* **1986,** *11*, (3), 177-198.
124. Bertilsson, L. Clinical Pharmacokinetics of Carbamazepine. *Clinical pharmacokinetics* **1978,** *3*, (2), 128-143.
125. Nielsen, P. B.; Mullertz, A.; Norling, T.; Kristensen, H. G. The effect of alpha-tocopherol on the in vitro solubilisation of lipophilic drugs. *Int J Pharm* **2001,** *222*, (2), 217-224.
126. Fujioka, Y.; Kadono, K.; Fujie, Y.; Metsugi, Y.; Ogawara, K. I.; Higaki, K.; Kimura, T. Prediction of oral absorption of griseofulvin, a BCS class II drug, based on GITA model: Utilization of a more suitable medium for in-vitro dissolution study. *J Control Release* **2007,** *119*, (2), 222-228.
127. bennett, J. E., *Goodman and Gilman's the Pharmacological Basis of Therapeutics*. 10 ed.; McGraw-Hill Inc.: US, **2001**; 1295-1313.
128. Develoux, M. Griseofulvin. *Annales de dermatologie et de venereologie* **2001,** *128*, (12), 1317-1325.
129. Crounse, R. G. Human pharmacology of griseofulvin: the effect of fat intake on gastrointestinal absorption. *The Journal of investigative dermatology* **1961,** *37*, 529-33.
130. Araujo, O. E.; Flowers, F. P.; King, M. M. Griseofulvin - a New Look at an Old Drug. *Dicp Ann Pharmac* **1990,** *24*, (9), 851-854.
131. http://www.drugs.com/pro/griseofulvin-tablets.

132. Hassan, P. A.; Rana, S.; Verma, G. Making sense of Brownian motion: colloid characterization by dynamic light scattering. *Langmuir* **2015,** *31*, (1), 3-12.
133. Svergun , D. I.; Koch, M. H. J.; Timmins , P. A.; May, R. P., *Small angle X-ray and neutron scattering from solutions of biological macromolecules*. ed.; Oxford University press: Oxford **2013**.
134. Gonzalez, R. J.; Tarloff, J. B. Evaluation of hepatic subcellular fractions for Alamar blue and MTT reductase activity. *Toxicol in Vitro* **2001,** *15*, (3), 257-259.
135. Carmichael, J.; Degraff, W. G.; Gazdar, A. F.; Minna, J. D.; Mitchell, J. B. Evaluation of a Tetrazolium-Based Semiautomated Colorimetric Assay - Assessment of Chemosensitivity Testing. *Cancer Res* **1987,** *47*, (4), 936-942.
136. Amidon, G. L.; Lennernas, H.; Shah, V. P.; Crison, J. R. A Theoretical Basis for a Biopharmaceutic Drug Classification - the Correlation of in-Vitro Drug Product Dissolution and in-Vivo Bioavailability. *Pharmaceut Res* **1995,** *12*, (3), 413-420.
137. Carey, M. C.; Lamont, J. T. Cholesterol gallstone formation. 1. Physical-chemistry of bile and biliary lipid secretion. *Progress in liver diseases* **1992,** *10*, 139-63.
138. Bates, T. R.; Gibaldi, M.; Kanig, J. L. Solubilizing properties of bile salt solutions. II. Effect of inorganic electrolyte, lipids, and a mixed bile salt system on solubilization of glutethimide, griseofulvin, and hexestrol. *J Pharm Sci* **1966,** *55*, (9), 901-6.
139. Kloefer, B.; van Hoogevest, P.; Moloney, R.; Kuentz, M.; Leigh, M. L. S.; Dressman, J. Study of a Standardized Taurocholate-Lecithin Powder for Preparing the Biorelevant Media FeSSIF and FaSSIF. *Dissolut Technol* **2010,** *17*, (3), 6-13.
140. Ilardia-Arana, D.; Kristensen, H. G.; Mullertz, A. Biorelevant dissolution media: Aggregation of amphiphiles and solubility of estradiol. *J Pharm Sci* **2006,** *95*, (2), 248-255.
141. Guinier, A., La. diffraction des rayons X aux tres petits angles; application a l'etude de phenomenes ultramicroscopiques. *Ann. Physique* **1939,** *12*, 161-237.
142. Nawroth, T.; Conrad, H.; Dose, K. Neutron Small-Angle Scattering of Liposomes in the Presence of Detergents. *Physica B* **1989,** *156*, 477-480.
143. Konefal, Z. Influence of Detergents on the Bleaching Process, Laser Properties of Rhodamine-6g and Rhodamine-B in Aqueous-Solution. *Z Naturforsch A* **1979,** *34*, (5), 551-556.
144. Lennernas, H.; Abrahamsson, B. The use of biopharmaceutic classification of drugs in drug discovery and development: current status and future extension. *J Pharm Pharmacol* **2005,** *57*, (3), 273-285.
145. Kataoka, M.; Masaoka, Y.; Yamazaki, Y.; Sakane, T.; Sezaki, H.; Yamashita, S. In vitro system to evaluate oral absorption of poorly water-soluble drugs: Simultaneous analysis on dissolution and permeation of drugs. *Pharmaceut Res* **2003,** *20*, (10), 1674-1680.
146. Carey, M. C.; Small, D. M. The characteristics of mixed micellar solutions with particular reference to bile. *Am J Med* **1970,** *49*, 590-608.
147. Wang, G.; Wang, T. Oxidative Stability of Egg and Soy Lecithin as Affected by Transition Metal Ions and pH in Emulsion. *J Agr Food Chem* **2008,** *56*, (23), 11424-11431.
148. Meyuhas, D.; Bor, A.; Pinchuk, I.; Kaplun, A.; Talmon, Y.; Kozlov, M. M.; Lichtenberg, D. Effect of ionic strength on the self-assembly in mixtures of phosphatidylcholine and sodium cholate. *J Colloid Interf Sci* **1997,** *188*, (2), 351-362.
149. Soderlind, E.; Karlsson, E.; Carlsson, A.; Kong, R.; Lenz, A.; Lindborg, S.; Sheng, J. J. Simulating Fasted Human Intestinal Fluids: Understanding the Roles of Lecithin and Bile Acids. *Mol Pharmaceut* **2010,** *7*, (5), 1498-1507.
150. Uppoor, V. R. S. Regulatory perspectives on in vitro (dissolution)/in vivo (bioavailability) correlations. *J Control Release* **2001,** *72*, (1-3), 127-132.
151. Moog, F. The Lining of the Small-Intestine. *Sci Am* **1981,** *245*, (5), 154-158.
152. Mu, H. L.; Holm, R.; Mullertz, A. Lipid-based formulations for oral administration of poorly water-soluble drugs. *International journal of pharmaceutics* **2013,** *453*, (1), 215-224.

153. Hofmann, A. F., The enterohepatic circulation of bile acids in man. In *Handbook of Physiology*, ed.; Schultz, S. G.Bethesda: U.S.A **1984,** pp 567-596.
154. Persson, E. M.; Nilsson, R. G.; Hansson, G. I.; Lofgren, L. J.; Liback, F.; Knutson, L.; Abrahamsson, B.; Lennernas, H. A clinical single-pass perfusion investigation of the dynamic in vivo secretory response to a dietary meal in human proximal small intestine. *Pharmaceut Res* **2006,** *23*, (4), 742-751.
155. Kleberg, K.; Jacobsen, F.; Fatouros, D. G.; Mullertz, A. Biorelevant Media Simulating Fed State Intestinal Fluids: Colloid Phase Characterization and Impact on Solubilization Capacity. *J Pharm Sci* **2010,** *99*, (8), 3522-3532.
156. Charman, W. N.; Rogge, M. C.; Boddy, A. W.; Berger, B. M. Effect of food and a monoglyceride emulsion formulation on danazol bioavailability. *J Clin Pharmacol* **1993,** *33*, (4), 381-386.
157. Buch, P.; Languth, P.; Kataoka, M.; Yamashita, S. IVIVC in Oral Absorption for Fenofibrate Immediate Release Tablets Using a Dissolution/Permeation System. *J Pharm Sci* **2009,** *98*, (6), 2001-2009.
158. Buch, P.; Holm, P.; Thomassen, J. Q.; Scherer, D.; Kataoka, M.; Yamashita, S.; Langguth, P. IVIVR in oral absorption for fenofibrate immediate release tablets using dissolution and dissolution permeation methods. *Pharmazie* **2011,** *66*, (1), 11-16.
159. Walter, A.; Vinson, P. K.; Kaplun, A.; Talmon, Y. Intermediate Structures in the Cholate-Phosphatidylcholine Vesicle Micelle Transition. *Biophys J* **1991,** *60*, (6), 1315-1325.
160. Nieh, M. P.; Katsaras, J.; Qi, X. Controlled release mechanisms of spontaneously forming unilamellar vesicles. *Biochimica et biophysica acta* **2008,** *1778*, (6), 1467-71.
161. Khoshakhlagh, P.; Johnson, R.; Nawroth, T.; Langguth, P.; Schmueser, L.; Hellmann, N.; Decker, H.; Szekely, N. K. Nanoparticle structure development in the gastro-intestinal model fluid FaSSIF(mod6.5) from several phospholipids at various water content relevant for oral drug administration. *Eur J Lipid Sci Tech* **2014,** *116*, (9), 1155-1166.
162. Berne, B. J.; Pecora, R., *Dynamic light scattering – with applications to chemistry, biology and physics* ed.; Dover book publications Inc.Mineola.: New York **1976**.
163. Radulescu, A.; Pipich, V.; Frielinghaus, H.; Appavau, M. S. In *KWS-2, the high intensity / wide Q-range small-angle neutron diffractometer for soft-matter and biology at FRM II*, Journal of Physics: Conference Series,351,012026 **2012**.
164. Jahn, M. R.; Nawroth, T.; Futterer, S.; Wolfrum, U.; Kolb, U.; Langguth, P. Iron Oxide/Hydroxide Nanoparticles with Negatively Charged Shells Show Increased Uptake in Caco-2 Cells. *Mol Pharmaceut* **2012,** *9*, (6), 1628-1637.
165. Buch, K.; Peters, T.; Nawroth, T.; Sanger, M.; Schmidberger, H.; Langguth, P. Determination of cell survival after irradiation via clonogenic assay versus multiple MTT Assay - A comparative study. *Radiat Oncol* **2012,** *7*.
166. Mosmann, T. Rapid Colorimetric Assay for Cellular Growth and Survival - Application to Proliferation and Cyto-Toxicity Assays. *J Immunol Methods* **1983,** *65*, (1-2), 55-63.
167. Nakayama, F.; Vanderli.W. Bile Composition - Sweden Versus Japan - Its Possible Significance in Difference in Gallstone Incidence. *Am J Surg* **1971,** *122*, (1), 8-13.
168. Helenius, A.; McCaslin, D. R.; Fries, E.; Tanford, C. Properties of detergents. *Methods in enzymology* **1979,** *56*, 734-49.
169. Muller, K. Structural Dimorphism of Bile-Salt Lecithin Mixed Micelles - a Possible Regulatory Mechanism for Cholesterol Solubility in Bile - X-Ray Structure-Analysis. *Biochemistry-Us* **1981,** *20*, (2), 404-414.
170. Kirby, C.; Clarke, J.; Gregoriadis, G. Cholesterol Content of Small Unilamellar Liposomes Controls Phospholipid Loss to High-Density Lipoproteins in the Presence of Serum. *FEBS letters* **1980,** *111*, (2), 324-328.

171. Raffy, S.; Teissie, J. Control of lipid membrane stability by cholesterol content. *Biophys J* **1999,** *76*, (4), 2072-2080.
172. Vanderkooi, G. Computation of Mixed Phosphatidylcholine-Cholesterol Bilayer Structures by Energy Minimization. *Biophys J* **1994,** *66*, (5), 1457-1468.
173. Ohvo-Rekila, H.; Ramstedt, B.; Leppimaki, P.; Slotte, J. P. Cholesterol interactions with phospholipids in membranes. *Prog Lipid Res* **2002,** *41*, (1), 66-97.
174. Silvius, J. R. Role of cholesterol in lipid raft formation: lessons from lipid model systems. *Bba-Biomembranes* **2003,** *1610*, (2), 174-183.
175. Wennberg, C. L.; van der Spoel, D.; Hub, J. S. Large Influence of Cholesterol on Solute Partitioning into Lipid Membranes. *J Am Chem Soc* **2012,** *134*, (11), 5351-5361.
176. Long, M. A.; Kaler, E. W.; Lee, S. P. Structural Characterization of the Micelle-Vesicle Transition in Lecithin-Bile Salt-Solutions. *Biophys J* **1994,** *67*, (4), 1733-1742.
177. Zumbuehl, O.; Weder, H. G. Liposomes of Controllable Size in the Range of 40 to 180 Nm by Defined Dialysis of Lipid-Detergent Mixed Micelles. *Biochimica et biophysica acta* **1981,** *640*, (1), 252-262.
178. Marinetti, G. V., *Disorders of cholesterol metabolism. In Disorders of lipid metabolism.* ed.; Springer, : New York **1990,** pp 63-74.
179. Tanaka, Y.; Hara, T.; Waki, R.; Nagata, S. Regional Differences in the Components of Luminal Water from Rat Gastrointestinal Tract and Comparison with Other Species. *J Pharm Pharm Sci* **2012,** *15*, (4), 510-518.
180. Sjogren, E.; Abrahamsson, B.; Augustijns, P.; Becker, D.; Bolger, M. B.; Brewster, M.; Brouwers, J.; Flanagan, T.; Harwood, M.; Heinen, C.; Holm, R.; Juretschke, H. P.; Kubbinga, M.; Lindahl, A.; Lukacova, V.; Munster, U.; Neuhoff, S.; Nguyen, M. A.; van Peer, A.; Reppas, C.; Hodjegan, A. R.; Tannergren, C.; Weitschies, W.; Wilson, C.; Zane, P.; Lennernas, H.; Langguth, P. In vivo methods for drug absorption - Comparative physiologies, model selection, correlations with in vitro methods (IVIVC), and applications for formulation/API/excipient characterization including food effects. *Eur J Pharm Sci* **2014,** *57*, 99-151.
181. Bevernage, J.; Brouwers, J.; Brewster, M. E.; Augustijns, P. Evaluation of gastrointestinal drug supersaturation and precipitation: Strategies and issues. *Int J Pharm* **2013,** *453*, (1), 25-35.
182. Buch, P.; Holm, P.; Thomassen, J. Q.; Scherer, D.; Branscheid, R.; Kolb, U.; Langguth, P. IVIVC for Fenofibrate Immediate Release Tablets Using Solubility and Permeability as In Vitro Predictors for Pharmacokinetics. *J Pharm Sci* **2010,** *99*, (10), 4427-4436.
183. Brouwers, J.; Augustijns, P. Resolving intraluminal drug and formulation behavior: Gastrointestinal concentration profiling in humans. *Eur J Pharm Sci* **2014,** *61*, 2-10.
184. Knoll, W.; Ibel, K.; Sackmann, E. Small-Angle Neutron-Scattering Study of Lipid Phase-Diagrams by the Contrast Variation Method. *Biochemistry-Us* **1981,** *20*, (22), 6379-6383.
185. Mahabir, S.; Small, D.; Li, M.; Wan, W. K.; Kucerka, N.; Littrell, K.; Katsaras, J.; Nieh, M. P. Growth kinetics of lipid-based nanodiscs to unilamellar vesicles-A time-resolved small angle neutron scattering (SANS) study. *Bba-Biomembranes* **2013,** *1828*, (3), 1025-1035.
186. Tenzer, S.; Docter, D.; Rosfa, S.; Wlodarski, A.; Kuharev, J.; Rekik, A.; Knauer, S. K.; Bantz, C.; Nawroth, T.; Bier, C.; Sirirattanapan, J.; Mann, W.; Treuel, L.; Zellner, R.; Maskos, M.; Schild, H.; Stauber, R. H. Nanoparticle Size Is a Critical Physicochemical Determinant of the Human Blood Plasma Corona: A Comprehensive Quantitative Proteomic Analysis. *Acs Nano* **2011,** *5*, (9), 7155-7167.

187. Manzo, G.; Carboni, M.; Rinaldi, A. C.; Casu, M.; Scorciapino, M. A. Characterization of sodium dodecylsulphate and dodecylphosphocholine mixed micelles through NMR and dynamic light scattering. *Magn Reson Chem* **2013,** *51*, (3), 176-183.
188. Adkin, D. A.; Davis, S. S.; Sparrow, R. A.; Huckle, P. D.; Phillips, A. J.; Wilding, I. R. The Effects of Pharmaceutical Excipients on Small-Intestinal Transit. *Brit J Clin Pharmaco* **1995,** *39*, (4), 381-387.
189. Hirtz, J. The gastrointestinal absorption of drugs in man: a review of current concepts and methods of investigation. *Br J clin Pharmac* **1985,** *19*, 77S-83S.
190. Chaudhary, A.; Nagaich, U.; Gulati, N.; Sharma, V. K.; Khosa, R. L. Enhancement of solubilization and bioavailability of poorly soluble drugs
by physical and chemical modifications: A recent review. *JAPER* **2012,** *2* (1), 32-67.
191. Khoshakhlagh, P.; Johnson, R.; Langguth, P.; Nawroth, T.; Schmueser, L.; Hellmann, N.; Decker, H.; Szekely, N. K. Fasted-State Simulated Intestinal Fluid "FaSSIF-C", a Cholesterol Containing Intestinal Model Medium for In Vitro Drug Delivery Development. *J Pharm Sci* **2015,** *104*, (7), 2213-2224.
192. Esezobo, S. The Effect of Some Excipients on the Physical-Properties of a Paracetamol Tablet Formulation. *J Pharm Pharmacol* **1985,** *37*, (3), 193-195.
193. Park, S. H.; Choi, H. K. The effects of surfactants on the dissolution profiles of poorly water-soluble acidic drugs. *Int J Pharm* **2006,** *321*, (1-2), 35-41.
194. Maggi, L.; Torre, M. L.; Giunchedi, P.; Conte, U. Supramicellar solutions of sodium dodecyl sulphate as dissolution media to study the in vitro release characteristics of sustained-release formulations containing an insoluble drug: Nifedipine. *Int J Pharm* **1996,** *135*, (1-2), 73-79.
195. Rangel-Yagui, C. O.; Pessoa, A.; Tavares, L. C. Micellar solubilization of drugs. *J Pharm Pharm Sci* **2005,** *8*, (2), 147-163.
196. Muellertz, A.; Ogbonna, A.; Ren, S.; Rades, T. New perspectives on lipid and surfactant based drug delivery systems for oral delivery of poorly soluble drugs. *J Pharm Pharmacol* **2010,** *62*, (11), 1622-1636.
197. Vemula, V. R.; Lagishettyn, V.; Lingala, S. Solubility Enhancement Techniques. *Int J Pharm Sci Rev Res* **2010,** *5*, (1), 41-51.
198. Nawroth, T. bifurcation of the nanoparticle- excipient mediated drug. **2015**.
199. Torchilin, V. P. Structure and design of polymeric surfactant-based drug delivery systems. *J Control Release* **2001,** *73*, (2-3), 137-172.
200. Ong, J. T. H.; Manoukian, E. Micellar Solubilization of Timobesone Acetate in Aqueous and Aqueous Propylene-Glycol Solutions of Nonionic Surfactants. *Pharmaceut Res* **1988,** *5*, (11), 704-708.
201. Kerwin, B. A. Polysorbates 20 and 80 used in the formulation of protein biotherapeutics: Structure and degradation pathways. *J Pharm Sci* **2008,** *97*, (8), 2924-2935.
202. Delamaza, A.; Parra, J. L. Vesicle-Micelle Structural Transition of Phosphatidylcholine Bilayers and Triton X-100. *Biochemical Journal* **1994,** *303*, 907-914.
203. Shoji, Y.; Igarashi, T.; Nomura, H.; Eitoku, T.; Katayama, K. Liposome Solubilization Induced by Surfactant Molecules in a Microchip. *Anal Sci* **2012,** *28*, (4), 339-343.
204. Lee, S. C.; Lee, K. E.; Kim, J. J.; Lim, S. H. The effect of cholesterol in the liposome bilayer on the stabilization of incorporated retinol. *J Liposome Res* **2005,** *15*, (3-4), 157-166.
205. Liu, D. Z.; Chen, W. Y.; Tasi, L. M.; Yang, S. P. The Effects of cholesterol on the release of free lipids and the physical stability of lecithin liposome. *J.Chin. Inst. Chem. Eng.* **2000,** *31*, 269-276.
206. Jogia, H.; Sola, S. P.; Garg, L. K.; Arutla, S.; Reddy, A. M.; Venkateswarlu, V. A Simple, Safe, and Environmentally Friendly Method of FaSSIF and FeSSIF Preparation Without Methylene Chloride. *Dissolution Technologies* **2014,** *21*, (1), 45-48.

207. Arnesjo, B.; Nilsson, A.; Barrowman, J.; Borgstrom, B. Intestinal digestion and absorption of cholesterol and lecithin in the human. Intubation studies with a fat-soluble reference substance. *Scandinavian journal of gastroenterology* **1969,** *4*, (8), 653-65.
208. Mansbach, C. M., 2nd; Cohen, R. S.; Leff, P. B. Isolation and properties of the mixed lipid micelles present in intestinal content during fat digestion in man. *The Journal of clinical investigation* **1975,** *56*, (4), 781-91.
209. Robinson, N. Lysolecithin. *J Pharm Pharmacol* **1961,** *13*, 321-54.
210. Buggins, T. R.; Dickinson, P. A.; Taylor, G. The effects of pharmaceutical excipients on drug disposition. *Adv Drug Deliver Rev* **2007,** *59*, (15), 1482-1503.
211. Granger, D. N.; Perry, M. A.; Kvietys, P. R.; Taylor, A. E. Permeability of intestinal capillaries: effects of fat absorption and gastrointestinal hormones. *Am J Physiol* **1982,** *242*, (3), G194-201.

8. Appendix

8.1 Procedures for DLS data export and scaling

8.1.1 Export and scaling of DLS data from Malvern Zetasizer

The zetasizer software allows different parameters (graphs, tables' data) to be exported to another application like Excel, Word, Wordpad. The export of the primary raw data without scaling, the particle size distribution "PSDi" is activated by an operation script "SOP" as an ASCII data file (one line per sample). This misses the size value table column, which can be completed external from a template file "Size master", as it is constant for all experiments (device property). After exporting the data in front of the sample data, Sizemaster table "containing size d (=s), radius r, r2, r3 … r6 should be copied. Data should be imported to Origin and after each sample a new column (=volume) should be created. After drawing the graphs they should be exported by TIF.
After import in Origin or Excel, the exponentials are calculated as radius r, r2, r3 … r6 as with the Malvern Zetasizer samples. The scaling to liposome contributions C_{m2} is obtained by division of the intensity by r^2, the scaling for contributions of massive particles C_{m3} ("PSD-v" in the Malvern software) is done by division of r^3.

index	1	2	3	4	5	6	7	8	9	10	11	12
	13	14	15	16	17	18	19	20	21	22	23	24
	25	26	27	28	29	30	31	32	33	34	35	36
	37	38	39	40	41	42	43	44	45	46	47	48
	49	50	51	52	53	54	55	56	57	58	59	60
	61	62	63	64	65	66	67	68	69	70		
ln-d	-0,91629		-0,76953		-0,62277		-0,476	-0,32924		-0,18248		-
0,03571		0,11105		0,25781		0,40457		0,55134		0,6981	0,84486	
	0,99162		1,13839		1,28515		1,43191		1,57868		1,72544	
	1,8722	2,01896		2,16573		2,31249		2,45925		2,60602		
	2,75278		2,89954		3,0463	3,19307		3,33983		3,48659		
	3,63335		3,78012		3,92688		4,07364		4,22041		4,36717	
	4,51393		4,66069		4,80746		4,95422		5,10098		5,24775	
	5,39451		5,54127		5,68803		5,8348	5,98156		6,12832		
	6,27508		6,42185		6,56861		6,71537		6,86214		7,0089	
	7,15566		7,30242		7,44919		7,59595		7,74271		7,88948	
	8,03624		8,183	8,32976		8,47653		8,62329		8,77005		
	8,91681		9,06358		9,21034							
d	0,4	0,46323		0,53646		0,62126		0,71947		0,8332	0,96492	
	1,11745		1,29409		1,49866		1,73557		2,00993		2,32766	
	2,69561		3,12173		3,61521		4,1867	4,84853		5,61498		
	6,5026	7,53052		8,72094		10,09954		11,69607		13,54497		
	15,68615		18,1658		21,03744		24,36302		28,21431		32,6744	
	37,83955		43,82119		50,74841		58,77068		68,0611		78,82015	
	91,27997		105,70944		122,4199		141,77194		164,18314		190,13708	
	220,19379		255,00185		295,31234		341,99507		396,05738		458,66581	
	531,17134		615,13848		712,37907		824,99138		955,40536		1106,43507	
	1281,33944		1483,89255		1718,46509		1990,11867		2304,71504		2669,04254	

	3090,96264	3579,57953	4145,43659	4800,74388	5559,64162	6438,5053	
	7456,29905	8634,98481	9999,99628				
r	0,2	0,23162	0,26823	0,31063	0,35974	0,4166	0,48246
	0,55872	0,64705	0,74933	0,86779	1,00496	1,16383	
	1,34781	1,56087	1,80761	2,09335	2,42427	2,80749	
	3,2513	3,76526	4,36047	5,04977	5,84803	6,77249	
	7,84308	9,0829	10,51872	12,18151	14,10715	16,3372	
	18,91977	21,9106	25,37421	29,38534	34,03055	39,41007	
	45,63999	52,85472	61,20995	70,88597	82,09157	95,06854	
	110,0969	127,50092	147,65617	170,99754	198,02869	229,33291	
	265,58567	307,56924	356,18954	412,49569	477,70268	553,21754	
	640,66972	741,94627	859,23255	995,05934	1152,35752	1334,52127	
	1545,48132	1789,78977	2072,71829	2400,37194	2779,82081	3219,25265	
	3728,14952	4317,49241	4999,99814				
r2	0,04	0,05365	0,07195	0,09649	0,12941	0,17356	
	0,23277	0,31217	0,41867	0,5615	0,75305	1,00995	
	1,3545	1,81658	2,4363	3,26744	4,38212	5,87707	7,88201
	10,57094	14,17719	19,0137	25,50018	34,1995	45,86657	
	61,51383	82,49912	110,64348	148,38922	199,01181	266,90418	
	357,95786	480,07426	643,85036	863,49825	1158,07846	1553,15394	
	2083,00841	2793,62137	3746,65811	5024,82089	6739,0256	9038,02685	
	12121,32645	16256,48578	21802,34407	29240,15765	39215,3622	52593,5821	
	70535,7473	94598,836	126870,9855	170152,6957	228199,85	306049,6417	
	410457,6894	550484,2739	738280,5675	990143,0834	1,33E+06	1,78E+06	
	2,39E+06	3,20E+06	4,30E+06	5,76E+06	7,73E+06	1,04E+07	
	1,39E+07	1,86E+07	2,50E+07				
r3	0,008	0,01243	0,0193	0,02997	0,04655	0,0723	0,1123 0,17442
	0,2709	0,42075	0,65349	1,01497	1,5764	2,4484	3,80274
	5,90624	9,17331	14,24757	22,12869	34,36928	53,38082	
	82,90869	128,77004	199,99982	310,6307	482,45761	749,33142	
	1163,8278	1807,60489	2807,49045	4360,46765	6772,48184	10518,7136	
	16337,19194	25374,19029	39410,04888	61209,91192	95068,47679	147656,0739	
	229332,7599	356189,3079	553217,1815	859231,9957	1,33E+06	2,07E+06	
	3,22E+06	5,00E+06	7,77E+06	1,21E+07	1,87E+07	2,91E+07	
	4,52E+07	7,02E+07	1,09E+08	1,69E+08	2,63E+08	4,08E+08	
	6,34E+08	9,85E+08	1,53E+09	2,38E+09	3,69E+09	5,73E+09	
	8,90E+09	1,38E+10	2,15E+10	3,34E+10	5,18E+10	8,05E+10	
	1,25E+11						
r4	0,0016	0,00288	0,00518	0,00931	0,01675	0,03012	
	0,05418	0,09745	0,17528	0,31528	0,56709	1,02001	
	1,83466	3,29996	5,93557	10,67616	19,20296	34,53991	
	62,12612	111,74479	200,99273	361,52088	650,25908	1169,60568	
	2103,74216	3783,95141	6806,10418	12241,9791	22019,35915	39605,7021	
	71237,84248	128133,8275	230471,2942	414543,2825	745629,2275	1,34E+06	
	2,41E+06	4,34E+06	7,80E+06	1,40E+07	2,52E+07	4,54E+07	
	8,17E+07	1,47E+08	2,64E+08	4,75E+08	8,55E+08	1,54E+09	
	2,77E+09	4,98E+09	8,95E+09	1,61E+10	2,90E+10	5,21E+10	
	9,37E+10	1,68E+11	3,03E+11	5,45E+11	9,80E+11	1,76E+12	
	3,17E+12	5,70E+12	1,03E+13	1,85E+13	3,32E+13	5,97E+13	
	1,07E+14	1,93E+14	3,47E+14	6,25E+14			

r6	6,40E-05	1,54E-04	3,72E-04	8,98E-04	0,00217	0,00523
	0,01261	0,03042	0,07339	0,17703	0,42705	1,03016
	2,48504	5,99465	14,46083	34,88371	84,14964	202,99336
	489,6789	1181,24764	2849,51217	6873,85044	16581,72241	39999,92734
	96491,43485	232765,3478	561497,5797	1,35E+06	3,27E+06	7,88E+06
	1,90E+07	4,59E+07	1,11E+08	2,67E+08	6,44E+08	1,55E+09
	3,75E+09	9,04E+09	2,18E+10	5,26E+10	1,27E+11	3,06E+11
	7,38E+11	1,78E+12	4,30E+12	1,04E+13	2,50E+13	6,03E+13
	1,45E+14	3,51E+14	8,47E+14	2,04E+15	4,93E+15	1,19E+16
	2,87E+16	6,92E+16	1,67E+17	4,02E+17	9,71E+17	2,34E+18
	5,65E+18	1,36E+19	3,29E+19	7,93E+19	1,91E+20	4,61E+20
	1,11E+21	2,69E+21	6,48E+21	1,56E+22		

8.1.2 Export and scaling of DLS data from ALV-Nanovel ProSpecD

The ALV DLS software 3.0 enables a complete data export as ASCII files via an intermediate copy at the windows surface (Zwischenablage). After pasting this in a text file with any editor, e.g. “WordPad”, the data are saved at the hard disc. The ASCII file contain 6 columns, which contain the individual size values as first column, and the corresponding intensities (= “PSDi” in Malvern files) as second column. After import in Origin or Excel, the exponentials are calculated as radius r, r2, r3 … r6 as with the Malvern Zetasizer samples. The scaling to liposome contributions C_{m2} is obtained by division of the intensity by r^2, the scaling for contributions of massive particles C_{m3} (“PSD-v” in the Malvern software) is done by division of r^3.

9. Personal data

9.1. Publications

1. "Nanoparticle Structure Development in the Gastro-Intestinal Model Fluid $FaSSIF_{mod6.5}$ from several Phospholipids at various Water Content relevant for oral Drug Administration." *Pooneh Khoshakhlagh, Raphael Johnson, Thomas Nawroth, Peter Langguth, Lars Schmueser, Nadja Hellmann, Heinz Decker, Noemi Kinga Szekely*.Eur. J. Lipid Sci. Technol. 2014, 116, 1155–1166.

2. "Fasted-State Simulated Intestinal Fluid "FaSSIF-C", a Cholesterol containing Intestinal Model Medium for *in vitro* Drug Delivery Development." *Pooneh Khoshakhlagh, Raphael Johnson, Peter Langguth, Thomas Nawroth, Lars Schmuese, Nadja Hellmann, Heinz Decker, Noemi Kinga Szekely*. J. Pharmaceutical Sciences 2015, 104 (7), 2213–2224.

3. "Amphotericin B Microparticles "AmbiShell" from Phospholipid and Gelatin: Development and investigation by combined DLS and SANS resolves the Core-Shell Structure." *Raphael Johnson, Pooneh Khoshakhlagh, Thomas Nawroth, Peter Langguth, Lars Schmueser, Nadja Hellmann, Heinz Decker, Noemi Kinga Szekely*. Eur. J. Lipid Sci. Technol. 2014, 116 (9), 1167–1173.

4. "Bifurcation of the Nanoparticle-Excipient mediated Drug Solubilization Pathways of oral Formulations in the Gastro-Intestinal model Fluid $FaSSIF_{mod6.5.}$" *Thomas Nawroth, Pooneh Khoshakhlagh, Philipp Buch, Raphael Johnson, Peter Langguth, Lars Schmueser, Nadja Hellmann, Heinz Decker, Noemi Kinga Szekely*. International Journal of Pharmaceutics, submitted.

5. "Excipient effect on the colloidal structure and drug solubility in cholesterol containing biorelevant intestinal medium (FaSSIF-7C) with Fenofibrate" *Pooneh Khoshakhlagh, Philipp Buch, Raphael Johnson, Peter Langguth, Thomas Nawroth, Lars Schmueser, Nadja Hellmann, Heinz Decker, Noemi Kinga Szekely*. J. Pharmaceutical Sciences, submitted.

9.2. Contributions to international conferences

1. Khoshakhlagh P., Nawroth T., Johnson R., Langguth P., Schmueser L., Decker H.,Hellmann N., Szekely N., Excipient effect on colloidal structure and BCS-II drug solubility in cholesterol containing biorelevant intestinal medium (FaSSIF-7C). Phospholipids in Pharmaceutical Research, Heidelberg, Germany, 21 th-22 September, 2015.

2. Johnson R, Khoshakhlagh P, Nawroth T, Langguth P, Schmueser L, Decker H, Hellmann N, Szekely N., Structural Dynamics of Liposomal Amphotericin B in FaSSIF by combined SANS and DLS. Trends in Neutron Science – MLZ User Meeting, Ismaning, Munich, Germany, 23rd – 24th February, 2015.

3. Khoshakhlagh P., Johnson R., Nawroth T., Langguth P., Schmueser L., Decker H., Hellmann N., Szekely N., Structural Dynamics of Novel Gastrointestinal Model Fluids by combined SANS and DLS. Deutsche Pharmazeutische Gesellschaft Annual meeting, Frankfurt, Germany, 24th – 26th September, 2014.

4. Khoshakhlagh P, Johnson R, Nawroth T, Langguth P, Schmueser L, Decker H, Hellmann N, Szekely N., Nanoparticles in gastrointestinal fluids drug solubility and structure development. Deutsche Pharmazeutische Gesellschaft Annual meeting, Frankfurt, Germany, 24th – 26th September, 2014.

5. Johnson R, Khoshakhlagh P, Nawroth T, Langguth P, Schmueser L, Decker H, Hellmann N, Szekely N., Structural Dynamics of Liposomal Amphotericin B in FaSSIF by combined SANS and DLS. Deutsche Pharmazeutische Gesellschaft Annual meeting, Frankfurt, Germany, 24th – 26th September, 2014.

6. T. Nawroth, P. Khoshakhlagh, S. Kindgen, L. Krebs, R. Johnson, P. Langguth, N. Szekely and R. Schweins., Gastro-Intestinal Simulator for in vitro Drug and Nanoparticle Tracing in Oral Drug Development. Deutsche Pharmazeutische Gesellschaft Annual meeting, Frankfurt, Germany, 24th – 26th September, 2014.

7. Johnson R, Khoshakhlagh P, Nawroth T, Langguth P, Schmueser L, Decker H, Hellmann N, Szekely N., Oral Amphotericin B Nano-Formulations: Structure and Development in Gastrointestinal Fluids. ORBITO Workshop, Mainz, Germany, 17th – 19th September, 2014.

8. T. Nawroth, P. Khoshakhlagh, R. Johnson, P. Buch, P. Langguth, L. Schmueser, N. Hellmann, H. Decker, N. Szekely and R. Schweins., Nanoparticles in the human Gastro-Intestinal System and Drug Uptake – Modelling and Investigation by Time Resolved Neutron Scattering. Neutrons in Biology and BioTechnology, Grenoble, France, 19th-21st February 2014.

9. Khoshakhlagh P., Nawroth T., Johnson R., Langguth P., Schmueser L., Decker H., Hellmann N., Szekely N., Gastrointestinal BCS 2-drug resolution in intestinal model fluids containing physiological lipids-drug dissolution and intestinal nanoparticle structure estimated by DLS and neutron scattering. Deutsche Pharmazeutische Gesellschaft Annual meeting, Freiburg, Germany, 9th – 11th October, 2013.

10. Raphael Johnson, Pooneh Khoshakhlagh, Thomas Nawroth, Peter Langguth, Lars Schmueser, Heinz Decker, Nadja Hellmann, Noemi Szekely., Amphotericin B lipid Nanoparticles for oral administration. Deutsche Pharmazeutische Gesellschaft Annual meeting, Freiburg, Germany, 9th – 11th October, 2013.

11. Khoshakhlagh P., Nawroth T., Johnson R., Langguth P., Schmueser L., Decker H.,Hellmann N., Szekely N., Lipid-Drug Nanoparticles in Gastrointestinal Model Fluids . Phospholipids in Pharmaceutical Research, Heidelberg, Germany, 16 th-17 th September, 2013.

12. Raphael Johnson, Pooneh Khoshakhlagh, Thomas Nawroth, Peter Langguth, Lars Schmueser, Heinz Decker, Nadja Hellmann, Noemi Szekely., Structural dynamics of lipid complexes of Amphotericin B. Phospholipids in Pharmaceutical Research, Heidelberg, Germany, 16th -17th September, 2013.

13. T. Nawroth, P. Khoshakhlagh, R. Johnson, P. Buch, P. Langguth, L. Schmueser, N. Hellmann, H. Decker, N. Szekely and R. Schweins., Drug-uptake by Nanostructures in the GI-System: Simulator with DLS-SANS. Innovative Tools for Oral Biopharmaceutics OrBiTo, Uppsala, Sweden, 26th-27th June 2013.

9.3. Curriculim vitae